ADVANCED MASTERS IN STRUCTURAL ANALYSYS
OF MONUMENTS AND HISTORICAL CONSTRUCTIONS

Master's Thesis

Elsa Anglade

Study of the seismic vulnerability of Catalonian Romanseque churches: Church of the cathedral of La Seu d'Urgell and church of the Monastery of Vilabertran

Spain | 2019

DECLARATION

Name:	Elsa Anglade
Email:	Elsa.anglade@ens-paris-saclay.fr

Title of the Msc Dissertation:	Study of the seismic vulnerability of Catalonian Romanesque churches: Church of the cathedral of La Seu d'Urgell and church of the Monastery of Vilabertran
Supervisor(s):	Professor Pere Roca and Professor Luca Pelà
Year:	2019

I hereby declare that all information in this document has been obtained and presented in accordance with academic rules and ethical conduct. I also declare that, as required by these rules and conduct, I have fully cited and referenced all material and results that are not original to this work.

I hereby declare that the MSc Consortium responsible for the Advanced Masters in Structural Analysis of Monuments and Historical Constructions is allowed to store and make available electronically the present MSc Dissertation.

University:	Universitat Politècnica de Catalunya
Date:	16/06/2019
Signature:	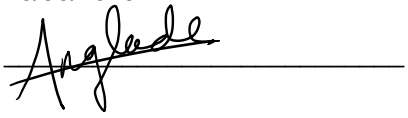

This page is left blank on purpose.

ACKNOWLEDGEMENTS

I would like to thank Professors Pere Roca and Luca Pelà for their help during this thesis. I am extremely grateful for their guidance, knowledge and numerous hours spent helping me complete this thesis. It would not have been possible to finish this thesis without their support. I am also grateful to Ellen Key, who helped me during the inspection of the churches and the application of the different methods used in this thesis.

I would like to thank the professors of the Advanced Master in Structural Analysis of Monuments and Historical Construction for the all knowledge they transmitted me. I am grateful for my admission in this master, which made me meet people from different countries. I learnt a lot this year about historical building but also about the cultures of the other students.

I would like to thank the SAHC consortium for the major financial support granted in the form of a scholarship. Their financial support provided the opportunity to participate to the SAHC course.

Finally, I would like to thank my parents and my family for their unwavering support.

This page is left blank on purpose.

ABSTRACT

As illustrated by the damage assessment made after an earthquake, churches are particularly vulnerable to seismic action. The vulnerability assessment of this type of construction is necessary in order to determine the best retrofitting intervention. The vulnerability assessment of two Romanesque churches, the church of La Seu d'Urgell and the church of Vilabertran, was carried out by using two different methods. The vulnerability index method is a widely used method to quickly assess the vulnerability of a church during the survey. It can be done before or after an earthquake to identify the most vulnerable buildings. This method is also used to determine the amount of damages that would occur for a specific earthquake. The second method, the kinematic limit analysis, is used to analyze local failure mechanisms such as the overturning of the main façade or the failure of the bell tower. This analysis is useful during the evaluation of the safety of a single building and the determination of the retrofitting strategy. These two methods applied to both churches highlighted the vulnerable elements of each church. Finally, remarks about the applicability of these methods to this type of case studies are made as well as possible improvements to increase the accuracy of the results.

This page is left blank on purpose.

RESUMEN

Como lo ilustra la evaluación de daños realizada después de un terremoto, las iglesias son particularmente vulnerables a la acción sísmica. La evaluación de vulnerabilidad de este tipo de construcción es necesaria para determinar la mejor intervención de remodelación. La evaluación de la vulnerabilidad de dos iglesias románicas, la iglesia de La Seu d'Urgell y la iglesia de Vilabertran, se llevó a cabo utilizando dos métodos diferentes. El método del índice de vulnerabilidad es un método ampliamente utilizado para evaluar rápidamente la vulnerabilidad de una iglesia durante la encuesta. Se puede hacer antes o después de un terremoto para identificar los edificios más vulnerables. Este método también se utiliza para determinar la cantidad de daños que se producirían en un terremoto específico. El segundo método, el análisis de límite cinemático, se utiliza para analizar mecanismos de falla locales, como el vuelco de la fachada principal o la falla del campanario. Este análisis es útil durante la evaluación de la seguridad de un solo edificio y la determinación de la estrategia de modernización. Estos dos métodos aplicados a ambas iglesias resaltaron los elementos vulnerables de cada iglesia. Finalmente, se hacen comentarios sobre la aplicabilidad de estos métodos a este tipo de estudios de caso, así como las posibles mejoras para aumentar la precisión de los resultados.

This page is left blank on purpose.

TABLE OF CONTENTS

TABLE OF FIGURES

1. INTRODUCTION

During the last centuries, strong earthquakes around the world have destroyed numerous historical monuments. For this reason, it is important to assess the vulnerability of these constructions before or after the earthquake in order to better preserve them from heavy damages with some retrofitting strategies.

Some example of historical constructions' typologies are palaces, churches, monasteries or towers. All these typologies are characterized by a different response, behavior or damage after an earthquake. However, they all have construction features and dimensions that increase largely their vulnerability such as slender towering, large openings or thin and long span vaults.

The vulnerability assessment of churches can be used after an earthquake in order to classify the buildings according to the priority of the intervention to preserve them. A second approach is to use the vulnerability assessment in order to predict the comportment of a church for a given earthquake and to anticipate the probable damages. This method can be used to plan preventive retrofitting interventions. In this thesis, the objective is to perform a seismic vulnerability analysis of two churches in order to identify the weaknesses of the structure and to conclude about the resistance of a building to the seismicity of the region.

This thesis will only focus on the vulnerability assessment of churches and in particular of Romanesque churches of Catalonia. These churches are very ancient constructions and their shape and dimensions make them vulnerable to earthquake. The region of Catalonia is a region with moderate seismicity. However, the presence of the fault of the Pyrenees induces earthquakes that can damage vulnerable constructions. The two churches analyzed in this thesis, the church of La Seu d'Urgell and the church Santa Maria de Vilabertran, are located near the Pyrenees, which means that they are located in the part of Catalonia with the highest seismicity. The church of La Seu d'Urgell is one of the most important of this area and its dimensions are large, while the church of Vilabertran is a more modest construction. Some damages in the churches already indicate some vulnerable element of the constructions.

Two main analysis will be done for both churches: first the vulnerability index method and then the kinematic limit analysis. The first method is based on the observations made during the survey of a building. The different vulnerable elements are recorded in order to determine a vulnerability index which can be used in a large scale to identify the most vulnerable buildings that need immediate intervention or at the building scale to predict with probabilistic analysis the damages occurring for a given earthquake intensity. Moreover, the predicted damages can be compared to the observed damages during the survey. The second method is based on the analysis of local failure

mechanisms. During the inspection the most vulnerable mechanisms are identified and then a kinematic limit analysis is made. With this method, the vulnerability of each local mechanism is determined, which can help determining the part of the church that should be reinforced in priority.

The first part of the thesis reports the different methods that can be applied in order to assess the vulnerability of a building and in particular of a church. In a second part the seismicity of the region and the history of each church are analyzed. Moreover, this part also contains the actual state of conservation of the churches and the localization of their damages. The third part concerns the assessment of the vulnerability of the churches through the vulnerability index method and the applications of this index to identify different vulnerability parameters such as the fragility curves or the ground acceleration corresponding to a certain limit state. In the fourth part, the kinematic limit analysis is explained, and the results of the method are used to identify the most vulnerable local mechanism. Finally, in the last part the results from both churches are compared and a discussion about the application of both methods is presented.

2. STATE OF THE ART

Seismic vulnerability assessment is made in order to determine the probability of a certain damage level to occur in a specific type of building under a given earthquake scenario. Several methods have been created in order to estimate the possible losses and can be divided in two main categories : empirical and analytical methods. In empirical methods the damage scale established by Grünthal [1] is used to produce the post-earthquake damage statistics, while in analytical methods it is related to limit-state mechanical properties of the building. These two methods can be regrouped in a hybrid method considering damage survey in order to identify the failure mechanisms that could occur and thus be analytically studied. However, both methods require first a complete knowledge of the structure studied in order to make relevant assumptions. The following paragraphs will describe first the minimum of knowledge required to start an analysis and then the two different procedures to assess the vulnerability of a church. [2]

2.1 General methodology according to the Italian Guidelines for the Evaluation and Mitigation of Seismic Risk in Cultural Heritage

The study of a specific church requires an important knowledge of the entire structure to better understand the connections between each elements of the structure. The Italian Guideline [3] gives clear instructions regarding the information that should be collected before any analysis. The following paragraphs will describe all the steps needed before performing the seismic vulnerability of a church.

The first important step before starting any analysis is to have a complete knowledge of the seismicity of the region. Regarding this, it is important to know which type of soil and foundation the building has. The classification of soils is based on the speed of the shear waves in the ground and the number of different type of grains under the building at a certain depth. Then, an analysis of the country seismic code help identifying the horizontal peak ground acceleration and thus the response spectrum corresponding to the studied area. Finally, the last factor needed to understand of the seismic action is the presence of site amplification around the structure. All these data are necessary in order to compare the results of the analysis with the seismic demand of the concerned area.

When the seismic demand is understood, an important part of a church analysis is knowing/understanding the building. The data needed is:

- The identification of the organism in charge of the building and its location. The different functions of the building should also be identified in order to better understand the motivation under some later addition in the construction.

- A geometrical survey in order to identify all the structural elements, their shape and their connections. Thanks to this step, the in-plan and in-elevation characteristics of the church can be identified (vaults, arches, …). The difficulty of this rely on the accessibility of each part of the structure and specially the vaults and the roof.
- The historical survey of the church, which gives information about the phases of construction, the interventions but also the historical earthquakes that already occurred.
- The inspection of the church giving relevant information concerning the damages of the structure and the monitoring dispositions already in place. A damage mapping needs to be done in order to understand the actual state of the structure.
- The identification of the materials and their state of conservation, which are important parameters to predict the structure comportment. Materials properties should also be determined in the case of a numerical study of the church. However, this step is one of the most complicated because of the composition of a masonry wall. Most of the time, the external walls are really thick and are composed of multiple leaves. Only the two external leaves are visible and are generally a good quality masonry, but the infill of the walls in most of the time rubble masonry. Moreover, it is not possible to evaluate the connection between all the leaves. It is thus possible to do experiment on samples from the existing building in order to have an idea of the compressive and tensile strength or the Young modulus.
- And finally, the knowledge concerning the ground and the foundations. As for the seismic demand, it is fundamental in order to understand the behaviour of the structure.

In the Italian Guideline, four forms (A, B, C and D) are presented in the Appendixes A and B to help understanding the requirements for all the information needed to be collected.

According to the data collected in the previous step, it is possible to determine a confidence factor F_C. This factor is ranging from 1 to 1.35 and grades the reliability of the structural model and the seismic safety index. This factor is applied in different ways depending on the type of analysis: in a first case, the confidence factor can be applied to the material properties, while in a second case it can be applied directly to the structure capacity. The Equation 2.1 and the Table 2.1 define how to calculate the confidence factor.

$$F_C = 1 + \sum_{k=1}^{4} F_{Ck} \qquad 2.1$$

Table 2.1. Relative partial confidence factors [3]

Geometric Survey	Material and Construction Survey	Mechanical Properties of the Materials	Terrain and Foundations
The geometric survey has been completed $\boldsymbol{F_{C1} = 0.05}$	Limited survey of materials and constructive elements $F_{C2} = 0.12$	Mechanical parameters deduced from available data $F_{C3} = 0.12$	Limited survey of terrain and foundations, in absence of geological data or availability of information about the foundation $F_{C4} = 0.06$
The geometric survey has been completed along with the graphic rendering of cracking and deformities $\boldsymbol{F_{C1} = 0}$	Extensive survey of materials and constructive elements $F_{C2} = 0.06$	Limited research of mechanical parameters of materials $F_{C3} = 0.06$	Geological data and information regarding the foundation structure is available, limited research on terrain and foundation $F_{C4} = 0.03$
	Exhaustive survey of materials and constructive elements $F_{C2} = 0$	Extensive research of mechanical parameters of materials $F_{C3} = 0$	Extensive or exhaustive research on the terrain and foundation $F_{C4} = 0$

Once all this information is collected, it is possible to start the analysis according to one of the two methods described below.

2.2 Empirical methods

In order to assess vulnerability of building at a large geographical scale, empirical procedures have been developed since the early 70's. These procedures were first developed and calibrated in function of the macroseismic intensity. This intensity is a scale defined in order to classify the severity of the ground shaking on the basis of observed effects in a limited area. Different intensity scales are used in function of the countries. For example, the European countries use the EMS-98 scale while Hong Kong and the United States used the Modified Mercalli scale and some other countries use the Medvedev-Sponheuer-Karnik scale.

Later, as the seismic hazard is not expressed anymore in terms of intensity but in terms of Peak Ground Acceleration (PGA), some correlations have been done to relate both of them. Empirical methods are the only reasonable way in terms of cost and effectiveness employed to analyse seismic risk at a large scale. The two principal empirical methods are based on the observation of damages after earthquake and are the damage probability matrices and the vulnerability functions. [2]

2.2.1 Damage Probability Matrices

The Damage Probability Matrices method (DPM) was first developed by Whitman et al [4] in 1973. The concept of this procedure is to predict the damage of a building by considering that all the constructions belonging to a same structural typology would have the same probability of reaching a same damage level under a specific earthquake. The initial format of the matrix proposed by Whiteman et al. is illustrated in Figure 2.1. The damage of a building is described by a damage state while the intensity of the earthquake is described by the Mercalli intensity scale, which was the most used scale at this period. The damage state is described by two elements: a description of the structural and non-structural damages and a damage ratio determined as the cost of repairing the damages over the cost of replacing the building. The damage ratio is a better method to identify the damage state, however it may be complicated to find the cost of the damages in the records of past earthquake. The Modified Mercalli intensity was used to describe the strength of ground shaking because, in the United States, all the historical records were expressed in this scale. The DPM was created for different structural typologies according to the damage survey of 1600 buildings after the 1971 San Fernando earthquake. [2], [4]

Damage State	Structural Damage	Non-structural Damage	Damage Ratio (%)	Intensity of Earthquake				
				V	VI	VII	VIII	IX
0	None	None	0-0.05	10.4	-	-	-	-
1	None	Minor	0.05-0.3	16.4	0.5	-	-	-
2	None	Localised	0.3-1.25	40.0	22.5	-	-	-
3	Not noticeable	Widespread	1.25-3.5	20.0	30.0	2.7	-	-
4	Minor	Substantial	3.5-4.5	13.2	47.1	92.3	58.8	14.7
5	Substantial	Extensive	7.5-20	-	0.2	5.0	41.2	83.0
6	Major	Nearly total	20-65	-	-	-	-	2.3
7	Building condemned		100	-	-	-	-	-
8	Collapse		100	-	-	-	-	-

Figure 2.1. Format of the DPM proposed by Whiteman et al [4]

In 1982, a first European version of this methodology was proposed by Braga et al [5] based on the damage data from Italian buildings after the Irpinia earthquake. This new version introduced the binomial distribution in order to describe the distribution of damage for a certain intensity and a certain type of building. The buildings were separated in three vulnerability classes (A, B and C) and a DPM was created for each of it. This method was also called "direct" method because the relation between building typology and observed damage is direct. [2]

This method was widely used in Italy and adapted to different seismic scales during the past decades. One of the last update of the method was made by Giovinazzi and Lagomarsino [6] in order to adapt it to the EMS-98 [1] scale. Some issues related to the "incompleteness" of the matrices, due to the lack of information for all the intensities, and the "vagueness" of the matrices, due to the qualitative description, have been solved by the same authors [6]. Concerning the first issue, a beta distribution instead of the previous binomial distribution and the application of the Fuzzy Set Theory reduced the problem. [2]

Even though the DPM proved to be an efficient and cost-effective method in the case of a large-scale study, many disadvantages can be noticed. First, the seismic intensity and the damage state are based on the same observations of the damages of a building stock which means that they are both deduced by the same judgement of an expert. Then in order to determine seismic vulnerability, a lot of buildings with the same ground characteristics and different earthquakes of all intensities are required, but the limited number of past earthquakes does not allow enough examples of strong earthquakes. Finally, the actual seismic hazard maps are defined in terms of PGA which means that a relation between seismic intensity and PGA needs to be found in order to apply this method to recent earthquakes. [2]

2.2.2 Vulnerability Index Method

The vulnerability index method developed in 1993 [7] has been widely used in Italy in the past years. It is based on a large data survey from the past earthquakes. This method is called "indirect", on the contrary of the DPM method, because the relation between the seismic action and the response of the building is evaluate through a vulnerability index. Some important parameters regarding the vulnerability of buildings are reported in a form, which is used during the survey in order to collect data about the damage state. This method was developed for the case of standard masonry buildings. The 11 parameters are related to the plan and elevation configuration, type of foundation of material quality. During the years, this form was adapted for different countries, type of buildings or type of analysis as illustrated by Brando et al [8], Aguado et al [9] and Ferreira et al [10]. In the case of churches, a specific form, the Italian Survey Form (ISF), was developed through the years and the visual inspection of damages caused by earthquakes. The following paragraphs indicate the evolution of this form, the actual procedure and the improvements that could be done. [2]

2.2.2.1 First versions of the Italian Survey Form

On the contrary to standard buildings, churches are characterized by particular elements. The aspect of non-structural elements does not exist as each element of a church is created in order to support a specific weight. After the observation of the damages created by the Friuli earthquake of 1976, it was observed that the response of churches to a seismic action is a recurrent phenomenon.

The description of the damages of structural parts called macroelements and their collapse mechanisms is similar in different churches. The response of the total structure can be deduced from the individual responses of each macroelement. Such elements are for example the façade, the bell tower, the apse or the chapels.

The first form created by Angeletti et al [11] in 1997 was composed of 16 indicators representing a possible failure mechanism of 8 different macroelements. Each indicator was illustrated by a drawing in order to better understand the failure. In order to fill the form, it was necessary to indicate for each of it: the presence or not of the macroelement, the damage level and the vulnerability of this mechanism through two indicators linked to the construction's weaknesses. These vulnerability indicators highlight the ability of the mechanism to occur. In this form, the damage level was divided in four grades: 0 no damage, 1 light damages, 2 fully developed mechanism and 3 severe damages / near collapse. The Figure 2.2 illustrate one of the mechanisms of the form. [12]

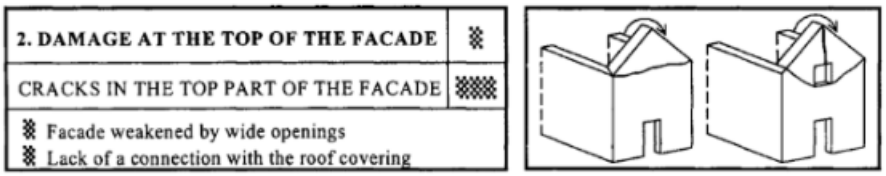

Figure 2.2. Example of one of the mechanism of the first form [12]

Some improvements of this form were made in 1998 by Lagomarsino et al [12]. These improvements first consist in the addition of two other failure mechanisms, the change in the mechanisms order in the form to improve the effectiveness of the inspection and the modification of the damage level scale. The second form composed of 18 mechanisms with the illustration description, the damages description and the vulnerability indicator are presented in Appendix A. Most of the damage mechanisms are related to one single macroelement well identified in the church such as the façade, while some others are related to different elements of the church such as the nave and the transept and take into consideration widespread cracking.

The main issue with the previous damage level scale was the difficulty to understand the relation between cracking or deformation and activation of the mechanism. The identification of precise damage level and thus the formation of technicians for post-earthquake survey was complicated. In order to improve it, the damage level scale developed by the European Macroseismic Scale EMS-98 [1] was adopted. This scale, illustrated in Figure 2.3, is composed of five levels which consider the structural and non-structural damages separately and with different importance. [12]

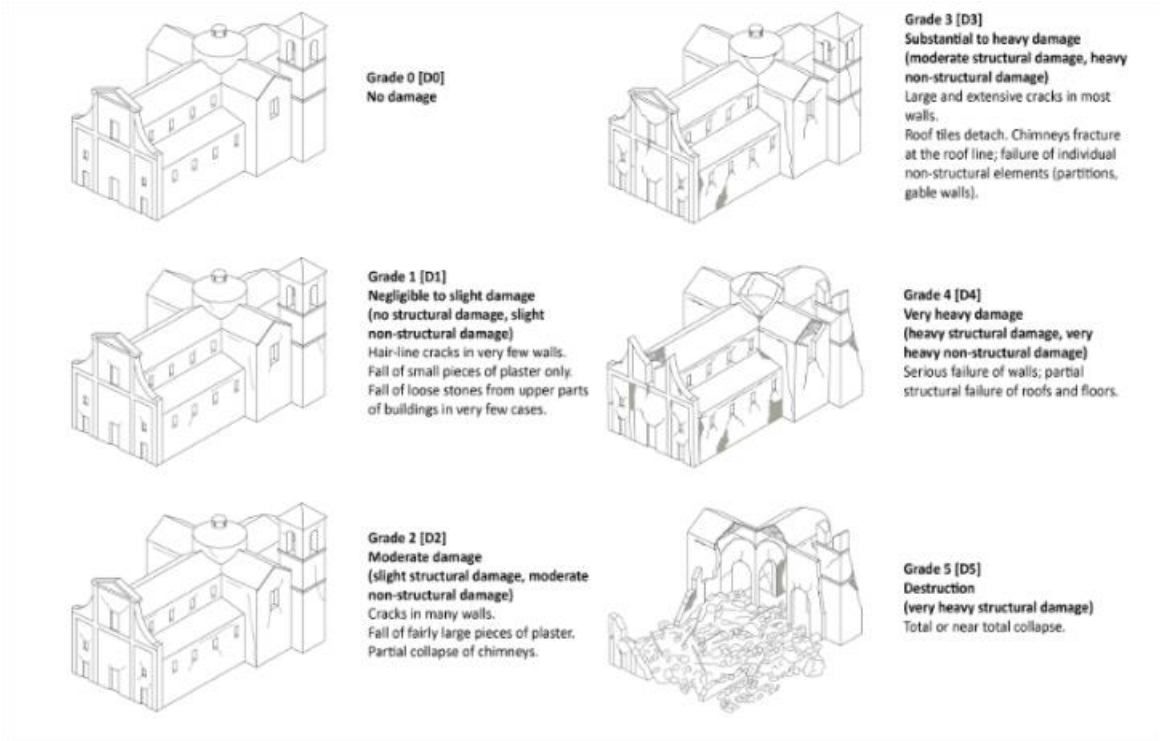

Figure 2.3. EMS-98 damage scale adapted to churches [13]

The information from the inspection, the damage grade and the number of vulnerability indicators, can thus be used in order to determine two important parameters: the damage index i_d and the vulnerability index i_v. The first one is a number between 0 and 1 measuring the mean level of damage of the church and is defined by Equation 2.2, while the second one is also a number between 0 and 1 linked to the tendency of the church to be damaged by the earthquake and is defined by the Equation 2.3. [12]

$$i_d = \frac{1}{5N} \sum_{k=1}^{18} d_k \qquad 2.2$$

Where d_k is the damage observed in the k-th mechanism and N is the number of mechanisms that can eventually activate.

$$i_v = \frac{1}{2N - m} \sum_{k=1}^{18} v_k \qquad 2.3$$

Where v_k is the number of vulnerability indicators of the k-th mechanism, N is the number of mechanisms that can eventually activate and m is the number of questions about the vulnerability for which there was no answer because of the inaccessibility of the area during the inspection.

The damage index as aforementioned is a useful tool during a post-earthquake inspection. It can hierarchise the buildings in function of the importance of the damages created by the earthquake. This is an essential step in the planning of potential interventions or preventive solutions for future earthquakes.

2.2.2.2 Actual version of the ISF

The last version of the form concerning churches' inspection was elaborated in 2005 by the Italian Guideline for evaluation and mitigation of seismic risk to cultural heritage with reference to technical construction regulation [3]. The first improvement of this new form is the increase of the number of failure mechanisms to 28, as shown in Appendix B. In this version, 9 macroelements can be easily identified as illustrated by Lagomarsino [14]: façade, nave, transept, triumphal arch, dome, apse, roof covering, chapel and bell tower. The other improvements concern the inclusion of a weight assigned to each mechanism, an increasing number of vulnerability indicators and the creation of anti-seismic parameters, which is described below.

The description of the 28 mechanisms is detailed in the appendix C of the Guideline. This appendix is divided in two part. The first part is composed of a list of all the possible vulnerability factors or anti-seismic measures for each mechanism. The anti-seismic measure is an element of the construction, initially present or added in interventions, which retain the activation of the mechanism. The second part of the appendix describes with drawings the failure mechanisms. The Table 2.2 shows an example of typical information that can be found in this appendix.

As for the previous version of the method, it is necessary to calculate a vulnerability index. However, the formula was adapted to the new parameters of the vulnerability assessment as shown in Equation 2.4:

$$i_v = \frac{1}{6}\frac{\sum_{k=1}^{28}\rho_k\,(v_{ki}-v_{kp})}{\sum_{k=1}^{28}\rho_k}+\frac{1}{2} \qquad 2.4$$

Where for each mechanism ρ_k is the weight of the mechanism and v_{ki} and v_{kp} are respectively the grades obtained by the vulnerability survey and the anti-seismic measures. These grades were assigned regarding the number of factors presents and their effectiveness as shown in Table 2.3.

Table 2.2. Example of data provided by the appendix C of the Italian Guideline for the mechanism 2 [3]

2 - Damage at the top of the façade	
Overturning of the gable, with horizontal or V-shaped cracking. Disaggregation of masonry or shifting of tie beams. Rotation of the trusses *Aseismic measures* • Presence of local connections to roof elements • Presence of roof braces • Presence of lightweight tie-beams *Vulnerability indicators* • Presence of large openings (rose window) • Presence of large and heavy towering gable • Rigid tie-beams in R-C, heavy roof covering in R-C	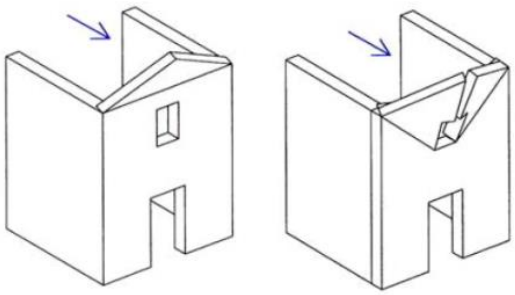

According to this method, if there is only one vulnerability indicator, it is possible to increase the vulnerability grade if we consider that it has a large influence on the failure mechanism. The weight of each mechanism is indicated in the appendix C of the Guideline. For some mechanisms, this weight is assigned to 1 or 0.5, and for other mechanisms the weight is chosen during the survey according to the dimensions of the macroelement concerned. In absence of the macroelement corresponding to the mechanism, the weight is assumed to be 0. The Table 2.4 resumes the corresponding weight to all the mechanisms.

Table 2.3. Evaluation of vulnerability grades for each mechanism [3]

Number of vulnerability indicators or anti-seismic measures	**Judgement of effectiveness**	**v_k**
At least 1	3	3
At least 2	2	
1	2	2
At least 2	1	
1	1	1
none	0	0

Table 2.4. Weight assigned to each mechanism [3]

Mechanisms	ρ_k
1, 2, 3, 5, 6, 7, 8, 9, 13, 14, 16, 17, 19, 21, 27, 28	1
4, 15	0.5
10, 11, 12, 18, 20, 22, 23, 24, 25, 26	$0.5 < \rho_k < 1$

As for the previous version of the form, a damage index is calculated. A new formula, which take into consideration the weight associated to each mechanism, is shown in Equation 2.5:

$$i_d = \frac{1}{5} \frac{\sum_{k=1}^{28} \rho_k \, d_k}{\sum_{k=1}^{28} \rho_k} \qquad 2.5$$

Where d_k is the damage grade assigned to the k-th mechanism according to the EMS-98 scale [1].

The vulnerability index and the damage index as calculated in the Italian Guideline can be used to determine the vulnerability of the church in different ways as explained in section 4.1.1.2.

2.2.2.3 Limitations of the Italian Survey Form and possible improvements

The Italian Survey Form aforementioned ([3]) is an efficient method regarding the assessment of Italian churches. However, it was shown in many studies that this method has some limitations regarding its application to other countries. As this method is subjective, it requires a complete analysis of the structure which is not always possible in a large-scale analysis. In order to improve the performance of the Italian methodology and to adapt it to fast survey or to other countries, some ameliorations are proposed by different authors.

The first proposition of modification of the method was proposed by Lagomarsino [15]. It is based on the fact that during the inspection only limited information is available, which induce the necessity of making a lot of assumptions. In order to reduce it, the new method considers that the vulnerability analysis of a church should start with the assignment of a typological vulnerability score V_0 equal to 0.89. This value was determined according to the Italian stock of churches studied after past earthquakes. This value of vulnerability score does not take into consideration the specificities of each church that could influence its seismic response. In order to compute such peculiar features, a rapid survey should be done by looking for example at the quality of materials, the structural regularity or the slenderness of structural elements. Thanks to this rapid survey, some modifier scores V_s can be identified in order to adapt the vulnerability score to the specific case of the church.

These modifier scores are reported in Lagomarsino [15] and are based on the judgement of experts. The final vulnerability value V is calculated according to the Equation 2.6:

$$V = V_0 + \sum V_s \qquad 2.6$$

The main problem with this method is in the fact that the direct summation of the modifier scores does not consider the possibility of interaction between two of them. Regarding this, the final result will be an overestimation of the real vulnerability of the church.

As aforementioned, the application of the ISF to other countries has highlighted some issues regarding the robustness of the damage index and the flexibility of the tool considering churches with macroelements not common in Italy. It was observed by the analysis of churches in New Zealand by Lagomarsino [16] that the damage index computed with the Italian method tends to be small in presence of severe damages. A first explanation of this phenomenon is that peaks of damages, which can occur as a severe damage in one single macroelement, are not accounted for. A second explanation considers that the attribution of the weight of each mechanism does not take into account the fact that for different churches types some macroelements are more important than in Italian churches. Moreover, in some cases macroelements can be present in several places, such as the chapels in New Zealand typical churches, and be only considered as one element. The lack of flexibility is based on the fixed number of mechanisms which were created according to the Italian stock of churches. However, it is possible to see in other countries some other macroelements, such as the choir in Portugal (Magalhães et al [17]), with a large influence on the vulnerability of the church. Regarding to the importance of this kind of macroelements, it is possible to add this new macroelement as a 29th mechanism. Regarding damages, when they do not correspond to a specific mechanism, it is possible to link them to the most similar damage mode or just describe them in the notes.

In order to solve these two principal issues, Lagomarsino [16] proposed a new methodology in order to assess the vulnerability of a church which is called the Church Assessment Form – Damage (CAF-D). In this method, a macroelement approach is also used. In total, 16 macroelements are taken into account as shown in the Table 2.5 and 10 seismic damage modes shown in Table 2.6 are considered. They were chosen in order to cover all the most recurring damages observed in churches. By associating each macroelement with the possible damage modes, in total 150 failure mechanisms are identified. In the presence of two similar macroelements, this method is well adapted to take into consideration the differences that might occur in both of them. With this principle, the flexibility issue of the ISF can be solved.

Table 2.5. Macroelements considered in the CAF-D form [16]

m	ID	Macroelements	*m*	ID	Macroelements	m	ID	Macroelements
1	Nc	Central Nave	7	D	Dome*	13	C	Chapels
2	Nr	Right Lateral Nave	8	L	Lantern	14	BT	Bell Tower
3	Nl	Left Lateral Nave	9	TA	Triumphal Arch	15	B	Belfry
4	F	Façade	10	P	Presbytery	16	Ch	Choir
5	Tr	Right Transept	11	A	Apse			
6	Tl	Left Transept	12	A/N	Atrium/Narthex			

*Dome or other standing-out element, over the height of the transept

Table 2.6. Seismic damage modes considered in the CAF-D form [16]

j	Structural elements*		Seismic damage modes
1	V	L, T	Out-of-plane of masonry walls
2	V	L, T	Out-of-plane at the top of walls
3	V	L, T	In-plane response
4	V	L, T	Rocking of multi macro blocks kinematism
5	V	L, T	Disintegration of masonry or hybrid mechanism**
6	H	–	Cracks in vaults, domes or diaphragms
7	H	–	Interaction between roof/diaphragms and walls
8	H	–	Damage in the roof structure
9	O	–	Damage due to interaction with other buildings or bell tower
10	O	–	Rocking of single blocks

* In this column, the structural elements relevant for each damage mode are listed

V: "Vertical structure", as the walls, which can be in longitudinal (L) and transversal (T) direction

H: "Horizontal structure" as every type of diaphragm

O: "Other buildings or the bell tower"

**Where "hybrid" means that is not clearly attributable to distinct in-plane or out-of-plane damage mode

In order to solve the robustness issue of the ISF, the CAF-D form has a new method to select the proper weight of each mechanism. Instead of having imposed weights and weights that should be selected regarding the dimensions of the macroelements, all the weights are assigned regarding some geometrical features of the macroelement considered. For example, the weight corresponding to the main façade is calculated by comparing the area of this façade to the global dimensions of the structure.

In this method, the damage grade can be attributed in different ways in function of the type of inspection. During a rapid inspection, usually in an emergency phase, a damage grade is assigned to each macroelement and then a global damage grade is assigned to the entire church. During a detailed inspection, a damage grade is assigned to each failure mode of each macroelement. Then the damage of each macroelement is computed and finally the damage grade associated to the church is also computed as for the rapid inspection. The detailed assessment of damage grade can be used as a tool in order to improve the capacity of evaluating the damage grade of the entire macroelement. The description of the method to compute the damage grade of the entire church is detailed in Lagomarsino [16]. This method also allows to attribute a damage index in both longitudinal and transversal direction and to take into consideration the peak of damage.

2.3 Analytical methods

The evaluation of seismic hazard in terms of spectral ordinate instead of macroseismic intensities or PGA has developed new methods to assess the seismic vulnerability of buildings. These methods, called analytical methods, give more detailed vulnerability assessment with direct physical meaning than empirical methods. It is thus possible to use analytical methods to do parametric studies, which aim to define or calibrate urban planning, retrofitting and other similar initiatives. [2]

2.3.1 Collapse Mechanism-Based Methods

In order to determine whether a mechanism will form, and damages occur, some methods using collapse multipliers were developed. These methods were applied a lot to masonry buildings. The first method, called VULNUS uses the fuzzy-set theory and the definition of collapse multipliers defined by Bernardini et al [18]. A first multiplier I_1 is defined for the in-plane behaviour of the structure by considering the shear failure at the ground level. This multiplier is the ratio of the in-plane shear strength of the system of walls to the total weight of the structure as explained below:

$$I_1 = \frac{\min(V_x, V_y)}{W} \qquad 2.7$$

Where V_x and V_y are the strength at mid-storey height of the ground in the x and y direction and W is the total weight of the structure.

A second multiplier I_2 is defined for the out-of-plane behavior of the structure. This multiplier is the ratio between the out-of-plane flexural strength of the most critical wall and the total weight of the structure. The evaluation of this multiplier considers both the resistance of vertical and horizontal strips. [2]

The second method is called FaMIVE (Failure Mechanism Identification and Vulnerability Evaluation) and it is also based on collapse multipliers. A static equivalent analysis aims to predict the ultimate load factor of the lateral loads which activate a specific failure. A number of possible out-of-plane, see Figure 2.4, and in-plane failure mechanisms are assumed, and the most likely mechanism is identified as the one with the lowest capacity. [19]

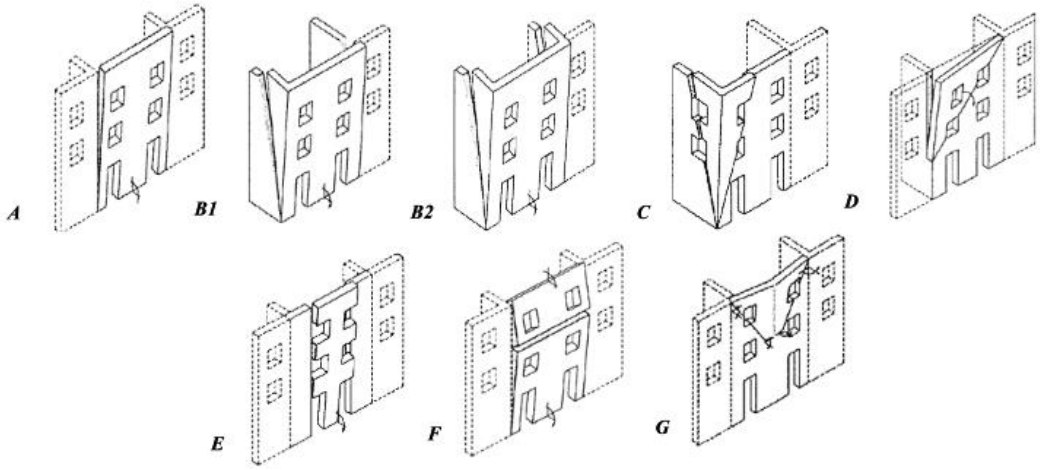

Figure 2.4. Examples of out-of-plane failure mechanisms [2]

One of main issues of these two methods is the fact that the uncertainties of geometry and material properties are not considered in the models. The second problem regarding FaMIVE method is the absence of clear relation to calculate the probability of exceeding a given limit state. This problem is not present with the VULNUS method; however, it is only possible to obtain the probability of damage for the collapse limit state. [2]

2.3.2 Capacity Spectrum-Based Methods

The Capacity Spectrum Method, first developed by ATC-40 [20], aims to find the performance point of a building by finding the intersection between an acceleration-displacement spectrum, representing the ground motion, and a capacity curve, representing the horizontal displacement of the structure under increasing vertical load. In order to facilitate the comparison of the two curves, the capacity curve is converted to the spectral base according to the modal properties of the building. The demand spectrum can be reduced to take into consideration damping or duration effects. In order to find the performance point, Freeman and Fajfar developed two different methods: respectively the capacity spectrum method (CSM) and the N2 method, which can be used. [2], [21]

2.3.2.1 **Capacity spectrum method (Freeman[20])**

The method developed by Freeman [22] consists in:

1. Developing a relation between the base shear and the roof floor displacement known as the pushover curve;
2. Converting the pushover curve to a capacity diagram by using the modal parameters of the structure;
3. Converting the elastic response spectrum from the standard pseudo-acceleration a versus natural period T format to the a-d format where d is the deformation spectrum ordinate, in order to obtain the demand spectrum;
4. Plotting the demand spectrum and the capacity curve in the same graph in order to determine the performance point and thus the displacement demand;
5. Converting the displacement demand to a global displacement and individual component deformation to compare them to the limiting values for the specified performance goals.

The steps 1 to 3 and 5 will be detailed for the specificities of the cases studies in section 4.2.1, while the step 4 is detailed below.

The performance is obtained through an iterative process where the changing parameter is the damping of the demand spectrum. This damping is first assumed to be 5%. The Italian Circolare [23] recommend assuming as first performance point the displacement corresponding to an equivalent elastic structure with the same initial stiffness as the real structure as illustrated in Equation 2.8.

$$d_{max}^{*(0)} = d_e \qquad 2.8$$

Considering all the values under this first performance point, an equivalent bilinear curve to the capacity curve in energy terms is calculated. In order to determine this new curve, the first slope is assumed to be tangent to the capacity curve, which means that there are identical initial stiffnesses. Then the second slope is calculated in order to have an equality between the two areas subtended by the curves. The Figure 2.5 represents this bilinearization in the case of a capacity curve given in a F-d format. In order to convert it to a a-d format, the force should be divided by the mass.

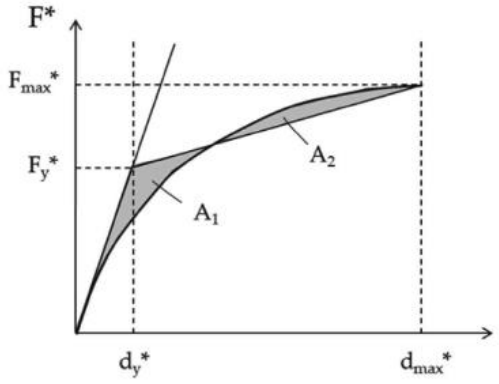

Figure 2.5. Equivalent bilinear curve according to the Capacity Spectrum Method

From this bilinear curve, it is possible to determine an equivalent damping ratio according to the following equation:

$$\xi_{eq}^{(1)} = k\frac{63.7(F_y^{*(0)}d_{max}^{*(0)} - F_{max}^{*(0)}d_y^{*(0)})}{F_{max}^{*(0)}d_{max}^{*(0)}} + 5 \qquad 2.9$$

Where *k* is the coefficient that take into consideration the dissipative capacity of the structure – in the case of masonry churches, the structure has a low dissipative capacity and thus *k* is equal to 0.33 – and the other variables are defined in the previous figure.

With this new damping ratio, it is possible to calculate the coefficient of reduction to apply to the demand spectrum. This reduction factor η can be determined according to the Equation 2.10. The demand spectrum is then multiplied by this factor and the intersection of this new spectrum with the capacity curve define the new performance point. If the displacement corresponding to the new performance point is close enough to the one of the previous iteration according to some criterion defined in function of the structure, then it is defined as the final one. Otherwise a new iteration should be performed with the definition of a new bilinear equivalent curve. The Figure 2.6 resumes the entire procedure to determine the performance point.

$$\eta = \sqrt{\frac{10}{\xi_{eq}^{(1)} + 5}} \qquad 2.10$$

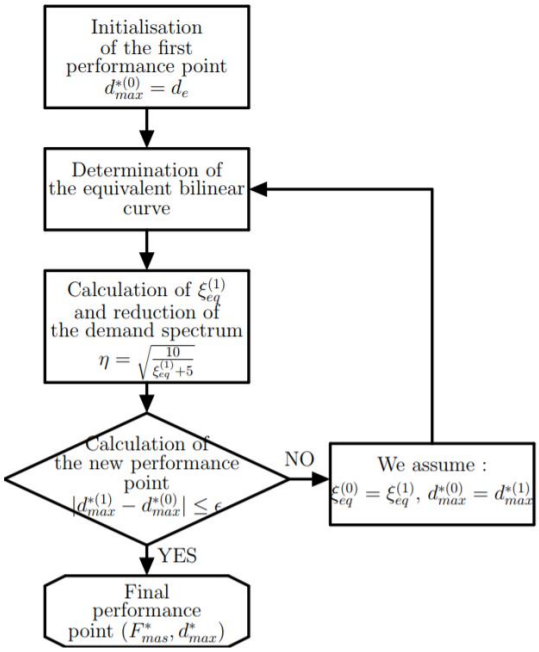

Figure 2.6. Explicative diagram of the Capacity Spectrum procedure

2.3.2.2 **N2 Method (Fajfar** [24]**)**

The N2 method, developed by Fajfar in the mid-1980s, is an evolution of the Q-model developed by Saiidi and Sozen [25]. This method is a variant of the capacity spectrum method developed by Freeman based on inelastic spectrum. This inelastic spectrum is determined from a typical smooth elastic spectrum. The general steps of the method are similar to the CSM; however, the determination of the performance point is different. The steps of the method, described in Fajfar (2000) [24], are given below.

1. Acquisition of the data regarding the structure and the elastic spectrum;
2. Conversion of the elastic spectrum in the a-d format and determination of the inelastic spectrum by using the ductility factor μ, which is the ratio between the maximum displacement and the yield displacement, and the reduction factor R_μ;
3. Determination of the base shear- top displacement;
4. Determination of an equivalent single degree of freedom model. Several methods can be used in this step in function of the system and the user;
5. In function of the elastic period of the equivalent SDOF model, the performance point can be found as illustrated in Figure 2.7 and with the equations 2.11 and 2.12.

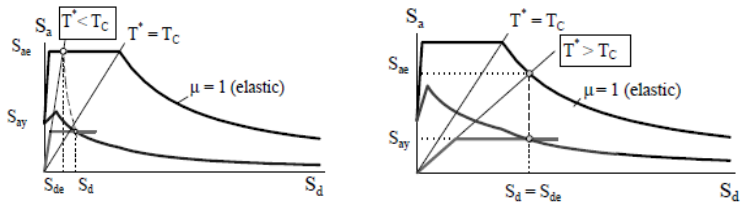

Figure 2.7. Determination of the performance point in function of T*

$$S_d = \frac{S_{de}}{R_\mu}\left(1 + (R_\mu - 1)\frac{T_C}{T^*}\right) \qquad T^* < T_C \tag{2.11}$$

$$S_d = S_{de} \qquad T^* \geq T_C \tag{2.12}$$

6. Conversion of the displacement demand to a global displacement and individual component deformation to compare them to the limiting values for the specified performance goals.

The main differences with the previous method are the use of an inelastic spectrum, the definition of an equivalent SDOF model and the method to determine the performance point. According to this, the steps 1, 2 (only the conversion in a-d format), 3 and 6 of this method are equivalent to the steps 1,2,3 and 5 of the CSM. The determination of the equivalent SDOF model will be detailed for these case studies in section 4.2.1.

3. PRESENTATION OF THE CASES STUDIED

3.1 Catalonia

Catalonia is a Spanish region located in the north-east of Spain as shown in Figure 3.1. This region is surrounded by the Pyrenees in the North, the Mediterranean Sea in the East and the region of Aragon in the West. This territory has been invaded during the middle age by numerous civilisation such as the Muslims, the Carolingians or the region of Aragon. These changes of population and civilisations deeply influenced the Catalan art and in particular the architecture.

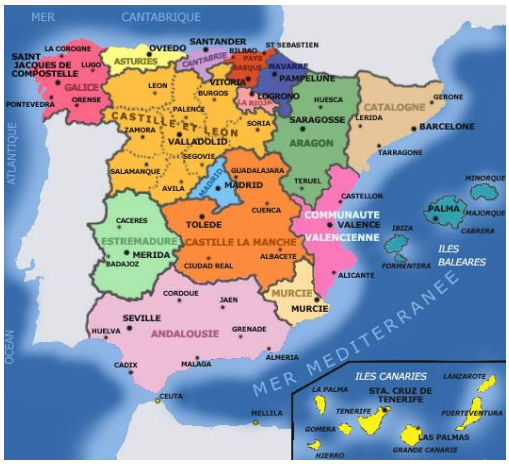

Figure 3.1. Location of Catalonia

3.2 The Romanesque style

The Romanesque style was developed during the middle-age, after the decline of the Greco-Roman civilization. This architecture was the first European style; however, its development and characterization were influenced by the location of the construction and thus the corresponding regional architectural style. The Carolingian's conquest of Europe induced the diffusion of this art to all the conquered countries. The period associated to the Romanesque style is not well established and includes several centuries between the 10th and the 12th centuries.

A Romanesque church can be characterized by a barrel vault in the central nave, which is a semi-cylinder supported by pillars or walls. The creation of this vault induces a large horizontal thrust in the wall which is supported by buttresses and an important thickness of the walls. The central barrel vault is often supported by lower cross-vaulted aisles. Because of this system, it is not possible to have large opening in the side walls, which create the darkening of the church. The plan of Romanesque churches is most of the time either a basilical plan without transept and with one to three naves or a Latin cross with a nave and a large transept. [26], [27]

The typical façade of a Romanesque church can be divided in three parts: the first part is composed of a unique portal with a rounded shape, the second part contains several small windows or a rose window, and the last part is a gable. However, some façade can also be vertically divided in three parts: the central one is the largest and is equivalent to the façade described early, the two external part are bell towers. This second type of façade is from the French region of Normandy, but it is widespread in all Europe. [26], [27]

The Romanesque style is present in all Catalonia. Moreover, it is possible to notice the presence of the first Romanesque style which was influenced by Lombardy and can be characterized by a masonry with small and irregular stone and few ornamentations. This style is mostly located in the north of Catalonia, in what was called the Old Catalonia. The later Romanesque style can be observed in all the Catalonia and is characterized by an external regular stone masonry which gives a feeling of sumptuousness to the church. [27]

3.3 Seismicity and geology of the region

Catalonia is a region with a moderate seismic activity. However, in the past some earthquakes with an intensity higher than VII have been observed in this area. These earthquakes were strong, with a return period of 500 years. The program SISMICAT implanted in the region has studied the seismic risk of the whole area. According to the information from the past earthquakes, a map of the probable intensity of earthquakes that could occur in each city has been created considering also the soil effect in the propagation of the earthquake as shown in Figure 3.2. The two churches studied in this report are situated in zones of intensity VII. This program includes the study of the seismic hazard of Catalonia, the vulnerability assessment of the buildings in this area and the emergency planning of the cities concerned. [28]

The epicenter of the largest earthquakes recorded in Catalonia are illustrated in Figure 3.3. La Seu d'Urgell is located between the epicenters of two important earthquakes, namely those of years 1373 and 1428. These two earthquakes were close enough to generate damages in the church. In order to find the maximal earthquake's intensity of this city, both earthquakes should be studied. In the case of Vilabertran, the city is located close to the epicenter of the 1428 earthquake. This earthquake is thus likely to be responsible of the maximal intensity corresponding to the church.

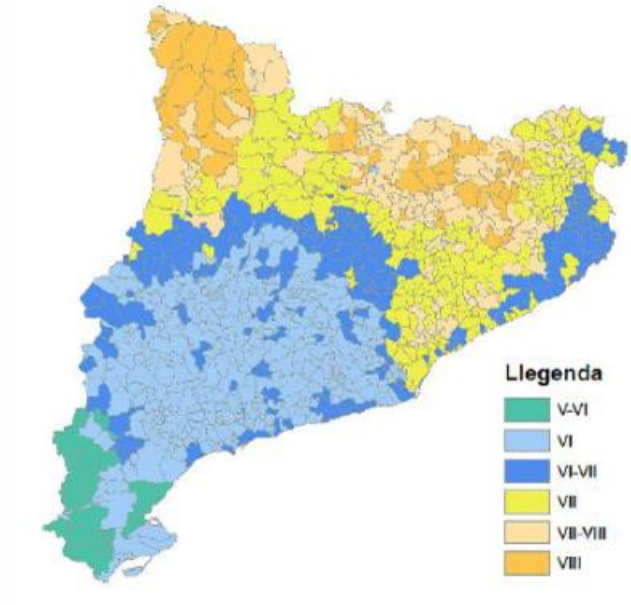

Figure 3.2. Map of seismic intensity in Catalonia [28]

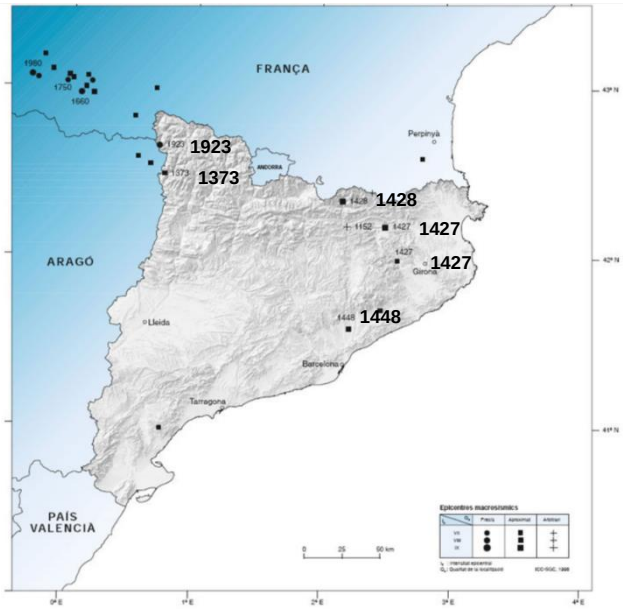

Figure 3.3. Map of the largest earthquakes of Catalonia [29]

The 3rd of March 1373, an earthquake of intensity VIII-IX occurred in the north of Ribagorça, a Pyrenean city. According to the numerous documentation found in cities close to the epicentre, this earthquake caused a lot of damage in the region. The intensity corresponding to the damages has been identified and is illustrated in the intensity map of the Figure 3.4. According to this figure, the intensity recorded in La Seu d'Urgell for this earthquake is VI-VII while in Vilabertran it is V-VI. [30]

Figure 3.4. Intensity map of the earthquake of 1373 [30]

In 1427 and 1428, several earthquakes of intensity higher than VIII occurred. The most intense occurred the 2nd of February 1428. This earthquake was the most important of this region and caused severe damages in many town and buildings. As for the precedent one, documentations from the damages of the surrounding cities helped to understand the intensity of the earthquake. The Figure 3.5 shows the intensity map of this earthquake. It is possible to notice that the intensity in La Seu d'Urgell is VI-VII while the intensity in Vilabertran is VII.

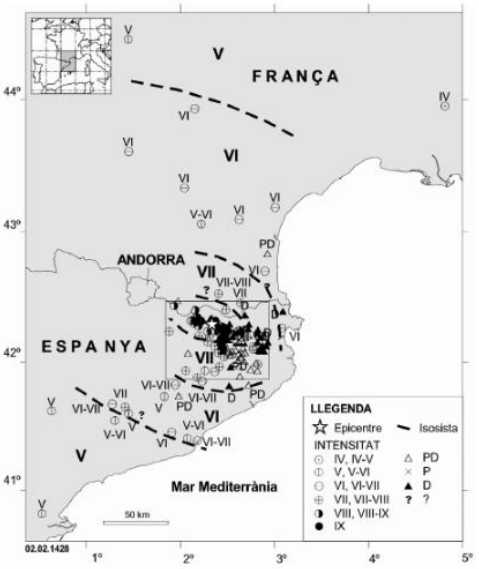

Figure 3.5. Intensity map of the earthquake of 1428 [30]

As the soil effect is an important parameter in order to determine the propagation of the wave of an earthquake, a study has been done to identify the type of soil in Catalonia. The Figure 3.6 illustrates the repartition of the type of soil according to the Eurocode classification [31]. In this classification, 6 types of soil are identified: hard rock (A), soft rock or rigid soil with a depth lower than 100m (B), soft rock or rigid soil with a depth higher than 100m (B'), soft soil with a large depth (20-100m) (C), very soft soil with a depth (20-100m) (D) and soft soil with a small depth (5-10m). According to this map, La Seu d'Urgell has a soil of type A while Vilabertan has a soil of type B'. However, specific geological and geotechnical studies are necessary for a more accurate identification of the soil types on which the studied buildings are founded.

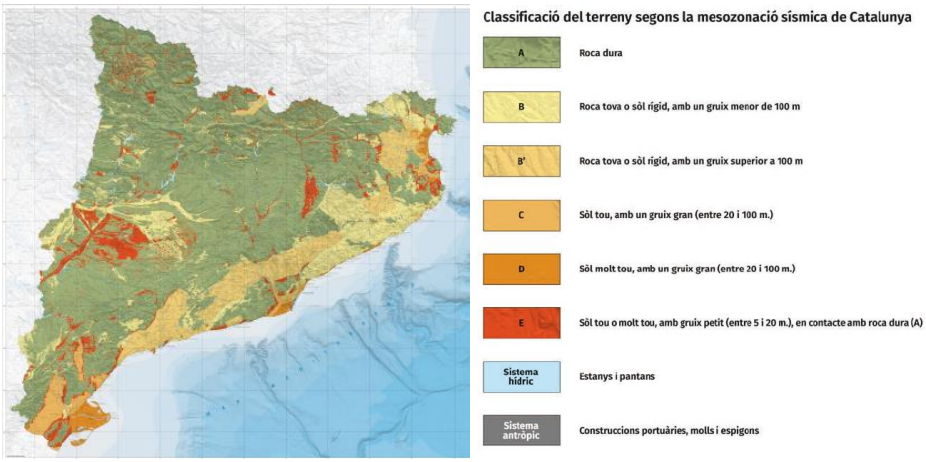

Figure 3.6. Map of the type of soil of Catalonia [32]

3.4 La Seu d'Urgell

The city of La Seu d'Urgell is a municipality from the region of Lérida in Catalonia. It is the comarca of Alta Urgell. The city is in the south of the Pyrenees, close to Andorra and the French border, as shown in Figure 3.7. Hercules l'Egipcia founded the city in 1699 BC in a place called Castellciutat. In 527, the first bishop Sant Just was selected and after this the episcopal has been occupied without interruption. Castellciutat was destroyed in 793 during the expedition of the muslim Abd-al-Malik who wanted to punish the region of Cerdanya for heresy. After this destruction, a new city called La Seu d'Urgell was created close to the ruins of the previous one with the help of Charlemagne. During the reconstruction of the city, a new cathedral was built at the actual location of the cathedral of La Seu d'Urgell. This cathedral is located in the old city center and the church Santa Maria is surrounded by the cloister and other religious buildings as shown in Figure 3.7. The

cathedral is composed of three different churches: Santa Maria, the main church, Sant Pere and Sant Miguel, two secondary churches. The following report will only focus on the main church of Santa Maria. [33]

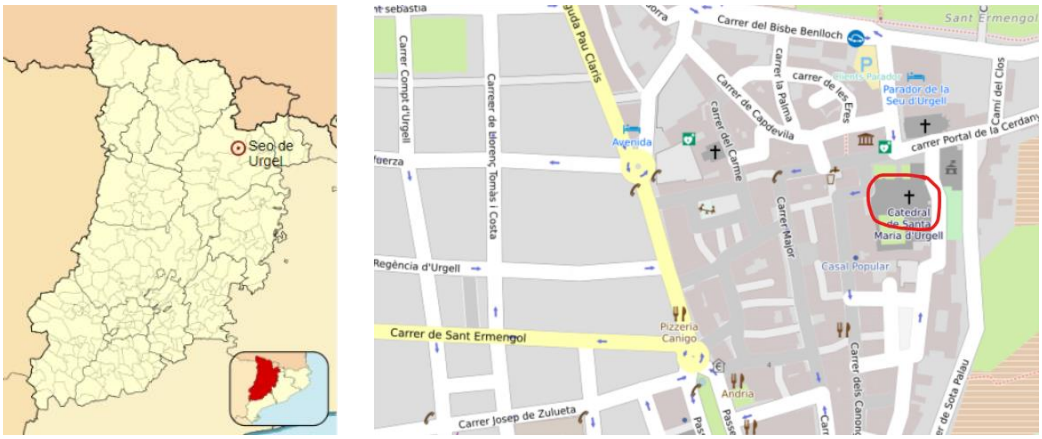

Figure 3.7. Location the cathedral of La Seu d'Urgell

3.4.1 Historical survey

The actual cathedral Santa Maria of La Seu d'Urgell is the fourth cathedral of this city. The first cathedral was in Castellciutat before the destruction of the city by Abd-al-Malik in 793 and the three others were built in the actual location. From these three churches, one was pre-Romanesque and the two others were Romanesque churches. [34], [35]

Information concerning the first cathedral of Castellcuitat is limited or inexistent. Some archeological surveys have proved its existence, but the actual constructions do not allow deeper inspection.

On the contrary, the second cathedral is documented, and some official documents help to understand how and when it was built. This cathedral was built around 819, close to the ruins of the previous city destructed by the Muslims. It was consecrated by Charlemagne and his son Louis le Pieux in 819. The exact date of this consecration is contested by many historians who consider the official document as false and the real date of the consecration might be in 831 or 839. During 823, Charlemagne supported the creation of a new episcopate situated in La Seu d'Urgell, as the previous one was situated in the destroyed city of Castellciutat. [35], [36]

According to the study of similar churches in the region, it is assumed that this church was constructed in pre-Romanesque style. The Figure 3.8 represents a hypothetical reconstruction of this cathedral and the representation in background of the actual church. It is composed of three naves, with a central nave larger than the two others, three apses and no transept. The apses have a rectangular shape. It is possible to notice that none of the walls or pillars are in the same location

in both churches, which means that the foundations of these two churches are not the same. According to this, it is possible to assume that this first construction did not impact the actual one. The pre-Romanesque church remained until the new construction led by bishop Sant Ermengol. [35]

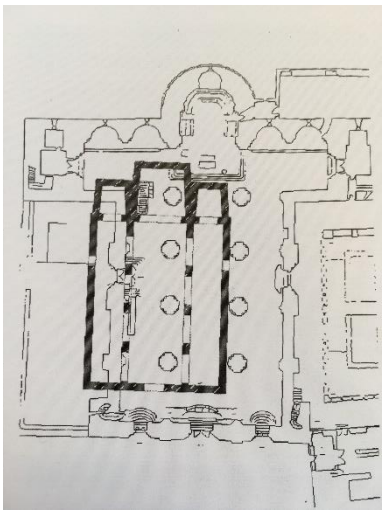

Figure 3.8. Hypothetical reconstruction of the second cathedral of La Seu d'Urgell [35]

Bishop Sant Ermengol decided in November the 8th, 1010 to restore the canonical life inside the cathedral. This bishop is also known for the large campaign of public work he started during his pontificate. A period of euphoric construction started with the creation of bridges and roads and more specifically with the creation of a new Romanesque church. This first Romanesque cathedral of La Seu d'Urgell was built according to construction and ornamental's rules from the Italian region of Lombardie. This church was consecrated in 1040, after the death of bishop Sant Ermengol. The Figure 3.9 shows a possible representation of the third cathedral of la Seu d'Urgell. It is possible to observe that the walls seem to be identic to the pre-Romanesque church. The main difference can be found in the shape of the apses. The three apses are circular and the central one is larger than the two others. Moreover, two circular transepts were added in both sides of the church. [35], [36]

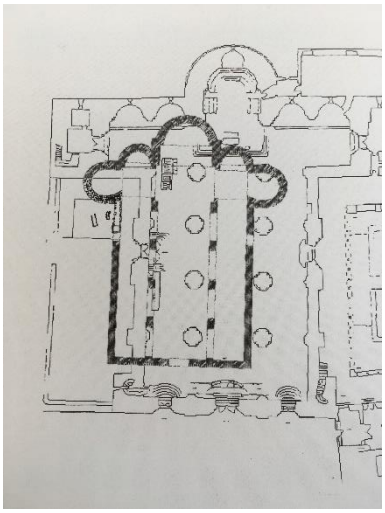

Figure 3.9. Hypothetical reconstruction of the third cathedral of La Seu d'Urgell [35]

At the beginning of the 12th century, the building was in really bad state of conservation. Indeed the bishop Sant Ot decided to build a new cathedral. In order to obtain enough money to start the construction, he asked for the financial help of the believers. Numerous donations were made during the whole period of construction to finance the project. Sant Ot died in 1122, few years after the beginning of the construction. The new cathedral was larger than the previous one and in order to maintain the functionality of the place of worship, it was not built in the position as the first Romanesque church as illustrated in Figure 3.9. The construction started with the south transept and the apse, which are the further parts from the old church, and then the construction was made on the top of it. [35]

Unfortunately, the construction was really slow and after more than 50 years the vaults were still not built. In 1175, bishop Arnau de Preixens decided to hire a new architect in order to resume the construction. The Italian architect Ramon Llambard was selected to finish the cathedral. Llambard was in charge of the construction but also of the administration of the building, which was new for an architect. Even though the cathedral was built in more than 50 years with different people in charge, the construction is homogenous and coherent with the initial plan of bishop Sant Ot. The wars against the vicomte of Castelbo from Andorra stopped the construction in 1195, before the completion of the two towers and the dome. [35]–[37]

After the end of its construction, some modifications and restorations were done. The first one occurred in 1567, the vaults and the walls of the cathedral were covered of white plaster. During the same century, some fortifications were constructed because of conflicts with the surrounding cities. The cathedral became the place of security of the city and was supposed to be able to resist to an external attack. Another important modification was planned in 1776 by the architect Antoni

Ginot. His objective was to turn the cathedral to baroque style. As the openings of the naves and the side walls were too small to do it, this modification was not possible. The only change that Ginot made was the modification of some opening in the transept's walls. In the 20th century, the architect Puig i Cadalfach led a new program of restoration. His objective was to restore the cathedral as it was during the middle age. Some of the white plaster from 1567 was removed from the walls but the vaults are still covered with it. [35], [37]

3.4.2 Geometry of the church

The church Santa Maria de La Seu d'Urgell (see Appendix C) is composed of three naves and a Latin cross plan (the previous cathedral did not have a Latin cross plan but a basilical plan). The central nave has a width of 5 m while the two externals have a width of 3 m as shown in Figure 3.10. The naves are separated by four pillars in each side with a cross section. These pillars are thick, 1.4 m, and 6.75 m height, which means that they are not slender and not supposed to deform a lot. The central vault supported by the pillars is a barrel vault and arches are present between each pillar in order to help supporting the weight of the vault. The side vaults are pointed vault with a small range and the side walls are thick, 0.85 m. Few openings are present in the side walls which reduce the risk of shear mechanism.

Figure 3.10. Plan and elevation of La Seu d'Urgell

As shown in Figure 3.11, the main façade is composed of a central part with a large door and a lot of small windows in the upper part and two symmetric sides with a tower. The thickness of the façade is important, 1.1 m. We will consider in the following study that the two towers are not part of the façade as their thickness is much larger, which could induce a different stiffness and thus a different comportment during an earthquake. The most remarkable element of the façade is the presence of a bell tower on the top of the gable. The bell tower in leaning in the façade wall but also

in the central vault. It is characterized by the presence of a lot of openings and slender elements such as thin pillars.

Figure 3.11. Main façade of La Seu d'Urgell

The church also contains a transept which is delimited on both sides by a tower. Regarding the size of the church this transept can be considered as not significant as the façade walls are part of the external towers. The vault of the transept is similar to the rest of the building, it is a barrel vault. A large circular apse is present in a central part of the transept, surrounded by four small chapels. These chapels are not visible from the outside of the church as the external wall mask their shape. The Figure 3.12 shows the external view of the apse and the presence of the tower at the extremity of the transept. We can notice in this picture and in Figure 3.10 the presence of a dome in the intersection between the nave and the transept. A drum and a heavy gable are sitting on top of the dome. The gable contains two small bells and is not center in the dome.

Figure 3.12. External view of the transept and the apse of La Seu d'Urgell

3.4.3 Actual state of conservation

The walls of the cathedral are made of three-leaf masonry. The two external leaves are in good masonry with rectangular stone of regular shape. According to the Italian Circolare [38], this type of masonry can be considered as "Matura a blocchi lapidei squadrati", which means square stone masonry. The internal leaf is probably a rubble masonry and can be classified according to the Circolare as "Matura in pietrame disordinata", which means rubble masonry with different size and shape of stone. The pillars are also made of good stone masonry. It was noticed during the inspection of the building that quality of the materials composing the church is good and they are still in good state of conservation. However, it was not possible to see the state of conservation of the vault's stones as they were recovered by plaster.

Even if the general aspect of the church is good and no severe damage has been noticed, some noticeable damages have been observed inside and outside the church. The crack mapping of Figure 3.13 and Figure 3.14 illustrate the location of some of these damages and the Appendix D illustrates these damages.

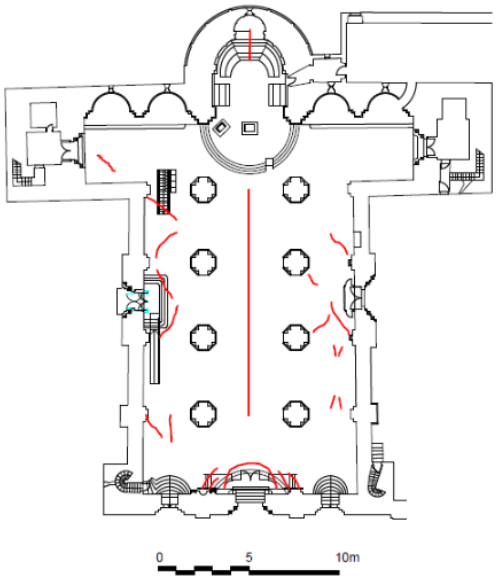

Figure 3.13. Crack mapping of the vaults of the cathedral La Seu d'Urgell

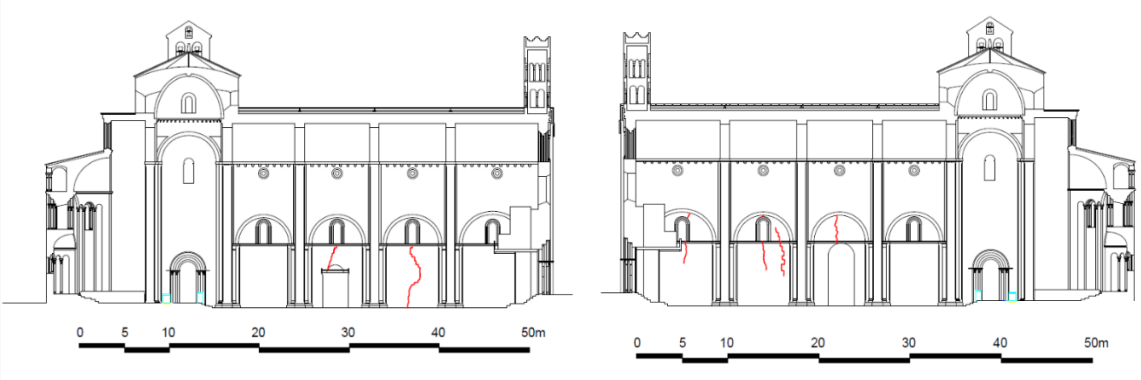

Figure 3.14. Crack mapping of the walls of the cathedral La Seu d'Urgell

The most significant damage concerns the tower leaning in the front façade. Indeed, this bell tower is leaning both in the façade and in the central vault. The resistance of the façade and the vault is significantly different and the vault cannot resist to the weight of the tower, inducing the presence of crack in the vault around the location of the tower as shown in Figure 3.15 and Figure 3.13. Because of this phenomenon, a deformation of the top of the tower can also be observed as illustrated in the Figure 3.15.

Figure 3.15. Damages due to the presence of the bell tower

The second phenomenon that can be observed in La Seu d'Urgell is the transversal deformation of the nave. This is the deformation of the central nave and the lateral walls due to the self-weight of the vault or some extra loads from the roof. In this case, during the inspection an important deformation of the vault and in particular of the arches that help supporting the vault has been noticed. Figure 3.16 illustrates this deformation. This deformation was accompanied by the presence of a crack along the whole central vault as shown in Figure 3.13.

Figure 3.16. Transversal deformation of the central vault of the nave

Some minor cracks have been noticed in the vault of the aisles as illustrated in the crack mapping of Figure 3.13. These cracks were thin and superficial. However, it seems that they are present in almost all the vaults. It can be explained by the load of the vault itself or some extra load due to the central vault and its deformation. Minor cracks are also present in some of the side walls as illustrated in the crack mapping of Figure 3.14. The origin of these cracks is not determined but it could be due to soil settlement or to past seismic action. The last location of cracks in one of the façades of the transept. This façade is vertically cracked as shown in the Appendix D.

3.5 Vilabertran

Vilabertran is a small town of the north of Catalonia, in the canton of Alt Emportada. This town of 907 inhabitants is located close to the city of Figueras as shown in Figure 3.17. In the middle-age, Vilabertran was in the commercial Roman road going from Barcelona to France. It was the easiest and fastest way to cross the region of Emportada. Two remarkable elements are present in the city center: the Torre d'en Reig and the canonical Santa Maria de Vilabertran composed by a church, a cloister and an abbey palace. [39]

Figure 3.17. Location of Vilabertran

3.5.1 Historical survey

The first document related to the church Santa Maria de Vilabertran mentions the presence of a hamlet and its church during the king Lothaire's reign (954-986). This small church was a modest pre-Romanesque construction in an isolated area that did not contain parish. During the Xth century, the church belonged to a devoted family. [37], [39], [40]

During the second half of the 11th century, the priest Pere Riguall decided to establish a canonical life in the city of Vilabertran in order to create a new religious community. In 1060, the clerics started to gather around Pere Riguall. Between 1066 and 1069, some rich people such as Guillem i Ponc donated to the priest in order to increase the properties of the religious community. In 1069 Pere Riguall was designed the person in charge of the administration of the church, the clerical life and the lands of the monastery. [37], [39], [40]

In 1080, the priest decided to start the construction of a new church for the monastery. This church is the actual Santa Maria de Vilabertran. This church would be dedicated to the cult of the Virgin Mary and the canonical life would be ruled by the Sant Augustin's order. In 1100, the church was officially consecrated, and the pope confirmed the presence of the Augustin's order in the monastery of Vilabertran. According to this, the clerics were allowed to elect their own administration and elected as first official priest Pere Riguall. [37], [39]

During the 12th century, the popes Pascual II and Alexandre III confirmed twice in 60 years the possessions of Santa Maria de Vilabertran and other churches of the region to the monastery of Vilabertran. During this time, they also confirmed the legitimacy of the Augustin's order in this monastery. [39]

In autumn of 1295, the wedding of the king Jaime II with Blanche of Anjou was celebrated in the canonical church Santa Maria de Vilabertran. These years were the most prosperous of the monastery. The church made a good impression on the queen Blanche, and she decided later to donate to the monastery.[37]

After this flourishing period, the region of Catalonia was in danger because of pirates coming from the Mediterranean Sea. In order to protect this church, king Pere III allowed the bishop to create some fortifications in the monastery. [37]

During the 16th century, the mentalities changed, and the Augustin rules were not respected anymore. The decline of this order started in Germany and it was followed by Spain few years later. In 1592, pope Clement III sent the order to secularize all the Augustin's communities of Catalonia. Starting from this, the monastery became a secular collegial composed of a prior and 14 monks. The number of monks was reduced to 12 in 1625. [37], [39]

During the Roussillon's campaign of 1794, the region of Alt Emportada was occupied by the French army. Because of it, the villager of Vilabertran escaped from the city and left it to the occupying forces. The church of the monastery, as other monuments of the region, was vandalized. [39]

After the Spanish Civil War, in 1941, restoration works were done in the monastery in order to preserve and restore it after the destruction of the past centuries. Figure 3.18 illustrates the state of the main façade before the restoration work. [39]

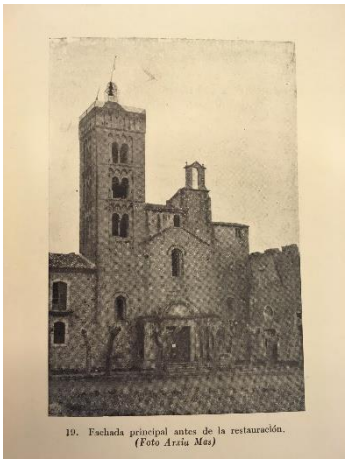

Figure 3.18. Main façade of Santa Maria de Vilabertran in 1941, before the restoration [39]

3.5.2 Geometry of the church

The church of Santa Maria de Vilabertran (see Appendix E) has a Latin cross plan and is composed of three naves characterized by a width of 8 m for the central one and 3 m for the two aisles as illustrated in Figure 3.19. 8 pillars of a thickness relatively high, 2 m, and a height of 3.5 m separate the naves. According to these numbers, the pillars cannot be considered as slender. The central vault is a barrel vault supported in some points by arches connecting the pillars. Before the beginning of the vault, the clerestory wall contains some small windows as illustrated in the elevation of Figure 3.19. The vaults of the aisles are semi-barrel vaults with a short span. The side walls are really thick, 1.5 m, with few openings, the only openings are the two doors that allow to go to the cloister and one of the external chapels.

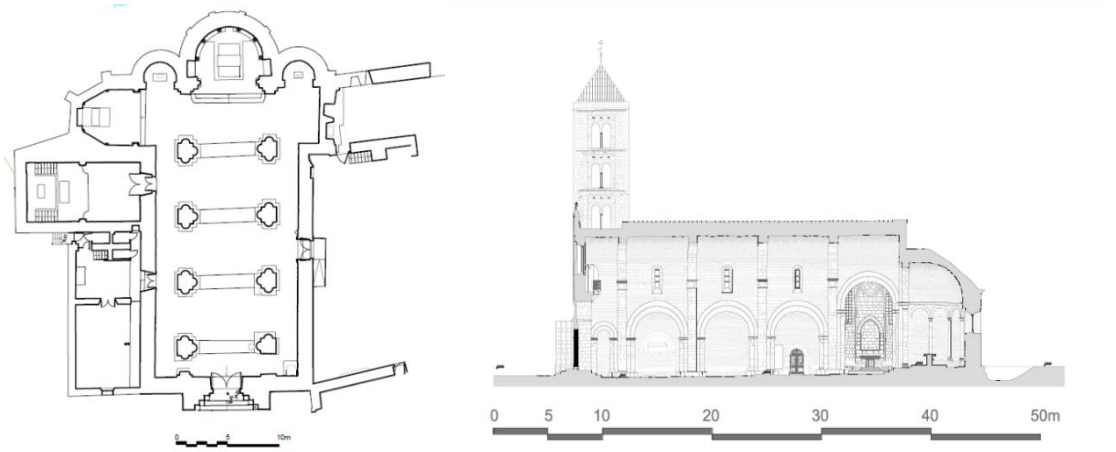

Figure 3.19. Plan and elevation of the church of Santa Maria de Vilabertran

The main façade of the church can be divided in three parts: the central part and the two towers. The central part contains a door, whose shape has been changed after the construction. The original shape was circular in the top and the actual shape is rectangular. This transformation can be easily seen in the Figure 3.20. We can also notice the presence of a small windows in the upper part of the façade. The two bell towers are situated on both sides of the façade. Only one of them was finished. It is possible to observe that the tower contains many large openings and is supported by the main façade, the first pillar of the nave and the first vault of the aisle. Initially, this façade was supposed to be a typical Romanesque façade with a style imported from Normandy as explained in section 3.2.

Figure 3.20. Main façade of Santa Maria de Vilabertran

The transept of the church is not significant regarding the dimensions of the church and it is also not symmetric. The North transept is circular and has two buttresses while the South transept is rectangular with dimensions much smaller than the other one. The church is also composed of a circular apse and two small circular chapels.

The church is surrounded by the monastery and its outbuildings such as the cloister, the dormitory, which is leaning in the south transept façade, and two chapels, that were added after the end of the construction along the north's side walls. These chapels are in rubble masonry and the connection with the main church is clearly weak, which can have consequences during an earthquake.

3.5.3 Actual state of conservation

The masonry of the church of Vilabertran is a three-leaf masonry with a thickness of 1.5 m in all the walls. The two external leaves are made of good quality masonry. According to the Italian Circolare [38], the corresponding type of masonry is called "Matura a blocchi lapidei squadrati", which means square stone masonry. The internal leaf is probably a rubble masonry and can be classified according to the Circolare as "Matura in pietrame disordinata", which means rubble masonry with different size and shape of stone. The inspection indicates that the general state of conservation of the material is good in the church. Moreover, the presence of repointing in some places illustrates in the fact that some restoration work has already been done.

A lot of damages have been observed inside and outside the church as shown in the damage map of Figure 3.21 and the Appendix F. None of the damage induced a partial collapse of the church but some of them indicate potential of collapse mechanisms that could be activated by possible earthquakes.

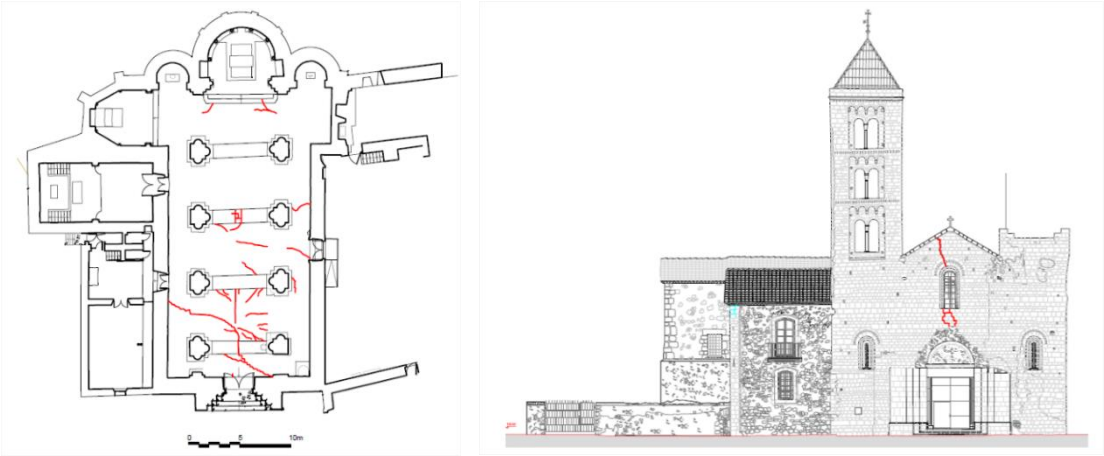

Figure 3.21. Crack mapping of the vaults and the main façade of Santa Maria de Vilabertran

The most important damage concerns the vaults of the church. As shown in Figure 3.21 and Figure 3.22, the central vault contains significant cracks. These cracks are mostly localized in the two first bays, where the first bay is the closest to the main façade. Some of them are already repointed, but their number shows the importance of the damages. It is also possible to notice a large crack starting from the main façade and going to the side wall in a diagonal. This crack is probably due to the presence of the tower in this corner. All of these cracks might be explained by the strong earthquake that occurred in 1428 and created similar damage to the churches of the region - the damages from this earthquake in the church of Vilabertran have not been documented on the contrary to other churches. However, these cracks could be also caused by soil settlement due to the weight of the tower in only one corner of the structure. In both cases, the presence of the tower might have influenced the development of the damages.

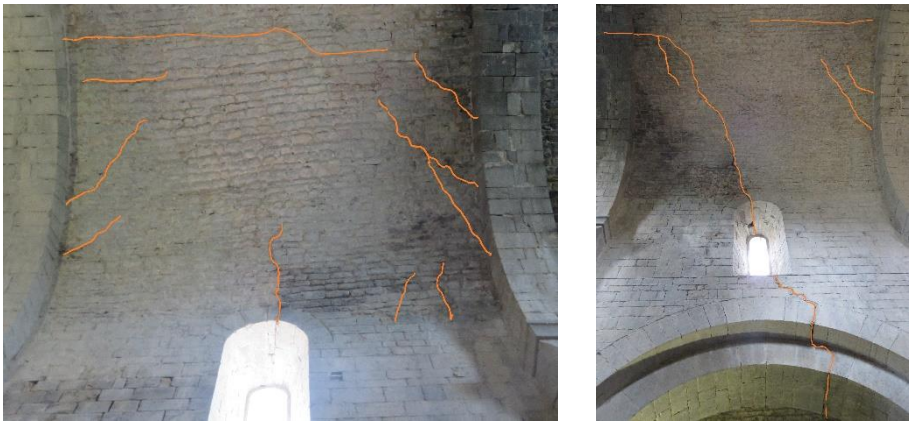

Figure 3.22. Cracks in the central vault of the nave

A second important damage can be observed in the main façade of the church as illustrated in Figure 3.23. A large crack of around 5 cm wide is visible in the top of the window and can be due to shear mechanism. Other diagonal cracks are present between the window and the door and a part of the first leaf of the masonry felt from the top of the door along the diagonal crack. Another observable damage is the displacement of the two stones under the lintel which seems recent. Moreover, the stones under these two ones are damaged in the corner. All the damages could have been induced by a shear mechanism that would have developed during the earthquake of 1428.

Figure 3.23. Damages in the main façade of Vilabertran

Some minor damages have been observed in the apse and in the rest of the church. These cracks are really small and do not represent any danger for the structure.

4. SEISMIC VULNERABILITY OF THE CHURCHES

4.1 Vulnerability index method

The vulnerability index method, as explained in section 2.2.2, is a method used to determine the vulnerability of the churches. The main issue of this methodology is the subjectivity of the application of the Italian survey form, and moreover the considerable number of assumptions that needs to be taken in order to perform the assessment. The following part will present the assumptions that were done for the two churches studied and the results of the method.

4.1.1 La Seu d'Urgell

4.1.1.1 Assumptions

Santa Maria of La Seu d'Urgell is a complex church with a structure comporting elements that could induce a collapse mechanism during an earthquake. According to section 2.2.2.2, 28 mechanisms can be identified in usual churches. All the elements of these mechanisms are not present in this specific church, which indicates that the first step of the inspection was to identify the mechanisms that could not occur because of a missing macroelement. La Seu d'Urgell does not include any nartex, lantern, timber roof structure or belfry. According to this, the mechanisms 4, 15, 19 to 21 and 28 detailed in the Appendix B are not possible.

Regarding all the mechanisms that can occur because of the presence of the macroelement corresponding, as explained in section 2.2.2.2, the presence of some vulnerability indicators or anti-seismic measures were listed during the inspection. Their efficiency was judged to assign a vulnerability grade to all the mechanism by following the Table 2.3 in section 2.2.2.2. As this judgement is subjective, the method used by Brando et al [8] in the case of the seismic assessment of historical city centre was used in order to better understand how to attribute the efficiency of each indicator. The crack mapping and the damages pictures inside of the church are also good indicators to determine the damage grade of each mechanisms. In order to use the vulnerability index method, it is necessary to make several assumptions regarding all the hidden elements of the church and the information that cannot be found. The following paragraphs will summarize these assumptions and the state of damage for all the possible mechanisms.

1 – Overturning of the façade: The observation of the façade indicates that there are no anti-seismic measures. Moreover, as the vault of the nave is a barrel vault, it is considered that there are no thrusting elements and the windows of the side walls were too small and too far from the corner to be considered as vulnerability indicators. No damage corresponding to this mechanism was noticed.

2 – Damage at the top of the façade: At the top of the façade, no anti-seismic measures were noticed. However, some vulnerability indicators were visible. First of all, the top of the façade is composed of a lot of medium to small openings. The presence of only one of these openings will not be considered as a vulnerability indicator, but as there are more than one, it can be considered as an indicator with a low effectiveness. Secondly, the presence of the tower on top of the façade leaning on the façade wall and the vault, as described in section 3.4.2, is an important vulnerability indicator. This element, as shown in Figure 3.11, is heavy and large and can largely influence on the failure mechanisms. According to this, the vulnerability indicator associated to this element should be considered of large effectiveness. The total vulnerability grade was thus set to 3. No damage corresponding to this mechanism was observed.

3 – Shear mechanism in the façade: For this mechanism, it was noticed that there are no anti-seismic measures. Regarding the vulnerability indicators, the main façade is composed of a large door and a lot of small windows. Considering the number, the size and the disposition of the openings, it was assumed that the effectiveness of the vulnerability indicator was low, which induced a vulnerability grade of 1. Inside of the church, some cracks were observed near the openings as illustrated in Figure 4.1. As these damages were located in different parts of the façade, a damage grade of 2 was assigned to this mechanism.

Figure 4.1. Shear cracks in the main façade of La Seu d'Ugell

5 – Transversal vibration of the nave: Regarding the anti-seismic measures, it was observed that an external buttress was added after the end of the construction of the church in order to help supporting the thrust of the vault. However, as only one buttress was built in just one side of the church, the efficiency of this anti-seismic measure can be considered as non-existent. The thickness of the walls and the pillars is too important to consider it as a vulnerability indicator; however, the vaults and arches of the central nave can be considered as vulnerability indicator with a low efficiency. The damages of this mechanism were easily observed during the inspection. As illustrated in section 3.4.3 with the Figure 3.13 and Figure 3.16, all the arches supporting the vault

are highly deformed and the central vault is cracked at midspan from the main façade to the dome. As the deformation of the arches can be considered as a structural damage, the damage grade attributed to this mechanism is 3.

6 – Shear mechanism in the side walls: This mechanism has no anti-seismic measures and it was assumed that there are also no vulnerability indicators. Indeed, the windows of the side walls are too small to be considered as a vulnerability indicator. However, the inspection of the wall revealed the presence of some superficial cracks in different locations of the side walls. These cracks, as illustrated in the crack mapping of Figure 3.14 and the Appendix D are not large and superficial, which induced a damage grade of 1 for the mechanism.

7 – Longitudinal response of the colonnade: The inspection of the church revealed that there are no anti-seismic measures in the church for this mechanism. The only vulnerability indicator is the presence of a heavy vault in the central nave, which can be considered as an indicator with a low efficiency. No damages were noticed in the pillars, which could indicate the activation of this mechanism.

8 – Vault of the nave: No tie-rods or buttresses were noticed as anti-seismic measures for the vault of the nave. Regarding the presence of a concentrated load from the roof, it was noticed that the bell tower on the top of the main façade is also leaning in the central vault. As the tower is a heavy element and there is no supporting element to help the vault at the location of the tower, this element is considered as contributing efficiently to the vulnerability of the mechanism. Regarding this, the vulnerability grade associated to this mechanism is 2. Regarding the damage of the central vault, it was assumed that the crack in the middle of the vault is not associated to this mechanism. However, the Figure 3.15 illustrate the presence of cracks due to the weight of the bell tower. These damages are moderate structural damages which induce the attribution of a damage grade of 3 for this mechanism.

9 – Vault of the aisles: As for the previous mechanism, no anti-seismic measures are noticed for this mechanism. The only vulnerability indicator in this case is the presence of two tower in the vaults of the first bay which are leaning on the top of the vault as illustrated in the Appendix C. As this element is only present in the first bay, it can be considered as low efficiency. As illustrated in the damage map of the vaults in Figure 3.13, almost all the vaults are cracked. Regarding the size of the cracks, it can be assumed that they are slight structural cracks, which induces a damage grade of 2.

10 – Overturning of the transept façade: The transept of this church is ended in both side by a tower. These two towers act like a buttress and block the rotation of the transept façades, that is why a value of 1 has been attributed to the anti-seismic measures. Regarding the vulnerability

indicators, none of them have been observed in this church. No damage corresponding to this mechanism has been noticed.

11 – Shear mechanism in the transept walls: During the inspection, it was observed that there are no anti-seismic measures for the shear mechanism of the transept walls. However, the façade walls of the transept are composed of a large door and an opening in the top of the wall. These opening can be considered as a vulnerability indicator of low effectiveness. As illustrated in Appendix D, some diagonal cracks between the openings were observed during the survey. The size of these cracks indicates that it is superficial cracks. According to it, the damage grade 1 is attributed to the mechanism.

12 – Vault of the transept: Regarding this mechanism, no anti-seismic measures or vulnerability indicators are present in the church. It is also observed that there is no damage corresponding to this mechanism.

13 – Triumphal arches: The triumphal arch of the church is maintained by stiff lateral wall which can be considered as an anti-seismic measure of low efficiency. The only vulnerability indicator is the presence of a dome in the top of the arch. According to this a vulnerability grade of 1 is attributed to the mechanism. No damage was noticed in the triumphal arch during the inspection.

14 – Dome, drum and tiburio: As explained in the previous mechanism, the dome is placed on top of a triumphal arch, which can be considered as an anti-seismic measure. Some small openings are present at the bottom of the dome, which can be considered as a vulnerability indicator. As their size is small, the efficiency of this indicator is low. No damage was observed on the dome.

16 – Overturning of the apse: The apse of the church does not include any reinforcement ring or propping elements that can act as an anti-seismic measure. Moreover, the size of the openings is too small to consider them as a vulnerability indicator. The only vulnerability indicator is the thrust created by the vault of the apse. This vault is a semi-dome, which induces a lot of horizontal forces on top of the apse and thus a vulnerability grade of 2. During the inspection, no damage was observed in the apse.

17 – Shear mechanism in the presbytery and the apse: This mechanism does not include any anti-seismic measure and the openings are not large enough to be considered as a vulnerability indicator. No damage corresponding to this mechanism was noticed during the survey.

18 – Vault in the presbytery and the apse: the vault of the apse does not include anti-seismic measure or vulnerability indicators. Some small cracks are visible; however, their size indicates that it is superficial cracks. A damage grade of 1 has been attributed.

22 – Overturning of the chapels: The chapels do not have large openings and the thickness of the walls is between 0.5 m close to the openings and 1.8 m between two chapels. The chapels shape is hidden in the thickness of the wall. This is why it can be considered that there is a good quality of end wall to side wall clamping which is an anti-seismic measure. No vulnerability indicators or damage were observed during the inspection.

23 – Shear mechanisms in the chapel walls: There are no anti-seismic measures or vulnerability indicators related to this mechanism. No damage was observed during the survey.

24 – Vault of chapels: There are no anti-seismic measures or vulnerability indicators related to this mechanism. No damage was observed during the survey.

25 – Interactions with adjacent buildings: The church is a part of a monastery, which means that there are adjacent buildings to the structure. The most important adjacent buildings are the two towers next to the transept. As these towers were built at the same time as the church, it can be considered that there is an adequate connection between the different phases of masonry construction, which is an anti-seismic measure. However, it is assumed that there might have a concentration of seismic action in connecting elements. This mechanism does not have damage corresponding to it.

26 – Projections (gable belfry, spires, pinnacle, statues): A gable belfry is leaning on the top of the tiburio. This projection does not have anti-seismic measures such as connecting pins. Moreover, some vulnerability indicators were noticed during the inspection. First of all, the gable belfry, as illustrated in Figure 4.2, is quite thin and the bells are still in place which add more weight. Secondly, the gable has an asymmetrical position on the tiburio. These two elements induce the vulnerability grade of 2 for this mechanism. During the inspection, no damage was observed.

Figure 4.2. Gable belfry on the top of the tiburio of La Seu d'Urgell

27 – Bell tower: The bell tower is one of the most vulnerable mechanism of this church. There are no anti-seismic measures; however, a lot of vulnerability indicators are present. The first vulnerability indicator is the presence of large openings in different heights as illustrated in Figure 3.15. Some slender elements are present such as thin columns. Secondly, the most important indicator is the asymmetrical support on the church at the base of the tower. As the tower is leaning both on the façade wall and the vault, a disequilibrium can appear and has a large impact on the vulnerability of the bell tower. According to these elements, a vulnerability grade of 3 is attributed. Some damage such as the deformation of the tower or the cracks in the supporting vault are visible. According to the EMS-98 scale, these damages are heavy structural damages inducing a damage grade of 4 for this mechanism.

The Italian Guideline, as evocated in section 2.2.2.2, assigned to each mechanism a certain weight. However, some of the weights had to be attributed manually in function of the importance of the element in the structure. In the case of the church of La Seu d'Urgell, all the mechanisms related to the transept (10, 11 and 12) have a weight of 0.5. This number has been chosen because of the small dimensions of the transept regarding the dimensions of the entire church. The weight of the mechanism related to the vault of the apse (18) is 1 because of the importance of this vault regarding the size of the apse. The chapels are small compared to the entire church, thus the weight assigned to the corresponding mechanisms (22, 23 and 24) is 0.5. The adjacent buildings were built at the same time as the church and are relatively large compared to the church which explained the weight of 1 for the mechanism 25. Finally, the gable belfry is small and present in only one location which induces a weight of 0.5 for the mechanism 26.

The Table 4.1 summarizes the anti-seismic grade, vulnerability grade, weight and damage grade for each of the 28 mechanisms of the Italian survey form. The highlighted lines correspond to the mechanisms which are not possible because of the lack of the corresponding macroelement.

Table 4.1. Variables assigned for each mechanism during the inspection of La Seu d'Urgell

Mechanism	v_{kp}	v_{ki}	ρ_k	d_k	Mechanism	v_{kp}	v_{ki}	ρ_k	d_k
1	0	0	1	0	15	0	0	0	0
2	0	3	1	0	16	0	2	1	0
3	0	1	1	2	17	0	0	1	0
4	0	0	0	0	18	0	0	1	1
5	0	1	1	3	19	0	0	0	0
6	0	0	1	1	20	0	0	0	0
7	0	1	1	0	21	0	0	0	0
8	0	2	1	3	22	1	0	0.5	0
9	0	1	1	2	23	0	0	0.5	0
10	1	0	0.5	0	24	0	0	0.5	0
11	0	1	0.5	1	25	1	1	1	0
12	0	0	0.5	0	26	0	2	0.5	0
13	1	1	1	0	27	0	3	1	4
14	1	1	1	0	28	0	0	0	0

4.1.1.2 **Results**

In order to perform a seismic assessment of a building, the Italian Guidelines [3] considers three seismic evaluation levels. The level 1 (LV1) is a quantitative analysis and evaluation with simplified mechanical models. The second level (LV2) is an evaluation of individual macroelements with local collapse mechanisms. It is applied during restoration interventions of parts or the entire building. The last level (LV3) is a global evaluation of the seismic response of the building. For this level, the entire construction is considered during the seismic assessment. It is used when interventions modified the use of the construction. The following vulnerability assessment is made according to the first seismic evaluation level.

As explained in section 2.2.2.2, the main objective of the vulnerability index method is to compute the vulnerability index and the damage index by using formulas of the equations 2.4 and 2.5 respectively. The results of these two indices are given in the Table 4.2. The vulnerability index is equal to 0.631, which is a high value of vulnerability. This means that the church is likely to be severely damaged by earthquakes. On the contrary, the value of the damage index seems to be really low. As explained in Table 2 of Lagomarsino et al [41], this damage index corresponds to a damage grade D1, which means negligible to light damage and does not correspond to the damages observed during the survey. According to the literature [16], this phenomenon is common

in the case of localised severe damages. When the damages are only in few macroelements, the damage index tends to be too small while when damages are in many macroelements this method gives results close to the observations made during the survey.

Table 4.2. Results of the vulnerability index method

I_v	I_d
0.631	0.178

By using the vulnerability index, different outputs can lead to the vulnerability assessment of the church. The first method consists in regarding the corresponding accelerations of two limit states. These limit states were established in order to guarantee the safety of the visitors of the building in case of a rare high intensity earthquake and limit economical losses in case of a moderate intensity earthquake. The two limit states are:

- The Ultimate Limit State (ULS): under this limit state, the structure is supposed to resist to severe damage and maintain a residual resistance and stiffness. The earthquake associated to this limit state is an earthquake with a probability of exceeding the limit ground acceleration of the code of 10% in 50 years.
- The Damage Limit State (DLS): under this limit state, the entire building is not severely damaged, and its use is not interrupted. The earthquake associated to this limit state is an earthquake with a probability of exceeding the limit ground acceleration of the code of 50% in 50 years.

From the vulnerability index, it is possible to deduce the corresponding acceleration value of each limit states described before by using a correlation. The relations are shown below:

$$a_{DLS} = 0.025 * 1.8^{2.75-3.44i_v} \quad 4.1$$

$$a_{ULS} = 0.025 * 1.8^{5.1-3.44i_v} \quad 4.2$$

The Table 4.3 shows the numerical values for both limit state. In order to determine if the church is able to sustain the seismic action of the area, a seismic safety index I_S is calculated according to the Equation 4.3.

$$I_S = \frac{a_{ULS}}{\gamma_i S a_g} \quad 4.3$$

Where a_{ULS} is the ground velocity of the ultimate limit state, γ_i is the coefficient of importance, S is the factor taking into account the terrain and a_g is the peak ground acceleration of the site.

In this case, the factor of importance is equal to 1.3. The soil of La Seu d'Urgell, as explained in section 3.3, is of type A in the Eurocode 8 classification [31], which means that the factor S is equal to 1 as explained in the Table 3.2 of the Eurocode 8. The peak ground acceleration of the site is also given by the Eurocode 8. According to the national annex of this document, the basic seismic acceleration for an earthquake with a return period of 500 years that should be considered is 0.116g. The numerical value of the seismic safety index is 0.93. As the value is lower than 1, the building is not able to sustain the seismic action for this area and some measures should be taken to solve this issue.

It is also possible to calculate this safety index according to the values given by the Spanish code [42]. The factor of importance is also equal to 1.3, but in the Spanish code the factor S in equal to 0.8 and the basic seismic acceleration is 0.06g. With these numerical values, the new safety index is equal to 2.26. In this case, the building is able to sustain the seismic action for this area. The two values calculated according to the Spanish annex of the Eurocode 8 or to the Spanish code give different results due to the high difference in the basic acceleration. The value given by the Spanish code seems to be too low regarding the location of the city and the presence of the Pyrenees. The values calculated according to the Eurocode 8 may be considered to represent better the seismicity of this location.

Table 4.3. Ground acceleration for two limit states

a_{DLS} (g)	a_{ULS} (g)
0.035	0.140

The second output of the vulnerability index method is the vulnerability curve. This curve help relating the macroseismic intensity of an earthquake to the vulnerability index through the calculation of a mean damage grade. The expression of the mean damage grade used in the case of buildings was adapted by Lagomarsino et al [41], during the study of the Umbrian and Marches earthquakes. A calibration of the original equation led to the final expression given in Equation 4.4.

$$\mu_d = 2.5 \cdot \left[1 + \tanh \cdot \left(\frac{I + 3.4375 \cdot i_v - 8.9125}{Q}\right)\right] \qquad 4.4$$

Where I is the macroseismic intensity given by the EMS-98 scale, i_v is the vulnerability index calculated before and Q is a ductility factor equal to 3 in the case of a church.

The vulnerability curved plotted in Figure 4.3 represents the mean damage grade of the church of La Seu d'Urgell for all the different macroseismic intensities. For intensities lower than V, the mean damage grade is low while for intensities higher than VI the mean damage increases significantly.

Another method to obtain the mean damage grade is to use the damage index. By multiplying the damage index by 5, it is possible to obtain the mean damage grade corresponding to the maximal macroseismic intensity that occurred in La Seu d'Urgell. The seismic analysis of Catalonia of section 3.3 indicates that this maximal macroseismic intensity is VII. The value of the mean damage grade calculated with the damage index is 0.89. As illustrated in the Figure 4.3, this value is less than half of the value calculated with the previous method. This result reinforces the idea that the damage index is too low. Another explanation of this difference might be in the calibration of the expression of the mean damage grade, which were done for the Italian stock of churches.

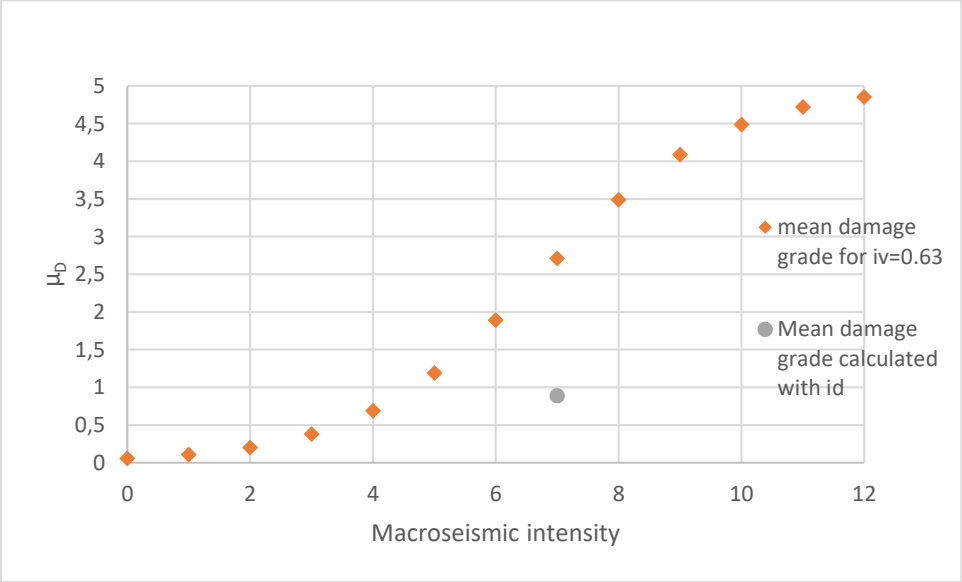

Figure 4.3. Vulnerability curve of La Seu d'Urgell

The last output of the vulnerability index method is the fragility curves. These curves are one of the best methods to define the probability of reaching or exceeding a certain level of damage for each macroseismic intensity. First, the probability of reaching one of the 6 level of the damage scale defined in the EMS-98 is calculated according to a binomial function depending of the mean damage grade as expressed in the Equation 4.5. Then, the probability of exceeding a certain damage level is calculated by cumulating the previous binomial functions.

$$_k = \frac{5!}{k!\,(5-k)!}\left(\frac{\mu_{D,0}}{5}\right)^k \left(1-\frac{\mu_{D,0}}{5}\right)^{5-k} \qquad 4.5$$

Figure 4.4 and Figure 4.5 represent the fragility curves of the church of La Seu d'Urgell. According to these curves, it is possible to know the damage grade that will occur for each macroseismic intensity and to plan the strengthening interventions according to the risk of damages to the church. As illustrated by these figures, for an intensity of VII, which correspond to the maximal historical intensity, the probability of exceeding a damage grade D4 is around 0.25, while the probability of exceeding a damage grade D3 is around 0.6. This indicate that the church in its actual state of conservation should have a damage grade close to D2-D3. As explained previously with the vulnerability curve, this does not correspond to the result obtained by the visual inspection and the corresponding attribution of the damage grade.

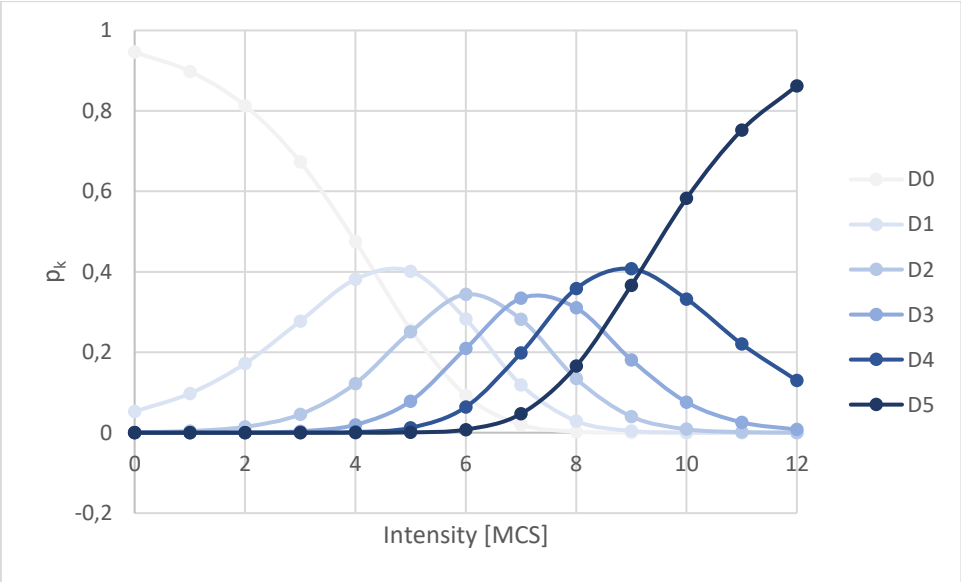

Figure 4.4. Fragility curves of La Seu d'Urgell: probability of reaching a damage level

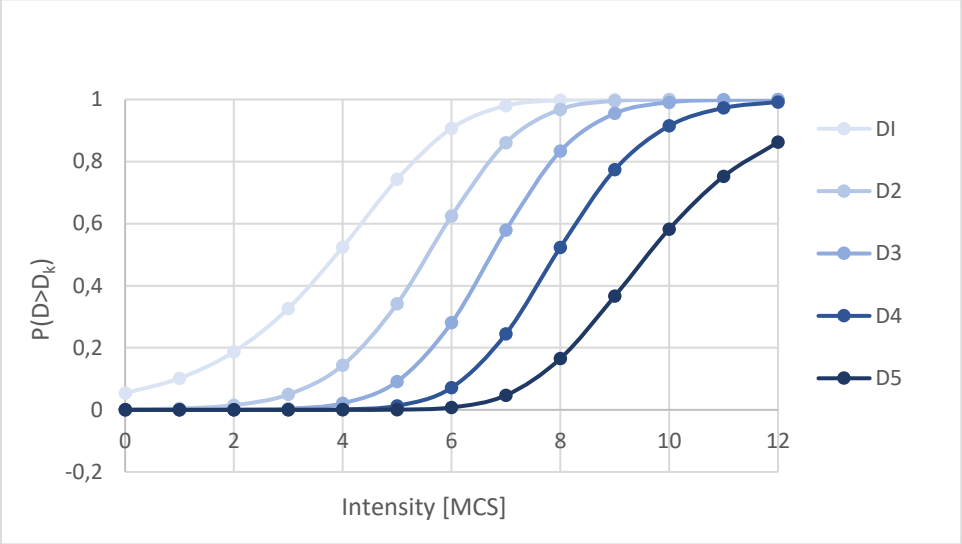

Figure 4.5. Fragility curves of La Seu d'Urgell: probability of exceeding a damage level

4.1.2 Vilabertran

The methodology for the vulnerability assessment of the church of Vilabertran and the processing of the results is similar to the ones used for La Seu d'Urgell.

4.1.2.1 **Assumptions**

The inspection of the church of Vilabertran revealed that this church does not have all the macroelements listed in the Italian Survey Form. The nartex, the dome, the lantern, the roof, the projection and the belfry are missing macroelements to the structure. According to this, the mechanisms 4,14, 15, 19 to 21, 26 and 28 detailed in the Appendix B are not possible. . The following paragraphs will resume the assumptions concerning all the other mechanisms.

1 – Overturning of the façade: The main façade of the church does not have any anti-seismic measures such as tie-rods or buttresses to reduce the vulnerability of the mechanism. Moreover, as the vault is a barrel vault, there is no horizontal thrust from the vault on top of the façade and the absence of openings in the side walls near the corner indicates that there are no vulnerability indicators of this mechanism. During the inspection, no damage corresponding to the overturning of the façade was noticed.

2 – Damage at the top of the façade: As for the previous mechanism, there are no anti-seismic measures related to this mechanism. However, the window on top of the façade, illustrated in Figure 3.20 can be considered as a vulnerability indicator. This window is not large but regarding to the

dimensions of the façade, it is assumed to be sufficiently large to be a vulnerability indicator of low efficiency. The inspection did not reveal any damage related to this mechanism.

3 – Shear mechanism in the façade: The adjacent leaning buildings of the church were built after the end of the construction of the church. In addition to the poor quality of their masonry, this indicates that they cannot be considered as anti-seismic measures regarding the shear mechanism of the façade. The façade is only composed of the main door and one window (the two other windows are too small to have any impact on this mechanism) but their dimensions and disposition can be a vulnerability indicator of low efficiency. As explained in section 3.5.3, the main façade has several damages, such as the diagonal cracks or the displacements of the piers under the lintel, which can be associated to a shear mechanism. In the case of moderate structural damage like this, a damage grade of 3 is attributed.

5 – Transversal vibration of the nave: As in the previous mechanism, the poor masonry quality of the adjacent building induces the absence of any anti-seismic measure. The church is a Romanesque church, which results in the presence of walls too thick to be a vulnerability indicator. However, the presence of the vault and the arches supporting the vault are vulnerability indicators. The inspection did not reveal damage related to this mechanism.

6 – Shear mechanisms in the side walls: The side walls of the church have really few openings (one door in each side), which reduces the vulnerability to this mechanism. Thus, we can conclude that there are no anti-seismic measure or vulnerability indicator for this mechanism. The only cracks present in the side walls cannot be associated to shear mechanism as they are a prolongation of cracks from the vaults.

7 – Longitudinal response of the colonnade: In this church, there is one longitudinal tie-rod at each side of the colonnade. However, in order to be efficient, it is necessary to have longitudinal tie rods between each pillar. According to this, it is not possible to consider it as an anti-seismic measure. As the Romanesque vaults are most of the time very thick, they can be considered as heavy vault and then become a vulnerability indicator. As the columns of the church are large, no damages corresponding to this mechanism are visible.

8 – Vault of the nave: This mechanism does not have any anti-seismic measures. The bell tower of the church is leaning on the first pillar of the church. However, it cannot be considered as a concentrated load on the central nave. It is assumed that the opening of the clerestory walls are not irregularities of the vault as this one starts on the top of the openings. According to this, there are no vulnerability indicators for this mechanism. A lot of damages were noticed during the inspection as illustrated with the crack mapping of Figure 3.21 and the pictures of Appendix F. Even if these cracks might be caused by soil settlement due to the tower or to the response of the

structure to a past earthquake. These damages were associated to this mechanism. As it is moderate structural damage, a damage grade of 3 is attributed.

9 – Vault of the aisles: There are no anti-seismic measures corresponding to this mechanism. However, the bell tower can be considered as a vulnerability indicator of low efficiency as it is leaning on the first bay of the church, starting from the main façade. Some damages are noticed in the aisles' vaults. Most of the cracks are the expansion of the ones from the nave's vault. Indeed, a damage grade of 2 is attributed to this mechanism.

10 – Overturning of the transept façade: One side of the transept has a circular shape with external buttresses to support the façade. On the other side of the transept, there is a dormitory that can be considered as an anti-seismic measure. As each façade of the transept has a different anti-seismic measure, it is assumed that the grade associated to it will only be 1. Some openings are present in both transept façades, but as their size is not large, the efficiency of this vulnerability indicator is low. No damage corresponding to this mechanism was observed in church.

11 – Shear mechanism in the transept walls: There are no anti-seismic measure for this mechanism. Regarding the vulnerability indicators, the openings can be considered as an indicator of low efficiency. Some superficial diagonal cracks are visible in the transept walls, which leads to a damage grade of 1 for the mechanism.

12 – Vault of the transept: This mechanism has no anti-seismic measures and no vulnerability indicators. During the survey, no damage was observed.

13 – Triumphal arches: The triumphal arch is not maintained by stiff lateral walls, which means that there are no anti-seismic measures. However, there are no dome or heavy roof covering on top of the arch which indicates that there are no vulnerability indicators neither. No damage was noticed during the inspection.

16 – Overturning of the apse: The apse of the church does not have any anti-seismic measures. The vault of the apse applies a vertical thrust on top of the apse. This can be considered as a vulnerability indicator of low efficiency. During the survey, no damage was noticed regarding this mechanism.

17 – Shear mechanism in the presbytery and the apse: The masonry of the apse seems to have different construction phase and the only opening is really small. According to this, it is possible to assume that there are no anti-seismic measures or vulnerability indicators. No damage was observed during the survey.

18 – Vault in the presbytery and the apse: There are no anti-seismic measures or vulnerability indicators corresponding to this mechanism. However, some cracks were noticed during the

inspection of the church. The Appendix F illustrated these superficial cracks. According to the EMS-98 scale, a damage grade of 1 is attributed to this mechanism.

22 / 23 / 24– Mechanisms related to the chapels: The chapels are small, with few openings and a bad quality masonry. According to this, there are no anti-seismic measures or vulnerability indicators for these mechanisms. No damage was noticed during the survey.

25 – Interactions with adjacent buildings: The church is surrounded by a lot of adjacent buildings. The dormitory of the monastery is leaning on the transept façade and two chapels were added along the side wall. These constructions have thinner walls than the church, which induces a great difference in stiffness between the buildings. Moreover, there is a possibility of concentration of seismic actions in connecting elements due to the bad quality masonry of the adjacent buildings. According to this, there are no anti-seismic measures but there are vulnerability indicators with a grade of 2. During the inspection, no damage corresponding to this mechanism were noticed.

27 – Bell tower: The bell tower, as illustrated in Figure 3.20, is leaning on the façade and on the first pillar of the nave. This asymmetrical support on the church at the base of the tower is a vulnerability indicator. Moreover, the second vulnerability indicator of this mechanism is the presence of large openings at different heights. These two indicators have a low efficiency. The inspection revealed that there are no damage and no anti-seismic measures for this mechanism.

The weight attributed to all the mechanisms related to the transept (10, 11 and 12) is 0.5 because of the small dimensions of the transept regarding to the dimensions of the church. The weight of the mechanism related to the vault of the apse (18) is 1 because of the importance of this vault regarding the size of the apse. The chapels are small compared to the entire church, thus the weight assigned to the corresponding mechanisms (22, 23 and 24) is 0.5. The church is surrounded by a lot of different buildings, which explained the weight of 1 for the mechanism 25.

The Table 4.4 summarizes the anti-seismic grade, vulnerability grade, weight and damage grade for each of the 28 mechanisms of the Italian survey form. The highlighted lines emphasize the mechanisms which are not possible because of the lack of the corresponding macroelement.

Table 4.4. Variables assigned for each mechanism during the inspection of Santa Maria de Vilabertran

Mechanism	v_{kp}	v_{ki}	ρ_k	d_k	Mechanism	v_{kp}	v_{ki}	ρ_k	d_k
1	0	0	1	0	15	0	0	0	0
2	0	1	1	0	16	0	1	1	0
3	0	1	1	3	17	0	0	1	0
4	0	0	0	0	18	0	0	1	1
5	0	1	1	0	19	0	0	0	0
6	0	0	1	0	20	0	0	0	0
7	0	1	1	0	21	0	0	0	0
8	0	0	1	3	22	0	0	0.5	0
9	0	1	1	2	23	0	0	0.5	0
10	1	1	0.5	0	24	0	0	0.5	0
11	0	1	0.5	1	25	0	2	1	0
12	0	0	0.5	0	26	0	0	0	0
13	0	0	1	0	27	0	2	1	0
14	0	0	0	0	28	0	0	0	0

4.1.2.2 **Results**

The same methodology used for the results of the church of La Seu d'Urgell will be used in the case of the church of Vilabertran. The Table 4.5 shows the vulnerability index and the damage index of this church. The vulnerability index is lower than for the previous church; however, the value is also quite high. Regarding the damage index, this value corresponds to a damage grade D1, which means negligible or light damages. This result does not correspond to the damages observed during the survey. As the damages were located in few mechanisms, the same explanation as for La Seu d'Urgell can explain this result.

Table 4.5. Results of the vulnerability index method

I_v	I_d
0.603	0.106

Regarding the ground accelerations of the two limit states analysed, the Table 4.6 indicates the numerical values calculated with the Equations 4.1 and 4.2. In order to obtain the seismic safety index, the factor of importance is equal to 1.3. According to the section 3.3, the soil type of

Vilabertran is a type B of the Eurocode 8 classification [31], which induces a factor S equal to 1.2 as illustrated in the Table 3.2 of the Eurocode 8. The basic seismic acceleration of Vilabertran given by the Eurocode 8 is 0.113g. The seismic safety index is 0.84, which is lower than 1. Hence, the structure is not able to sustain the seismic action of the area.

According to the Spanish code, the factor of importance is equal to 1.3, the factor S is equal to 1.04 and the basic ground acceleration is equal to 0.08g. The safety factor calculated with these values is equal to 1.37, which means that the building is able to sustain the seismic action for this area. This value is higher than the previous calculation, which indicates, as for La Seu d'Urgell, that the difference in the basic seismic acceleration given by the two codes can imply a significant difference in the results.

Table 4.6. Ground acceleration for two limit states

a_{DLS} (g)	a_{ULS} (g)
0.037	0.148

The vulnerability curved plotted in Figure 4.6 represents the mean damage grade of the church of Vilabertran for all the different macroseismic intensities. Before an intensity of V, the mean damage grade is low while for intensities higher than VI the mean damage increases considerably. The mean damage grade calculated with the damage index correspond to a seismic intensity of VII according to the seismic analysis of Catalonia of section 3.3. The value of the mean damage grade calculated with this method is 0.53. As illustrated in the Figure 4.6, this value is less than a quarter of the value calculated with the other method. This result reinforces the idea that the damage index is too low.

The Figure 4.7 and Figure 4.8 represent the fragilities curves of the church of Vilabertran. According to these curves, it is possible to know the damage grade that will occur for each macroseismic intensity and to plan the strengthening interventions according to the risk of damage of the church. As illustrated by these figures, for an intensity of VII, which correspond to the maximal historical intensity, the probability of exceeding a damage grade D4 is around 0.2, while the probability of exceeding a damage grade D3 is around 0.5. This indicate that the church in its actual state of conservation should have a damage grade around D2. As explained previously with the vulnerability curve and the results from the damage index, this does not correspond to the result obtain by the visual inspection and attribution of the damage grade.

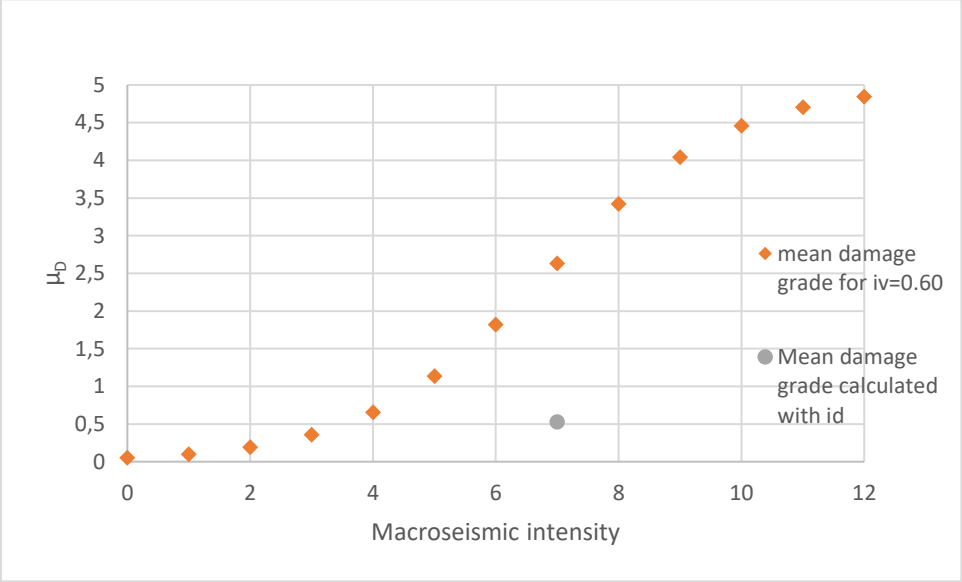

Figure 4.6. Vulnerability curve of Vilabertran

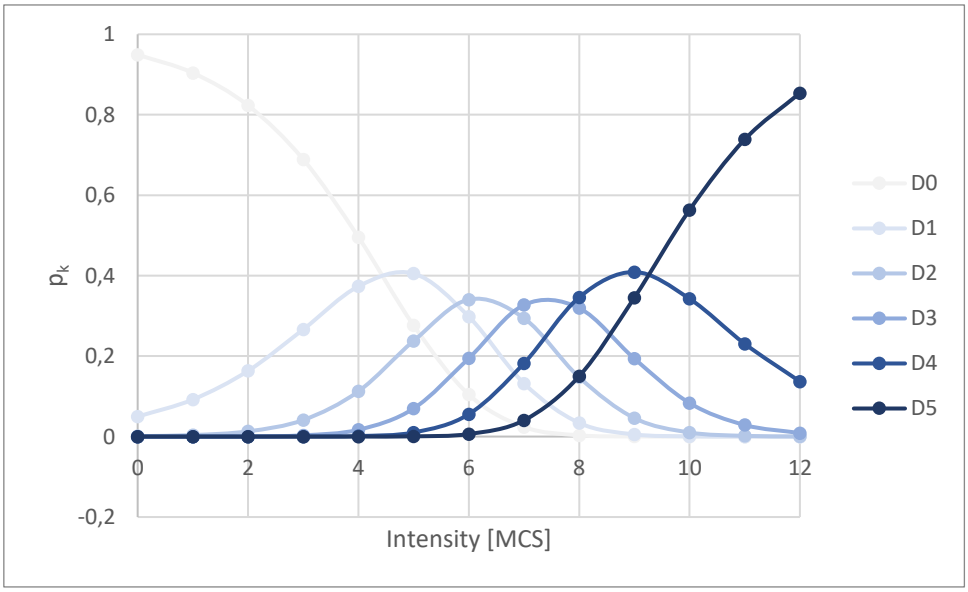

Figure 4.7. Fragility curves of Vilabertran: probability of reaching a damage level

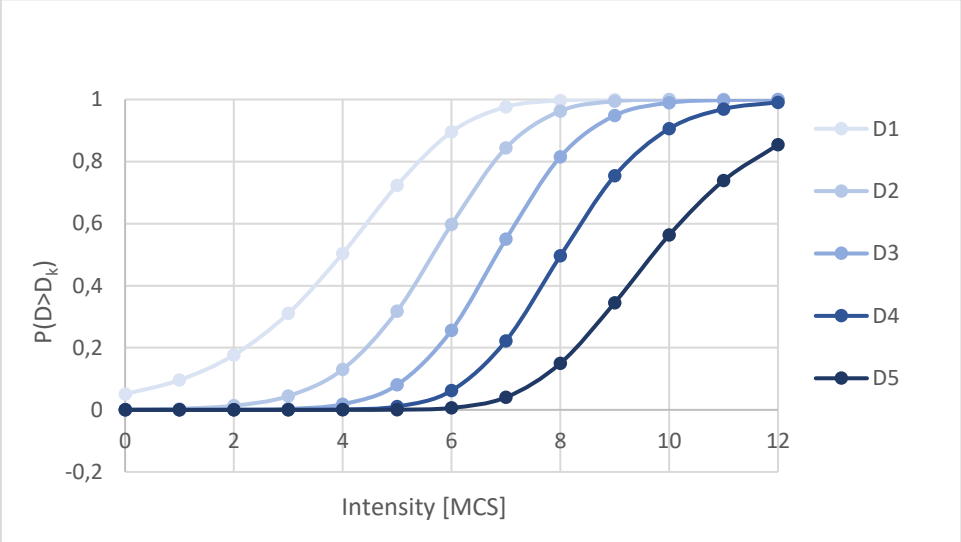

Figure 4.8. Fragility curves of Vilabertran: probability of exceeding a damage level

4.2 Kinematic Limit Analysis

The kinematic limit analysis is a method applied to a localized failure mechanism in order to determine the behavior of this mechanism under a typical earthquake. Once the capacity curve of each mechanism analyzed is determined, the two methods described in the section 2.3.2 are used in order to find the performance point. The following part will describe the local mechanisms studied, the method to obtain the capacity curve and finally the results obtained.

4.2.1 Methodology for the determination of the capacity curve and the demand curve

The first step of the determination of the capacity curve is to find the position of the rotation point of the wall. This point is linked to the compressive capacity of the wall and the total load supported by it. It is assumed that only the external leaf will fail under compression, which means that only the compressive strength of the external leaf is taken into account. The rotation point is calculated according to Equation 4.6.

$$t = \frac{2N}{\sigma_c \, l} \qquad 4.6$$

With t the position of the rotation point, N the vertical loads, σ_c the compressive strength of the external leaf and l the length of the façade.

If the position of the rotation point is not in the external leaf, a more detailed calculation is necessary. A first verification is needed, which consists on checking that the compression strength at the

interface is lower than the limit given by the internal leaf. Once this verification is done, it is possible to obtain the new position of the rotation point t by solving the following equation:

$$\frac{\sigma_{c1}\left(2-\frac{t_1}{t}\right)}{2} l_1 + \sigma_{c1}\left(1-\frac{t_1}{t}\right)\frac{E_2}{E_1}\,(t-t_1) = W \qquad 4.7$$

With σ_{c1} the compressive strength of the external leaf, σ_{c2} the compressive strength of the internal leaf, E_1 and E_2 the Young modulus of the two leaves, t_1 the thickness of the external leaf and W the total vertical load.

Once the position of the rotation center is determined, it is possible to calculate the horizontal load that will activate the rotation of the wall. This horizontal load is equal to the total of the vertical load multiplied by a coefficient α. An equilibrium between the moment of resistance and the moment of the horizontal loads permits to obtain the value of the multiplier α. Equation 4.8 and Figure 4.9 explain the calculation. This equation corresponds to the case of a wall divided in two monolithic blocks. However, it can be adapted in the case of a monolithic wall or of the presence of a horizontal thrust from a vault.

$$\alpha = \frac{N_1\left(\frac{b_1}{2}-t\right) + N_2\left(\frac{b_2}{2}-t\right)}{\frac{N_1 h_1}{2} + N_2\left(h_1+\frac{h_2}{2}\right)} \qquad 4.8$$

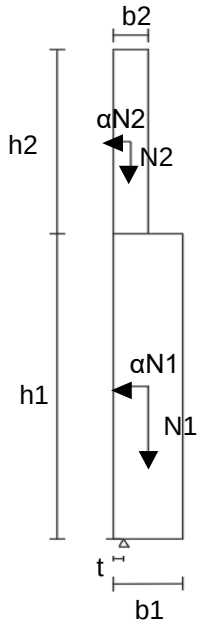

Figure 4.9. Drawing of the loads applied to the wall

It is then possible to determine the capacity curve by applying the same equilibrium to a wall with a small rotation as illustrated in Figure 4.10. The capacity curve represents the value of the multiplier α in function of the horizontal displacement of a reference point such as the barycenter of the forces. The multiplier α and the acceleration can be linked according to the following equation:

$$\frac{a}{g} = \frac{F}{W} = \frac{\alpha W}{W} = \alpha \qquad 4.9$$

Where a is the acceleration, g the gravity acceleration, F the horizontal loads and W the vertical loads.

The curve obtained represents the inelastic part of the capacity curve. It is a decreasing linear curve, which stops when the maximal displacement before the collapse of the wall is reached (which means an acceleration equal to zero to activate the mechanism). However, the Italian Circolare [23] recommends taking as a maximal value of displacement the displacement for an acceleration equal to 85% of the maximal acceleration. Figure 4.11 represents the part of the capacity curve obtained with this method.

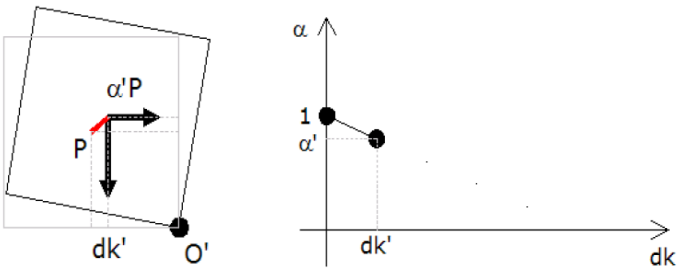

Figure 4.10. Determination of the capacity curve

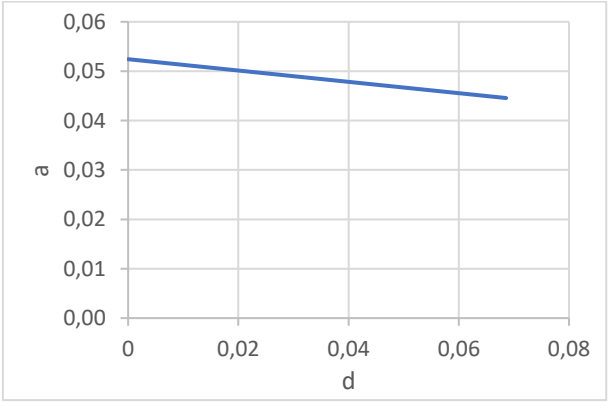

Figure 4.11. Inelastic part of the capacity curve

In order to obtain the elastic part of the capacity curve, the elastic period T_0 is calculated according to the following expression from the part C8.7.1.2.1.3 of the Italian Circolare [23]:

$$T_0 = k\lambda L \sqrt{\frac{W}{Eg}} \qquad 4.10$$

Where k is a coefficient equal to 6.2, λ the slenderness of the structure, L the length of the structure, W the weight, E the young modulus and g the gravity acceleration.

By using the relation between the period, the acceleration and the displacement (Equation 4.11), it is possible to find the elastic displacement d_{emax} corresponding to the maximal acceleration a_{max} determined previously. The elastic part of the capacity curve is a linear curve between the point 0-0 and the point a_{max} – d_{emax}. By joining the elastic and inelastic part of the capacity curve, the complete curve is obtained.

$$T_0 = 2\pi \sqrt{\frac{d}{a}} \qquad 4.11$$

In this analysis, the capacity curve will be compared with the spectrum from the Spanish code and the Eurocode 8. It is thus necessary to transform the capacity curve to the spectral coordinates a*-d*. The part C8.7.1.2.1.3 of the Italian Circolare [23] explains how to perform the transformation. First, the spectral acceleration is calculated according to the expression of Equation 4.12.

$$a^* = \frac{a(d_c)g}{e^* FC} \qquad 4.12$$

With d_c the point of control (which means the barycentre of the loads), g the gravity acceleration, FC the factor of confidence and e^* the participant masse. This variable is calculated with the following expression:

$$e^* = \frac{\left[\sum_{k=1}^{N}(P_k + Q_k)\delta_{PQx,k}\right]^2}{\left[\sum_{k=1}^{N}(P_k + Q_k)\right]\left[\sum_{k=1}^{N}(P_k + Q_k)\delta_{PQx,k}^2\right]} \qquad 4.13$$

With P_k the vertical gravity load applied to the k-th bloc, Q_k the vertical load applied to the k-th bloc and $\delta_{PQx,k}$ the horizontal virtual barycentre displacement of the vertical loads application.

Then the spectral displacement is calculated according to the following equation:

$$d^* = d_c \frac{\sum_{k=1}^{N}(P_k + Q_k)\delta_{PQx,k}^2}{\delta_{Cx}\sum_{k=1}^{N}(P_k + Q_k)\delta_{PQx,k}} \qquad 4.14$$

With δ_{Cx} the horizontal virtual displacement of the control point.

Once the capacity curve is plotted, it is necessary to determine the demand curve. The Spanish code [42] explains in the section 2.3 how to calculate the elastic response spectrum. The following equations define this spectrum:

$$\begin{aligned} &\text{If } T < T_A && a(T) = a_c\left(1 + 1.5\frac{T}{T_A}\right) \\ &\text{If } T_A < T < T_B && a(T) = 2.5\ a_c \\ &\text{If } T > T_B && a(T) = a_c K\frac{C}{T} \end{aligned} \qquad 4.15$$

With a_c the seismic acceleration of calculation, K the coefficient of contribution, C the coefficient related to the soil and T_A and T_B the characteristic periods of the spectrum.

The elastic response spectrum defined in the section 3.2.2.2 of the Eurocode 8 [31] can be calculated according to the following equations:

$$\begin{aligned} &\text{If } 0 < T < T_B && a(T) = a_g S\left[1 + \frac{T}{T_B}(2.5\eta - 1)\right] \\ &\text{If } T_B < T < T_C && a(T) = 2.5\ a_g\ S\ \eta \\ &\text{If } T_C < T < T_D && a(T) = 2.5\ a_g\ S\ \eta\frac{T_c}{T} \\ &\text{If } T_D < T < 4s && a(T) = 2.5\ a_g\ S\ \eta\frac{T_c T_D}{T^2} \end{aligned} \qquad 4.16$$

With a_g the calculation acceleration, S a soil parameter, η a coefficient of correction of the damping ration and T_B, T_C and T_D the characteristic periods of the spectrum.

The final step is to convert the spectrum from an a-T format to an a-d format by using the relation between the acceleration, the period and the displacement: $T = 2\pi\sqrt{\frac{d}{a}}$.

The Figure 4.12 shows an example of the final capacity curve that can be obtained by applying this method and two demand spectra calculated according to the Spanish code and the Eurocode 8.

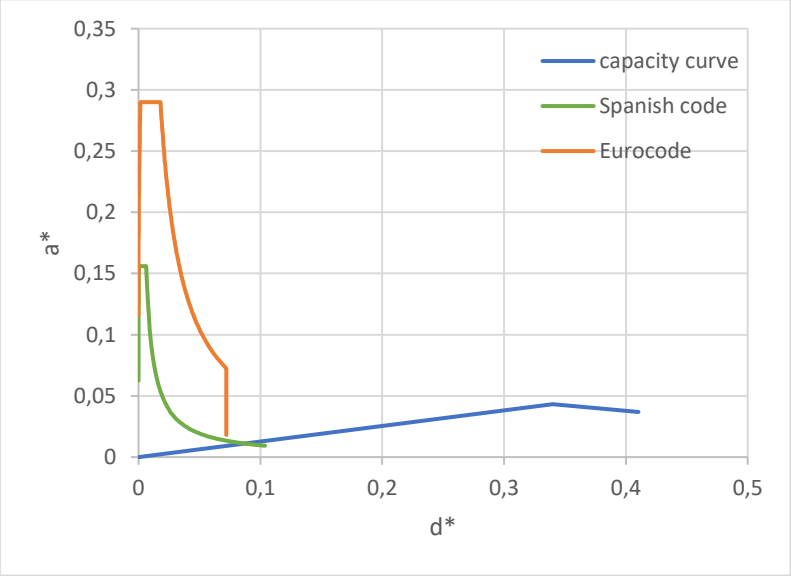

Figure 4.12. Capacity and demand curves of the case SU1

Once the capacity curve is determined, it is also possible to define damage threshold levels as explained in the RISK-UE [43]. The position of the performance point will indicate the level of damage expected and thus the vulnerability of the mechanism. These damage threshold levels are defined by the following expressions:

$$\overline{Sd_1} = 0.7\, D_y$$

$$\overline{Sd_2} = D_y$$

$$\overline{Sd_3} = D_y + 0.25(D_u - D_y) \qquad 4.17$$

$$\overline{Sd_4} = D_u$$

With D_y the elastic displacement and D_u the ultimate displacement.

4.2.2 La Seu d'Urgell

4.2.2.1 Presentation of the local mechanisms studied

In the case of La Seu d'Urgell, three main mechanisms are studied: the overturning of the main façade, the overturning of the bell tower on top of the main façade and the overturning of the apse. The overturning of the transept façades is not studied because the development of this mechanism is prevented by the two towers. The following paragraphs will describe all the cases analysed for these two mechanisms and the assumptions made for the calculations.

Case 1: Overturning of the main façade assuming deficient connection between orthogonal walls (SU1)

In this case, as the thickness of the external towers' walls is larger than the thickness of the central part, the behaviour of this part might be different. According to this, it is assumed that the overturning of the main façade only considers the part between the two towers as illustrated in Figure 4.13. It is also assumed that the façade of the bell tower leaning on top of the façade will participate to the overturning of the wall. Because of the difference of thickness between the bell tower and the façade, the wall is considered as two monolithic blocs, with a rotation point in the bottom of the wall as illustrated in Figure 4.14. It is also assumed in this case that the connection between orthogonal walls is deficient, which means that the orthogonal walls will not help in the resistance of the failure mechanism.

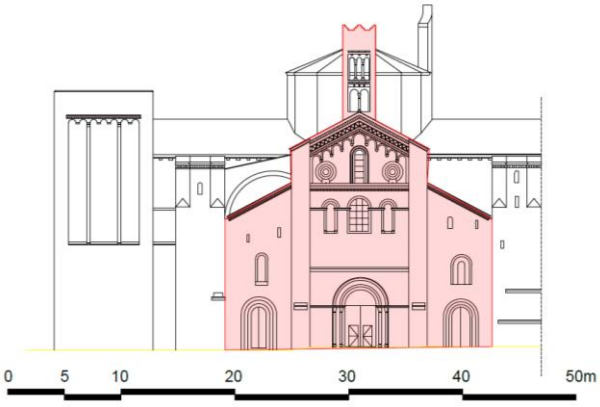

Figure 4.13. Overturning of the main façade of La Seu d'Urgell (SU1)

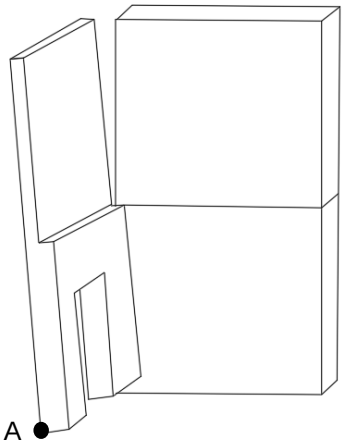

Figure 4.14. Rotation of the façade

As explained in the section 3.4.3, the main façade is a three-leaf wall. The thickness of each leaf is unknown because it was not possible to make any tests during the inspection. It was thus decided to consider an external leaf of 0.2 m of thickness, as it has been observed in other similar churches. The mechanical properties of the façade wall and the bell tower were determined according to the appendix of the Italien Circolare [23] and are summarized in the Table 4.7. The values of the compressive strength and the Young modulus for each material composing the wall are the mean value of the upper and lower bound given by the Circolare.

Table 4.7. Mechanical properties (SU1)

	Thickness (m)	**W (kN/m^3)**	**F_m (N/mm^2) external leaf**	**F_m (N/mm^2) internal leaf**	**E (N/mm^2)**
Main façade	0.2 – 0.7 – 0.2	20.09	7	1.5	1572
Bell tower	0.15	22	7	-	2850

Case 2: Overturning of the main façade with a good connection between orthogonal walls (SU2)

This case is similar to the previous one, the only difference is the fact that the connection between orthogonal walls is assumed to be effective, which involves the participation of a part of the orthogonal wall to the rotation of the façade. This part will add some vertical load, which will help to resist to the overturning mechanism.

In the bell tower, it is assumed that the orthogonal wall will crack in a weak point such as an opening. Usually, cracks are observed to develop in corner of openings or in the middle of them. In this case, it is assumed that the crack will occur in the middle of the opening, which coincides with the middle of the orthogonal wall. As the connection between the façade and the orthogonal walls is good, it is assumed that the failure will occur in the orthogonal wall as a diagonal crack with an angle of 15°. The Figure 4.15 illustrates the wall studied in this case.

Figure 4.15. View of the main façade with the orthogonal walls (SU2)

A specific point of this case is the participation of the weight of the vault of the resistance to the overturning mechanism. As the vault of the aisle is supported by the external wall, this weight should be taken into consideration. As no measurements were made during the survey, it is assumed that the thickness of the vault is 0.4 m, which is a value observed in similar churches. The shape of the vault is given by the drawing of the church and the density of the vault is assumed to be similar to the walls' one. In addition to the self-weight of the vault, the weight of the cover is also taken into consideration as a distributed load of 3kN/m².

The mechanical properties of the material of the façade are similar to the previous case.

Case 3 and 4: Overturning of the bell tower (SU3 and SU4)

Regarding the failure of a tower, five main mechanisms have been identified as shown in Figure 4.16. The first four mechanisms concern the overturning of the tower, and the last one a displacement of the tower due to base shear sliding. In this analysis, we will only consider the two first mechanisms: the rocking with a vertical splitting (SU3) and the monolithic rocking (SU4). In both cases, the rotating part will be considered as a monolithic block.

Figure 4.16. Failure mechanisms of a tower [44]

The mechanical properties of the material composing the tower's walls are similar to the case SU1. The main difference between the overturning of the tower and the main façade wall is the application of a coefficient to take into consideration the height of the tower in the construction. The Italian Circolare [23] recommends to apply an amplification factor to the capacity curve. This amplification factor is described in the equations C7.2.3 and C7.2.4 of the Circolare, which are reported below:

$$S_{am} = S_a R\left(\frac{T_a}{T_i}; \xi_a\right) \quad 4.18$$

$$R = \left[\left(2\xi_a \frac{T_a}{T_i}\right)^2 + \left(1 - \frac{T_a}{T_i}\right)^2\right]^{-\beta} \quad 4.19$$

With S_a the acceleration from the capacity curve, S_{am} the modified acceleration in the case of a tower, R the amplification factor, T_a the period of the tower, T_i the period of the main façade, ξ_a the damping ratio of the tower equal to 5% and β a coefficient equal to 0.5 in this case.

The amplification factor is equal to 1.52, which means that a significant amplification is done.

Case 5: Overturning of the apse (SU5)

This case is similar to the first case. The only difference between the overturning of the apse and the façade is the complex geometry of the apse. It is assumed that the failure due to the mechanism will appear as a diagonal crack from the top corners of the apse to the middle point of the bottom of the macroelement as illustrated in Figure 4.17. In this figure, the dome of the apse is not represented. The geometrical properties of this elements such as its volume or barycentre are given by the software used to model the element. The same procedure is done in order to determine the weight of the vault.

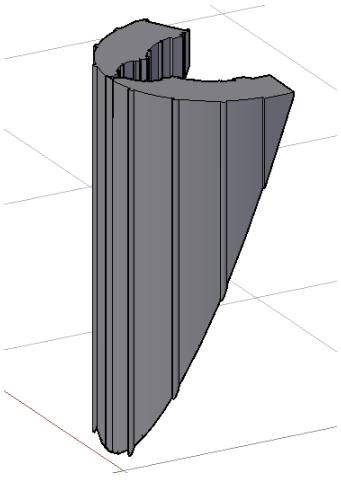

Figure 4.17. 3D view of the block whose detachment causes the failure of the apse (SU5)

In this case, the horizontal thrust of the vault has a large influence in the activation of the mechanism. This force H applied on top of the dome can be estimated according to the following equation:

$$H = P\frac{d_c}{h} \qquad 4.20$$

With P the weight of the vault, d_c the distance between the application of P and the external part of the apse and h the height of the vault.

4.2.2.2 **Results**

In order to perform the methodology and determine the performance, the spectra corresponding to La Seu d'Urgell have been calculated.

As illustrated in Figure 3.6, according to the Eurocode 8, the soil type of this city is a type A. This type corresponds to a velocity of the shear waves higher than 800 m/s. The corresponding type of soil in the Spanish code [42] is the type I. For this soil, the coefficient C is equal to one. Moreover, the annex of the document gives a value of 1 for K in the case of La Seu d'Urgell. This annex also indicates a value of 0.06g for the basic seismic acceleration considered for this city. As the building has a special importance, this value should be multiplied by 1.3. Finally, the basic acceleration should also be multiplied by a coefficient related to the amplification due to the soil. The expression of this coefficient S is given in the section 2.2 of the Spanish code and is equal to 0.8 in this case. The value of the acceleration of calculation a_c is 0.0624 g. The characteristic periods are related to the coefficients K and C as illustrated by the Equation 4.21.

$$T_A = K\frac{C}{10} = 0.1 \quad \text{and} \quad T_B = K\frac{C}{2.5} = 0.4 \qquad 4.21$$

According to the Spanish national annex to the Eurocode 8 [45], the acceleration a_g is equal to 0.116 g. Moreover, the elastic spectrum is calculated for a damping ratio of 5%, which means that the coefficient η is equal to 1. The rest of the parameters is given in the Table 3.2 of the Eurocode, for a soil of type A, and reported in the Table 4.8.

Table 4.8. Numerical values of the elastic spectrum's parameters

S	T_B (s)	T_C (s)	T_D (s)
1.0	0.15	0.4	2.0

For each case described in section 4.2.2.1, the CSM and the N2 method described in section 2.3.2 were applied to both spectra. The following section presents the results obtained.

The Figure 4.18 and Figure 4.19 show the position of the performance point calculated with the N2 method for the two cases related to the overturning of the main façade (SU1 and SU2). It is possible to see that the intersection of the capacity curve and the demand curve in all the cases is in the elastic part of the capacity curve. According to this, no reduction needs to be applied and the solution is the intersection of the two curves. Moreover, as the elastic period T^* is higher than T_B in the case of the Spanish code and T_C in the case of the Eurocode, the results from the CSM and the N2 method are similar.

It is noticed that the two demand spectrum are different. This difference is due to the value of the seismic acceleration of calculation. Indeed, this value is twice smaller in the case of the Spanish code and seems to be too low taking into account the proximity of the city with the Pyrenees, where the epicentres of several important past earthquakes have been located.

It is observed in the figures that in the two cases (SU1 and SU2) the performance points calculated with the Spanish code and the Eurocode are in the damage level D1. This means that these two failure mechanisms are not very vulnerable, and they will not cause severe damage to the structure in the case of an earthquake.

In both cases, the difference between the Spanish code and the Eurocode is low and the conclusion about the vulnerability of the mechanism is identic. However, the acceleration of the performance point of the case SU1 is smaller than for the case SU2. This is due to the stabilization effect of the orthogonal walls. This small difference does not have any impact in the vulnerability of the mechanism because in both cases it is small.

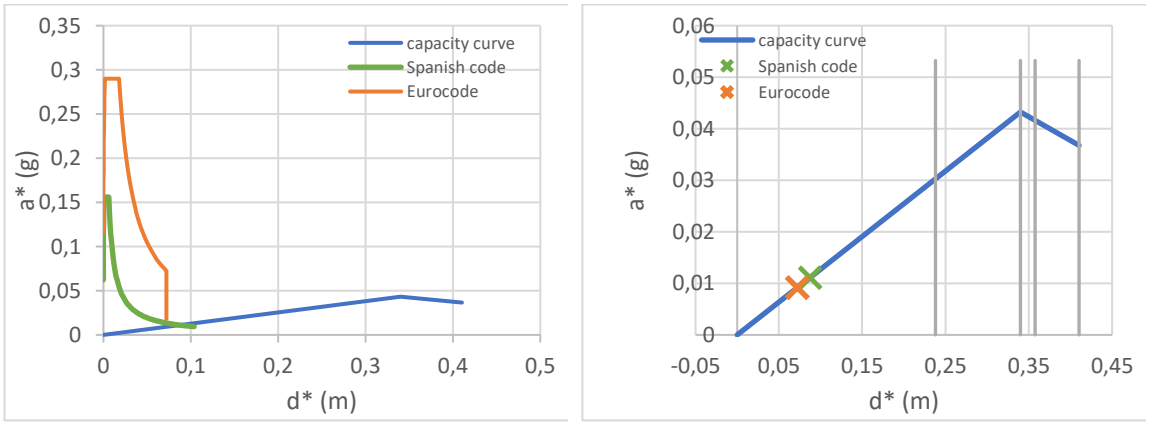

(a) (b)

Figure 4.18. Capacity curve and spectra (a) and Position of the performance point (b) (SU1)

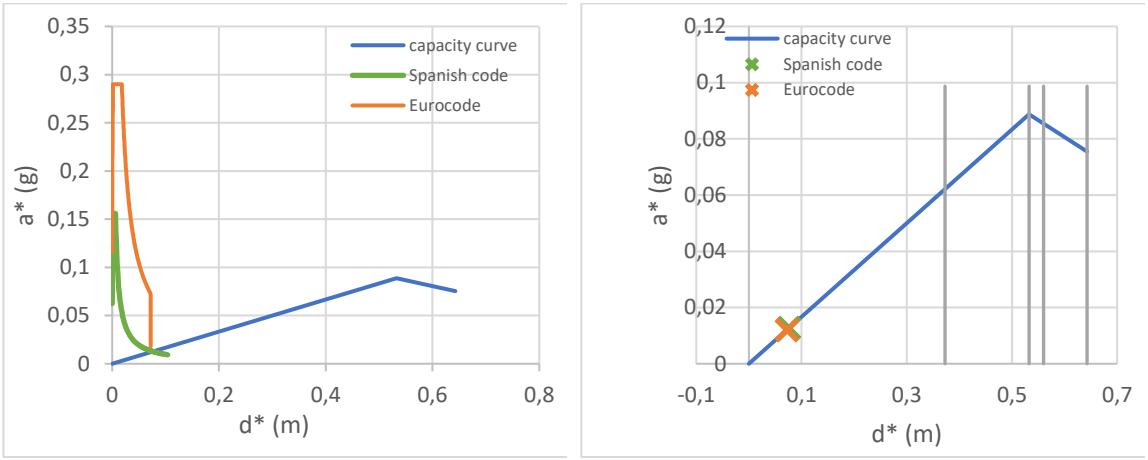

(a) (b)

Figure 4.19. Capacity curve and spectra (a) and Position of the performance point (b) (SU2)

The Figure 4.20 and Figure 4.21 represent the application of the N2 method and the CSM for the case SU3, which is the overturning of the bell tower with a vertical splitting. In this case, it is possible to begin the iteration process for the CSM for the Eurocode 8 as illustrated in Figure 4.21. After some iterations, it is possible to see that the solution tends to be the yielding point of the capacity curve. However, the criterion to stop the iterations has not been attained yet and a higher reduction is not applicable otherwise the result would be in the elastic branch. It is thus considered that the performance point is the yielding point.

By looking at the position of the performance points of the three different methods, it is possible to notice that except for the point from the Spanish code is in a damage level D1, while the points from the Eurocode are in a damage level D3 and D4, which correspond to an important vulnerability of the failure mechanism. This difference might be a consequence of the different values of reference accelerations. Moreover, during the survey, some important damages were noticed regarding the vulnerability of the bell tower. This analysis with the Eurocode 8 [31] shows results in agreement with the observations from the inspection, while the result from the Spanish code analysis are not in agreement with the survey observations.

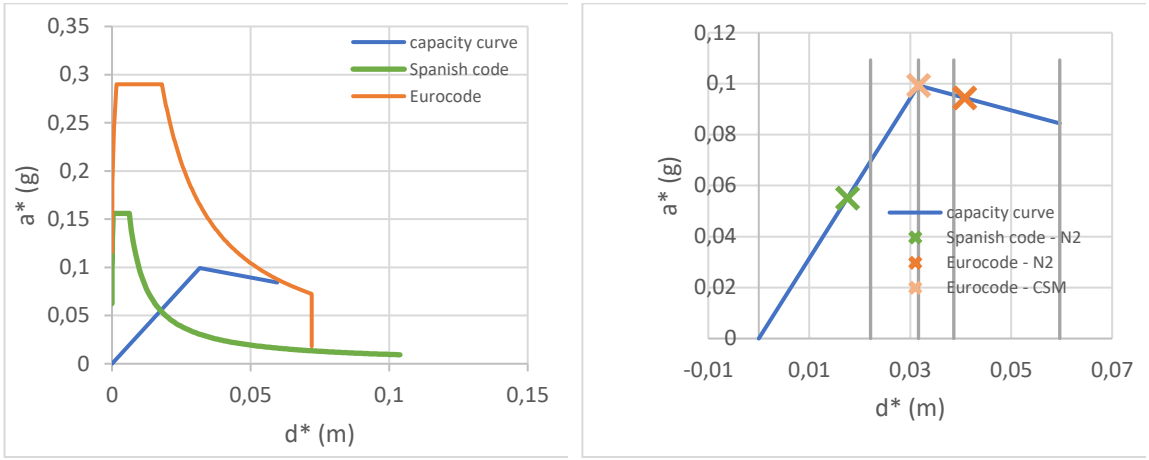

(a) (b)

Figure 4.20. Capacity curve and spectra (a) and Position of the performance point (b) (SU3)

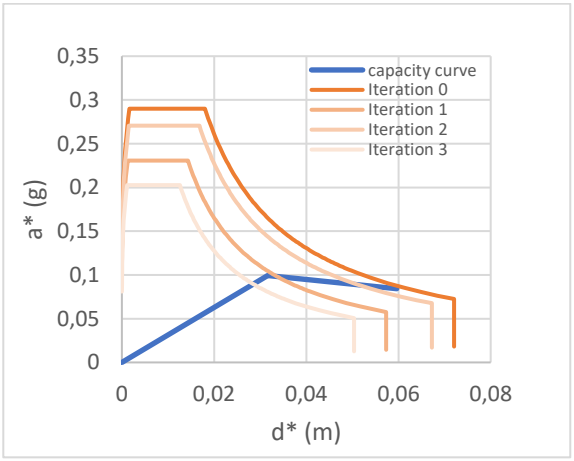

Figure 4.21. CSM for the Eurocode (SU3)

The Figure 4.22 represents the results of the case SU4, which is the overturning of the tower as a monolithic block. In this case, as the intersections of the capacity curve and the demand curves are in the elastic part, the solution from the CSM is directly these intersections and it is not necessary to reduce the spectra.

The two performance points indicate a damage level D1, which means a very low vulnerability of the mechanism. This results, different from the previous one, indicates that the failure of the bell tower might occur by a vertical splitting of the tower and not by the rotation of the entire tower as a monolithic block.

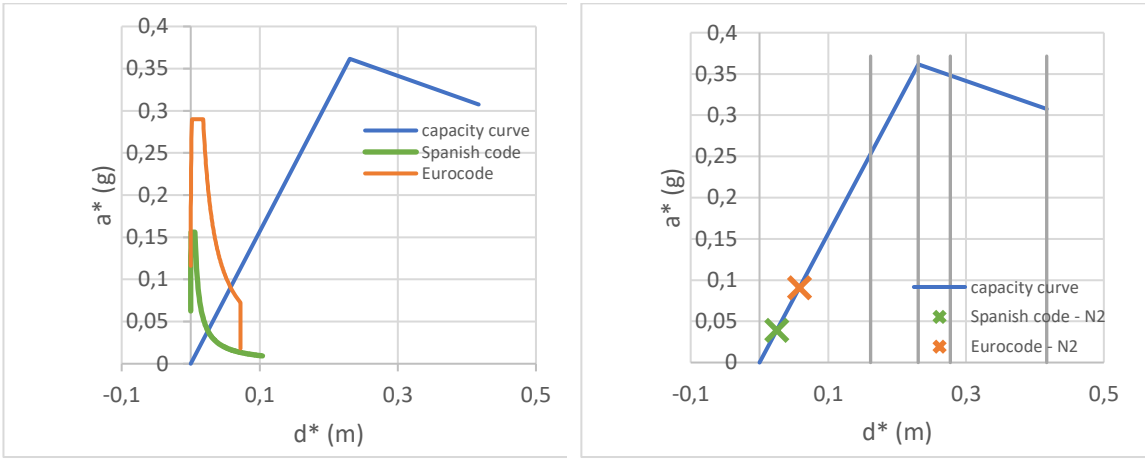

(a) (b)

Figure 4.22. Capacity curve and spectra (a) and Position of the performance point (b) (SU4)

In the case of the overturning of the apse, it is noticed that if the thrust of the dome is taken into account in the calculation, then the maximal acceleration become negative (-0.185 g). This means that the equilibrium is not possible, and the apse is not able to sustain the horizontal thrust. Another interpretation of this result is the fact that the dome of the apse could be decomposed as transversal arches instead of radial ones, which will produce a thrust against the lateral walls instead of the central nave.

An alternative solution is analyzed by considering a horizontal thrust equal to zero, which means that a cohesion exists between the blocs. The Figure 4.23 represents the results of this solution. In this case, the intersections of the capacity and the demand curves are in the elastic part of the capacity curve, which means that it is not necessary to reduce the spectra for the application of the CSM. In all the cases, the performance points are located in the damage level D1, which means that this mechanism has a low vulnerability. However, the assumption consisting in neglecting the horizontal thrust might be too strong, which means that in reality, this mechanism might be more vulnerable than illustrated with this alternative solution.

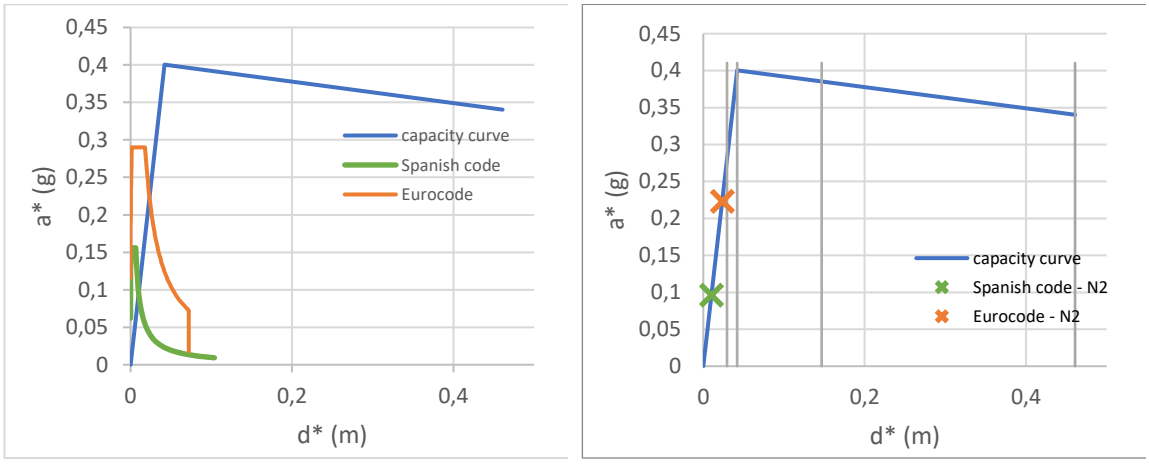

(a) (b)

Figure 4.23. Capacity curve and spectra (a) and Position of the performance point (b) (SU5)

According to the results, it is possible to say that the overturning of the main façade and the apse are not vulnerable mechanisms while the overturning of the bell tower is a mechanism more vulnerable. This conclusion is similar to the conclusions made during the inspection regarding the vulnerability of the tower due to its position and the damage already visible. However, a more detail analysis of the apse and of the transmission of the loads from the rest of the church and from the dome should be done to conclude about its vulnerability.

4.2.3 Vilabertran

4.2.3.1 Presentation of the local mechanisms studied

Three main mechanisms are studied for the church of Vilabertran: the overturning of the main façade, the overturning of the bell tower and the overturning of the apse. The overturning of the transept façade is not studied because the development of this mechanism is stopped by the dormitory in one side and the buttresses in the other side. The following paragraphs will describe all the cases analysed for these two mechanisms and the assumptions made for the calculations.

Case 1: Overturning of the central part of the main façade (V1)

In this first case, only the central part of the main façade is studied, as illustrated in Figure 4.24. This case was studied in order to study the overturning of the main façade without the participation of the bell tower in the mechanism. As the thickness is constant along the façade, the wall is considered as a monolithic block. There are no orthogonal walls connected to this part of the façade.

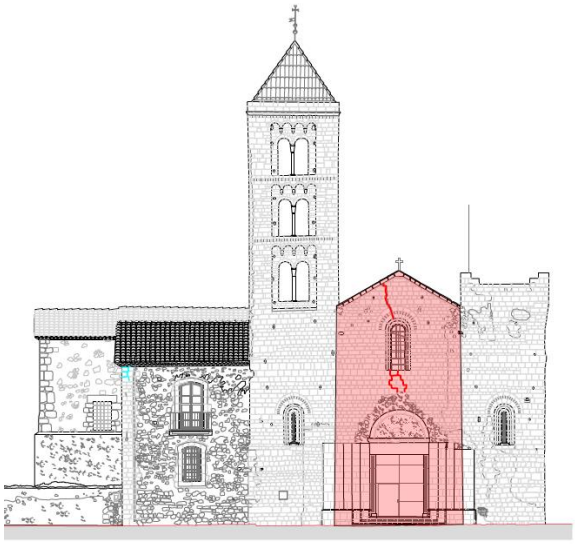

Figure 4.24. Overturning of the main façade of Vilabertran (V1)

As for the previous church, the walls are three-leave walls and similar assumptions are made for this church. The thickness of the external leaf is equal to 0.2 m and the mechanical properties of the façade are summarized in Table 4.9.

Table 4.9. Mechanical properties (V1)

Thickness (m)	W (kN/m^3)	F_m (N/mm^2) external leaf	F_m (N/mm^2) internal leaf	E (N/mm^2)
0.2 – 1.1 – 0.2	19.80	7	1.50	1385

Case 2: Overturning of the main façade with the bell tower (V2)

The second overturning mechanism takes into consideration the entire façade with the tower as illustrated in Figure 4.25. This case is similar to the case SU1: the main part of the façade and the bell tower are modelized as two monolithic blocks of different thickness. The connection between orthogonal walls is assumed to be deficient, which means that the orthogonal walls do not participate to the failure mechanism. As the thickness of the tower is lower than the main façade, the mechanical properties are different. The properties of the tower are summarized in Table 4.10.

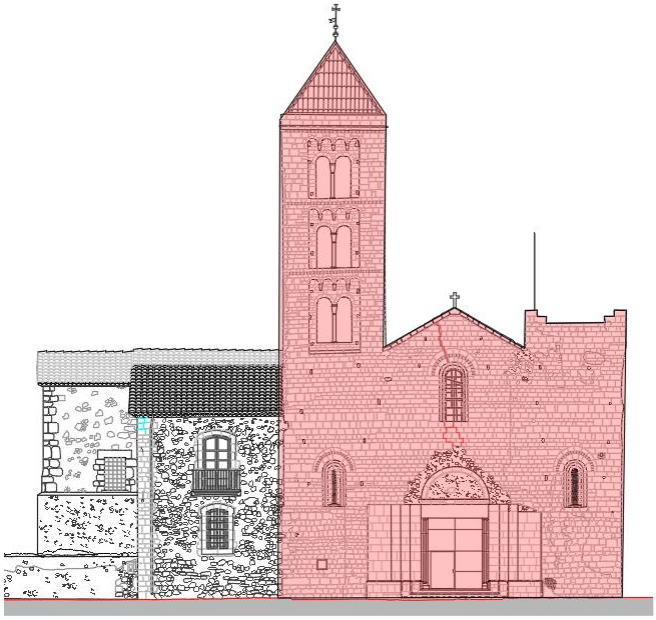

Figure 4.25. Overturning of the main façade of Vilabertran (V2)

Table 4.10. Mechanical properties of the tower

Thickness (m)	W (kN/m^3)	F_m (N/cm^2) external leaf	F_m (N/cm^2) internal leaf
0.1 – 0.3 – 0.1	20.80	700	140

Case 3: Overturning of the main façade with the participation of the vault (V3)

By looking at the cracks in the vault of the central nave, it is possible that the cracked part of the vault participates to the overturning mechanism. According to this, this case considers the entire façade and a part of the vault as illustrated in Figure 4.26.

The geometry of the vault given in the drawing allowed to determine the self-weight of the vault. Because of a lack of information regarding the composition of the vault, it is assumed that the density of the vault is similar to the façade wall. Moreover, the load from the cover on top of the vault is equal to 3 kN/m^2.

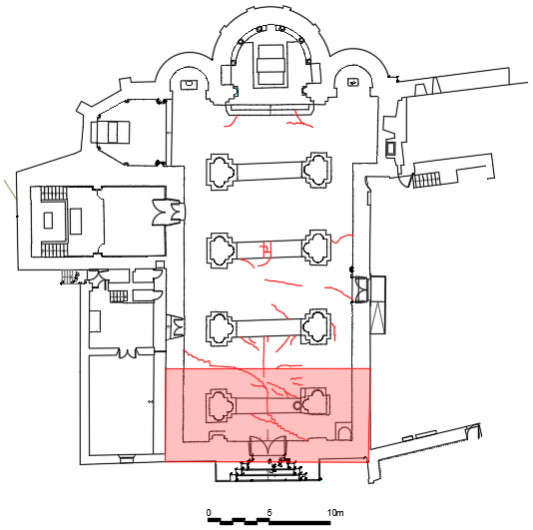

Figure 4.26. Part of the vault included in the mechanism (V3)

Case 4 and 5: Overturning of the bell tower (V4 and V5)

The cases V4 and V5 are similar to the cases SU3 and SU4 of the previous church. The same assumptions are made for both churches. The only differences are the material properties and the geometry of the tower. In this case, the amplification coefficient that should be applied because the tower is an element in a high position in the church is equal to 1.41.

Case 4 and 5: Overturning of the apse (V6)

This case is similar to the case SU5. The same calculation has been made to determine the horizontal thrust. The shape of the macroelement is given in Figure 4.27.

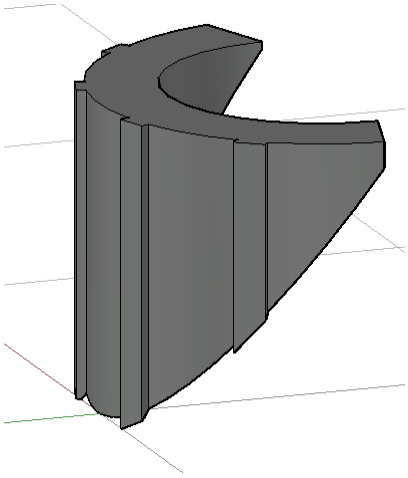

Figure 4.27. 3D view of the block whose detachment causes the failure of the apse (V6)

4.2.3.2 **Results**

For each case described in section 4.2.3.1, the CSM and the N2 method described in section 2.3.2 were applied to both spectra: from the Spanish code and from the Eurocode 8. In the case of Vilabertran, the constants of the Spanish code [42] and the Eurocode 8 [31] to determine the elastic spectrums are resumed in the Table 4.11 and Table 4.12. The following section presents the results obtained.

Table 4.11 Numerical values of the elastic spectrum's parameters from the Spanish code [42]

T_A (s)	T_B (s)	K	C	a_c (g)	S
0.13	0.52	1	1.3	0.108	1.04

Table 4.12. Numerical values of the elastic spectrum's parameters from the Eurocode 8 [31]

S	T_B (s)	T_C (s)	T_D (s)	a_g (g)
1.2	0.15	0.5	2.0	0.113

The Figure 4.28 illustrates the position of the performance points for the overturning of the central part of the façade and the Figure 4.29 represents the application of the CSM to the two spectra. It is possible to observe that except for the N2 method applied to the Eurocode spectrum; all the performance points are in the damage level D3. The last case corresponds to a damage level D4. In all cases, this means that the mechanism is vulnerable.

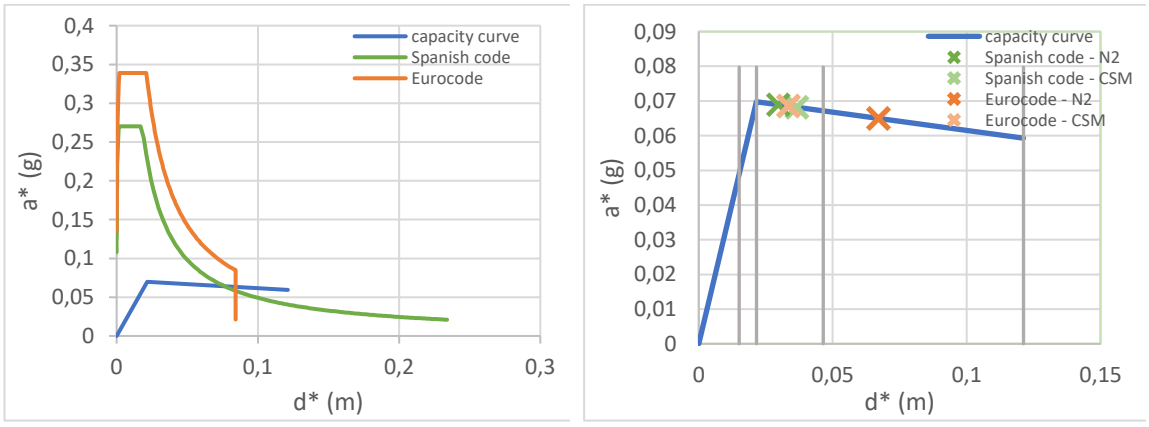

(a) (b)

Figure 4.28. Capacity curve and spectra (a) and Position of the performance point (b) (V1)

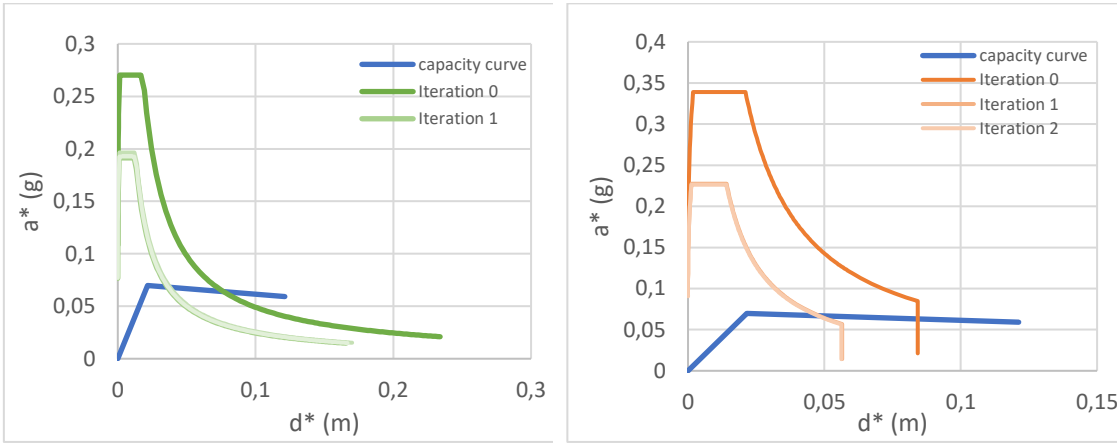

(a) (b)

Figure 4.29. CSM for the Spanish code (a) and CSM for the Eurocode 8 (b) (V1)

The Figure 4.30 shows the performance points of the overturning of the entire façade, including the bell tower. In this case, the application of the CSM consists on taking the intersection between the capacity curve and the demand curve without applying any reduction to the demand curve. Moreover, in both cases, Spanish code and Eurocode, the performance point corresponds to a damage level D1. This means that this mechanism is not very vulnerable in the sense that it will not experience meaningful damage subject to the earthquake considered. It is possible to observe that this mechanism is less vulnerable than the previous one due to the largest section considered.

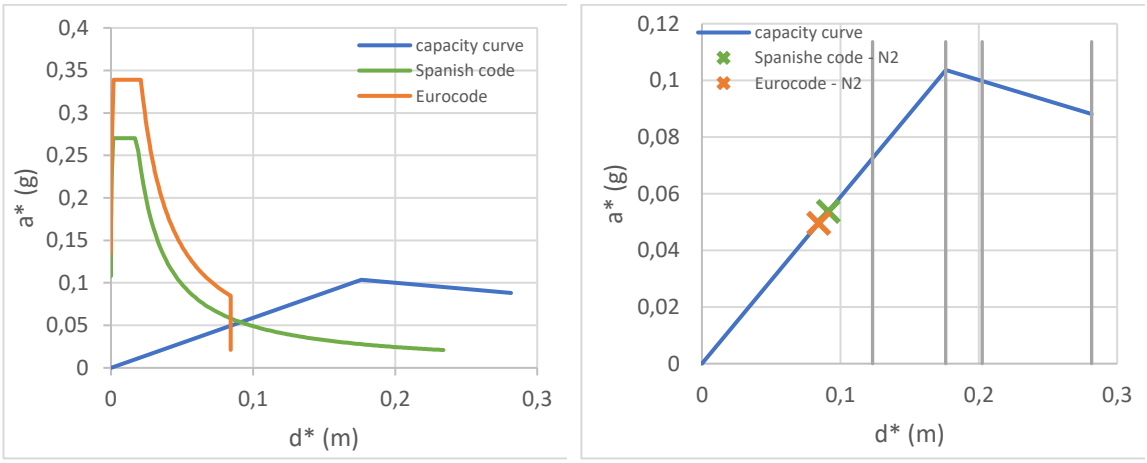

(a) (b)

Figure 4.30. Capacity curve and spectra (a) and Position of the performance point (b) (V2)

The Figure 4.31 represents the performance points of the overturning of the façade and a part of the vault. As expected, the maximal acceleration is higher than for the previous cases, there is a ratio of 10 between them. This large difference is due to the amount of mass participating to the failure mechanism, which help resisting to the activation of the mechanism in an easiest way than the two other cases. As this capacity curve is ten times higher than the previous ones, the maximal values of the demand curves are lower than the maximal value of the capacity curve. According to this, the performance points are located in the elastic part of the capacity curve and correspond to a damage level D1. This means that this failure mechanism presents a very low vulnerability.

This case was created because of the presence of some cracks in the vault. Regarding the results of the analysis, it is possible to assume that these cracks will not activate this mechanism, which is not very vulnerable, but they might be linked to another mechanism.

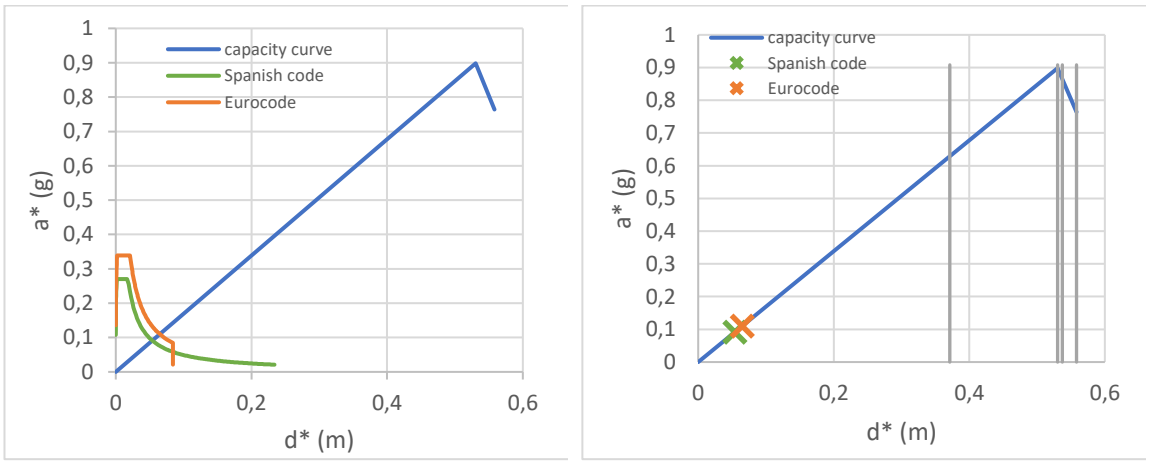

(a) (b)

Figure 4.31. Capacity curve and spectra (a) and Position of the performance point (b) (V3)

The Figure 4.32 represents the application of the N2 method to the overturning of the bell tower (V4). By looking at the position of the performance points, it is observed that they are all corresponding to a damage level D2. The value of the Eurocode 8 is close to the yielding point of the capacity curve.

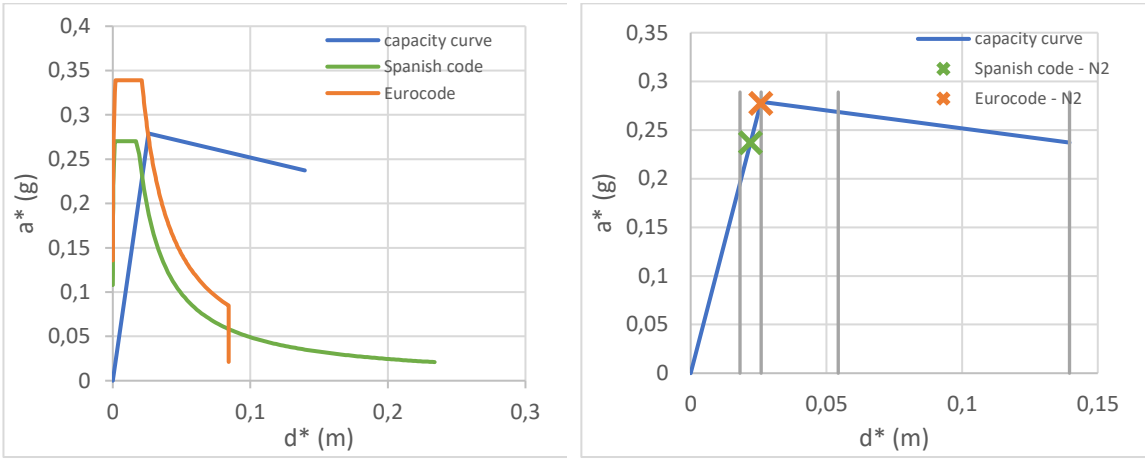

(a) (b)

Figure 4.32. Capacity curve and spectra (a) and Position of the performance point (b) (V4)

The Figure 4.33 illustrates the position of the performance points for the overturning of the bell tower (V5). The results from the Spanish code correspond to a damage level D1, while the results from the Eurocode to a damage level D1-D2. In both cases, the acceleration of the performance point is higher than the acceleration given by the codes. This means that this failure mechanism is not vulnerable. Moreover, as the values of the acceleration are lower than for the previous case and the damage level is lower, it is possible to conclude that the overturning of the tower as a monolithic block is less vulnerable than the overturning of the bell tower with vertical splitting.

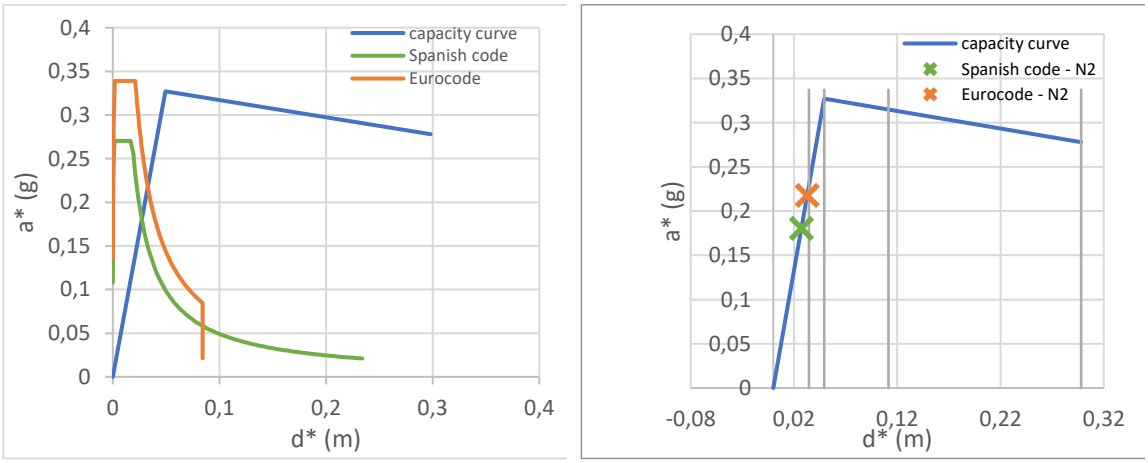

(a) (b)

Figure 4.33. Capacity curve and spectra (a) and Position of the performance point (b) (V5)

As for the apse of the church of La Seu d'Urgell, the results of the analysis by taking into consideration the horizontal thrust give a negative value of maximal acceleration (-0.205 g). The same alternative analysis is made in order to have an idea of the vulnerability of this mechanism.

The Figure 4.34 illustrates the results of this solution. It is possible to see that all the performance points are located in a damage level D1. This damage level indicates a low vulnerability which can corresponds to the damages observed during the survey. However, as for the apse of La Seu d'Urgell, this alternative solution might not correspond to the real performances of the structure.

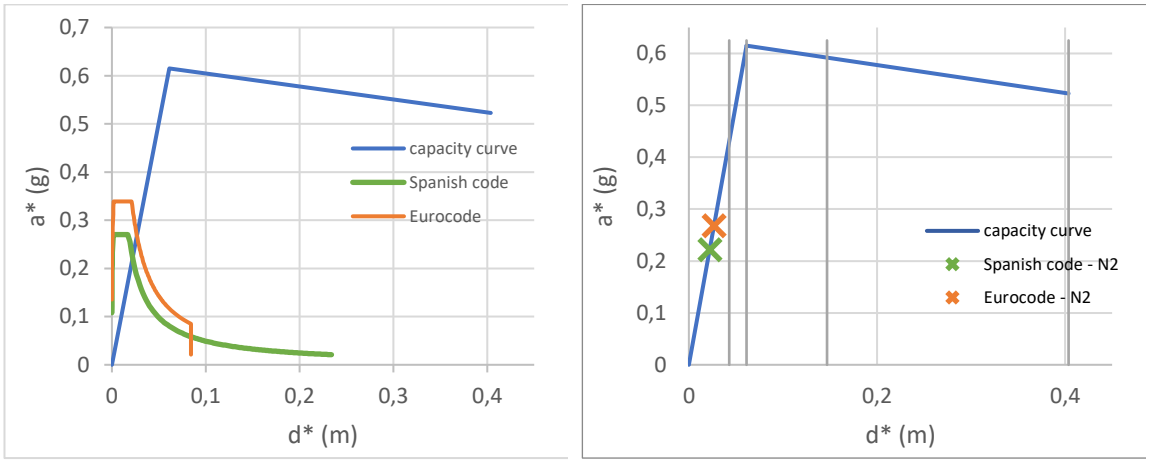

(a) (b)

Figure 4.34. Capacity curve and spectra (a) and Position of the performance point (b) (V6)

The results of the analysis indicate that the overturning of the main façade, the overturning of the bell tower and the overturning of the apse are not vulnerable mechanisms. According to the damages observed in the church, it would also be interesting to study the shear mechanism in the main façade or the mechanism related to the failure of the vaults.

5. CONCLUSIONS

5.1.1 Vulnerability index

By looking at the results of the vulnerability index for both churches, it is noticed that they both have a high vulnerability index. However, the church of La Seu d'Urgell seems to be more vulnerable than the church of Vilabertran.

During the inspection, the church of Vilabertran seemed to be more damaged than La Seu d'Urgell because of the numerous and large cracks in the vault and the main façade. In La Seu d'Urgell, the cracks were smaller and the only element that is really vulnerable is the bell tower leaning on top of the façade. However, the damage index indicates different results. The value for La Seu d'Urgell is higher than for Vilabertran. Moreover, these damage indices are too low compared to the probabilistic value obtained with the vulnerability index for an earthquake intensity corresponding to the maximal earthquake that occurred. This phenomenon has been observed in other studies and it is due to the fact that the damage index gives low results in the case of localized damages. With this method the peaks of damage are not taken into consideration. The amount of damages might also be influenced by the type of soil, which is not included in the parameters of the damage index or the vulnerability index.

Some steps of the vulnerability index method are susceptible to engineering judgement, which can lead to different results in function of the person applying the method. Moreover, in some buildings, it is possible to see some elements that seem to be vulnerable, but they are not in the list of the 28 mechanisms suggested by the Italian standards. During the inspection of these two churches, one of the issues noticed concerns the evaluation of a mechanism corresponding to a macroelement present in different places such as the transept façade or the chapels. In some cases, the vulnerability indicators were not the same in all the macroelements and the worst case was considered.

A second issue during the survey concerns the evaluation of the damages. In many cases, and in particular for the damages in the vault, it is complicated to identify the cause of the damages and thus to know which mechanism is responsible for these damages. It is also observed that some damages might not correspond to any mechanism and could be a result of degradation not caused by an earthquake but by some soil settlement or other factors.

The last problem observed during the application of the vulnerability index method concerns the calibration of the equation to determine the mean damage grade. This equation was calibrated for Italian churches and soils and might not be applied to the case of churches of Catalonia.

5.1.2 Kinematic limit analysis

The kinematic limit analysis is a good method to analyze quickly the behavior of a local mechanism. With this method, it was possible to determine that for the church of La Seu d'Urgell, the most vulnerable mechanisms are the overturning of the bell tower and the apse, while for the church of Vilabertran none of the mechanisms analyzed seem to have a significant vulnerability. In order to determine the most vulnerable element of a church, some other mechanisms should be analyzed such as the shear mechanism in the façade wall or some mechanisms related to the damage of the vaults.

The application of this method has pointed some issues linked to these specific cases studied or to more general cases. The first issue concerns the difficulty to identify the mechanism that should be studied and more specifically the connections within the macroelement studied and with the other elements surrounding it. Another difficulty is linked to the composition of the walls of a church. As in many cases it may not be possible to know exactly the material and the connection between the different leaves, it is complicated to determine how the failure will occur.

The last important issue is the large difference between the reference acceleration in the Spanish code [42] and in the national annex of the Eurocode 8 [45]. This difference in mainly observed for the church of La Seu d'Urgell, and it is observed that for some mechanisms the vulnerability is different for both codes. The value given by the Spanish code may be considered low regarding the localization of the city and the proximity of the Pyrenees.

5.1.3 General conclusion

The two methods applied in this thesis highlighted the vulnerability of the two churches studied. The church of La Seu d'Urgell is an important church of the Pyrenees, built in the 12th century, with some damages probably related to natural decay. The vulnerability index method indicates that this church is not able to sustain the seismicity of the region due to its high vulnerability. Moreover, the kinematic limit analysis highlighted the high vulnerability of the bell tower leaning on top of the façade. According to this, it might be necessary to analyze more in detail the behavior of this element and to think about some retrofitting strategy to improve the ability of the church to resist to an earthquake.

The church of Vilabertran is a more modest church built also in the 12th century, showing significant damage. The vault of the nave is severely cracked, and the main façade shows cracks related to shear mechanism. The damages of this church might be due to an important earthquake that occurred in 1428. The vulnerability index method indicates that the church might not be able to sustain the seismicity of the region if the references from the national annex of the Eurocode 8 are used. However, the kinematic limit analysis did not highlight vulnerable macroelements in the

church. In order to investigate other vulnerable macroelements of this church, it might be interesting to analyze other mechanisms such as the shear in the façade or the mechanisms related to the failure of the vault, which could induce the damages observed in the church during the survey.

In this thesis, it is observed that a fast and empirical method like the vulnerability index method or an analysis of simple macroelements can be sufficient to find the vulnerable points of an ancient church. However, in order to obtain more accurate results, the geometry and the properties of the material should be known in a more precise way. This would allow to find accurate models to represent the entire church or a part of it and to better identify the weaknesses of the structure.

In order to improve the results obtained and continue the analysis, it is possible in a first time to try to calibrate the formula of the mean damage grade to the churches of Catalonia. Then it might be interesting to apply the new version of the Italian Survey Form described in the state of art, which take into the consideration the peak of damage. This might lead to more accurate results in term of damage index. Concerning the kinematic limit analysis, it is possible to analyze other mechanisms or to try to improve the previous ones with experimental tests in order to identify the connections between macro elements. Finally, it is also possible to continue the analysis by trying to apply retrofitting strategy and analyzing the impact in the behavior of the structure.

6. REFERENCES

[1] G. Grünthal, *EMS-98*, A. Levret. Luxembourg, 2001.

[2] G. M. Calvi, R. Pinho, G. Magenes, J. J. Bommer, L. F. Restrepo-Vélez, and H. Crowley, "Development of seismic vulnerability assessment methodologies over the past 30 years," *ISET J. Earthq. Technol.*, vol. 43, no. 3, pp. 75–104, 2006.

[3] S. Lagomarsino, "Linee Guida per la valutazione e riduzione del rischio sismico del patrimonio culturale con riferimento alle norme tecniche per le costruzioni," pp. 73–80, 2008.

[4] R. V Whitman, "Damage Probabilty Matrices for Prototype Buildings," no. 380, 1973.

[5] F. Braga, M. Dolce, and D. Liberatore, "A Statistical Study on Damaged Buildings and an Ensuing Review of the MSK-76 Scale," *Proc. Seventh Eur. Conf. Earthq. Eng.*, pp. 431–450, 1982.

[6] S. Giovinazzi and S. Lagomarsino, "A Macroseismic Method for the Vulnerability Assessment of Buildings," *Proc. 13th World Conf. Earthq. Eng.*, 2004.

[7] GNDT, *Rischio sismico di edifici pubblici - Parte I: aspetti metodologici*. Bologna: Quasco Centro Servizi, 1993.

[8] G. Brando, G. De Matteis, and E. Spacone, "Predictive model for the seismic vulnerability assessment of small historic centres: Application to the inner Abruzzi Region in Italy," *Eng. Struct.*, vol. 153, no. December 2016, pp. 81–96, 2017.

[9] J. L. P. Aguado, T. M. Ferreira, and P. B. Lourenço, "The Use of a Large-Scale Seismic Vulnerability Assessment Approach for Masonry Façade Walls as an Effective Tool for Evaluating, Managing and Mitigating Seismic Risk in Historical Centers," *Int. J. Archit. Herit.*, vol. 12, no. 7–8, pp. 1259–1275, 2018.

[10] T. M. Ferreira, R. Vicente, J. A. R. Mendes da Silva, H. Varum, and A. Costa, "Seismic vulnerability assessment of historical urban centres: Case study of the old city centre in Seixal, Portugal," *Bull. Earthq. Eng.*, vol. 11, no. 5, pp. 1753–1773, 2013.

[11] P. Angeletti, M. Ferrini, and S. Lagomarsino, "Rilievo e valutazione della vulnerabilità sismica delle chiese: un esempio in Lunigiana e Garfagnana," *Proc. VIII ANIDIS Conf.*, vol. 2, 1997.

[12] S. Lagomarsino, "Damage survey of ancient churches: The Umbria-MArche experience," in *Seismic Damage to Masonry Buildings*, A. Bernardini, Ed. 1998, pp. 81–94.

[13] G. De Matteis, G. Brando, V. Corlito, E. Criber, and M. Guadagnuolo, "Seismic vulnerability

assessment of churches at regional scale after the 2009 L'Aquila earthquake," *Int. J. Mason. Res. Innov.*, vol. 4, no. 1/2, p. 174, 2018.

[14] S. Lagomarsino, "Damage assessment of churches after L'Aquila earthquake (2009)," *Bull. Earthq. Eng.*, vol. 10, no. 1, pp. 73–92, 2012.

[15] S. Lagomarsino, "On the vulnerability assessment of monumental buildings," *Bull Earthq. Engeneering*, 2006.

[16] S. Lagomarsino, S. Cattari, D. Ottonelli, and S. Giovinazzi, *Earthquake damage assessment of masonry churches: proposal for rapid and detailed forms and derivation of empirical vulnerability curves*, no. 0123456789. Springer Netherlands, 2019.

[17] J. Magalhães *et al.*, "Seismic vulnerability of churches in Faial and Pico islands, Azores.," *Proc. 15th world Conf. Earthq. Eng.*, 2012.

[18] A. Bernardini, R. Gori, and C. Modena, "Application of Coupled Analytical Models and Experimental Knowledge to Seismic Vulnerability Analyses of Masonry Buildings," *Eng. Damage Eval. Vulnerability Anal. Build. Struct.*, 1990.

[19] D. F. D'Ayala and E. Speranza, "An Integrated Procedure for the Design of Sustainable Products," no. January, pp. 1351–1356, 2002.

[20] ATC, *Seismic evaluation and retrofit of concrete buildings*. Redwood City: ATC 40, Applied Technology Council, 1996.

[21] N. Kircher, Charles A, "Development of Building Damage Functions for Earthquake Loss Estimation," *Earthq. Spectra*, vol. 13, no. 4, 1997.

[22] S. A. Freeman, "Development and use of capacity spectrum method," *Proc. ofthe 6th U.S. Natl. Conf. Earthq. Eng.*, 1998.

[23] Circolare 21 gennaio 2019 n. 617 Ministero delle Infrastrutture e dei Trasporti, "Istruzioni per l'applicazione delle 'Norme Tecniche per le Costruzioni' di cui al D.M. 14/01/2008," *G.U. n. 47 del 26/2/09 suppl. ord. n. 27*, 2019.

[24] P. Fajfar, "A Nonlinear Analysis Method for Performance-Based Seismic Design," *Earthq. Spectra*, vol. 16, no. 3, pp. 573–592, 2000.

[25] M. Saiidi and M. A. Sozen, "Simple nonlinear seismic analysis of R/C structures," *J. ofStructural Div.*, vol. 107, pp. 937–952, 1981.

[26] F. Conti, *Como reconocer el arte romanico*. .

[27] F. Espanol and J. Yarza, *El Romanic Catalan*. .

[28] Departament d'interior, "Pla especial d'emergències sísmiques a catalunya. SISMICAT," pp. 1–52, 2014.

[29] Institute Cartografic i Geologic De Catalunya, "Seismic Risk Assessment." [Online]. Available: http://www.icgc.cat/en/Public-Administration-and-Enterprises/Downloads/Geological-and-geothematic-cartography/Geophysical-and-seismic-maps/Seismic-risk-assessment.

[30] C. Olivera, E. Redondo, and A. R. Melis, *Els terratrèmols de segles XIV i XV a Catalunya*. 2006.

[31] E. C. D. E. Nantes, "NF EN 1998-1 / NA Eurocode 8 - Calcul des structures pour leur résistance aux séismes - Partie 1 : Règles générales , actions sismiques et règles pour les bâtiments - Annexe nationale à la NF EN 1998-1 (Indice de classement : P06-030-1 / NA)," vol. 1, no. décembre 2013, 2015.

[32] "ICGC soil map." .

[33] "La Seu d'Urgell medieval." [Online]. Available: http://www.laseu.cat/turisme/historia.

[34] J. Mestre i Godes and J.-A. Adell, *Les valls pirinenques, Viatge al romanic catala 1*. .

[35] J.-A. Adell, *La Catedral de La Seu d'Urgell*, Angle Edit. .

[36] *Catalunya romanica VI, L'Alt Urgell Andorra*. Barcelona, 1992.

[37] J. Cobreros, *Las rutas del romanico en espana volumen II*. .

[38] NTC 2008, "CIRCOLARE 617.2009 - Istruzioni per l'applicazione delle NTC 2008 (appendice)," pp. 355–434, 2009.

[39] M. Golobardes, *El Monasterio de Santa Maria de Vilabertran*. 1949.

[40] *Catalunya romanica IX, L'Alt Emportada*. Barcelona, 1992.

[41] S. Lagomarsino and S. Podestà, "Seismic vulnerability of ancient churches: II. Statistical analysis of surveyed data and methods for risk analysis," *Earthq. Spectra*, vol. 20, no. 2, pp. 395–412, 2004.

[42] A. Paniagua and J. C. R, "Norma de Construccion Sismorresistente," pp. 35898–35967, 2002.

[43] Z. V. Milutinovic and G. S. Trendafiloski, "RISK-UE An advanced approach to earthquake risk scenarios with applications to different European towns WP4: Vulnerability of current buildings," *Eur. Com.*, 2003.

[44] G. Milani, "Vulnerability Evaluation of Historical Masonry Structures: Italian Churches and Towers," in *Structural Analysis of Historical Construction*, Springer, Ed. 2019, pp. 19–32.

[45] F. N. Gazeta, "Anejo Nacional AN/UNE-EN 1998-1," 1998.

APPENDIX A: DESCRIPTION OF THE FIRSTS 18 MECHANISMS OF THE VULNERABILITY INDEX METHOD[2]

THE FACADE

1. OVERTURNING OF THE FACADE
   damage: separation of the facade from the lateral walls, in proximity to the corner or with curved cracks in the lateral walls
   vulnerability: 1. bad connection between the facade and the lateral walls
   2. lack of longitudinal tie rods or buttresses
2. OVERTURNING OF THE GABLE
   damage: separation of the top of the facade in parts
   vulnerability: 1. presence of wide openings that weaken the facade (rose window)
   2. lack of connection with the roof covering (hammering of the ridge beam)
3. SHEAR MECHANISMS IN THE FACADE
   damage: cracks in the facade with X trend; central vertical crack; arched crack near to the corner
   vulnerability: 1. presence of wide openings, even if closed with masonry
   2. roof thrusting on the lateral walls and lack of transversal tie rods

THE NAVE AND THE TRANSEPT

4. TRANSVERSAL VIBRATION OF NAVE OR OF THE TRANSEPT
   damage: cracks in the structural arches; rotation of the lateral walls, with crushing or opened cracks near to the base of the pillars
   vulnerability: 1. lateral walls too slender
   2. lack of transversal tie rods or buttresses

5. LONGITUDINAL VIBRATION OF THE CENTRAL NAVE
   damage: cracks in the longitudinal arches; crushing or opened cracks at the base of the column; diagonal shear cracks in the vaults of the lateral naves
   vulnerability: 1. slender columns and central nave very high with respect to the lateral ones
   2. lack of longitudinal tie rods
6. VAULTS OF THE CENTRAL NAVE
   damage: damage in the vaults, with disjointedness from the stiffening arches
   vulnerability: 1. vaults too lowered and/or too thin
   2. presence of concentrated actions from the roof covering (wooden prop)
7. VAULTS OF THE LATERAL NAVES AND OF THE TRANSEPT
   damage: damage in the vaults, with disjointedness from the stiffening arches
   vulnerability: 1. vaults too lowered and/or too thin
   2. presence of concentrated actions from the roof covering (wooden prop)

THE TRIUMPHAL ARCH

8. KINEMATISM IN THE TRIUMPHAL ARCHES
   damage: formation of hinges in the arch, with opened cracks, crushing of masonry and sliding of stone ashlar
   vulnerability: 1. thickness of the arch too thin or presence of masonry of bad quality
   2. lack of tie rods or bad positioned; insufficient propping from the lateral walls

THE DOME AND THE TIBURIO

9. COLLAPSE OF THE DOME AND THE TIBURIO
   damage: formation of a continuum arched crack in the dome; cracks in the tambour
   vulnerability: 1. tambour very high and slender (with big openings)
   2. lack of ringing tie rods and of external buttresses

THE APSE

10. OVERTURNING OF THE APSE
    damage: vertical cracks in correspondence of the windows; inclined arched cracks
    vulnerability: 1. lack of ringing tie rods or of longitudinal tie rods
    2. hammering roof covering or weakening for the presence of big openings
11. VAULTS OF THE APSE AND OF THE PRESBYTERY
    damage: damage in the vaults
    vulnerability: 1. vaults too lowered and/or too thin
    2. presence of concentrated actions from the roof covering (wooden prop)

WIDESPREAD MECHANISMS

12. OVERTURNING OF OTHER WALLS (TRANSEPT FACADE, CHAPELS)
    damage: separation of the end wall from the orthogonal walls
    vulnerability: 1. bad connection between the wall and the orthogonal walls
    2. lack of tie rods or buttresses
13. SHEAR FAILURE OF THE WALLS
    damage: inclined cracks in masonry; disjointedness in the lacks of continuity (closed windows)
    vulnerability: 1. masonry of poor quality or too thin
    2. weakening for the presence of too many openings
14. HAMMERING AND DAMAGE IN THE ROOF COVERING
    damage: cracks in proximity to the support of the beam; disjointedness from the r.c. ring beam and the masonry
    vulnerability: 1. hammering roof, with absence of a link from the wooden beam and the masonry
    2. increasing of the weight and the stiffness of the roof (substitution with a r.c. slab)
15. INTERACTION BETWEEN ELEMENTS OF DIFFERENT BEHAVIOUR
    damage: cracks due to the hammering between different parts
    vulnerability: 1. significant difference in the global stiffness of the two parts of the fabric
    2. lack of a good connection between the masonry in the two parts or of tie rods

THE BELL TOWER

16. GLOBAL COLLAPSE OF THE BELL TOWER
    damage: cracks near to the connection with the church; vertical cracks below the bell cell
    vulnerability: 1. bell tower too slender and made of walls of limited thickness
    2. masonry of poor quality and lack of connection between the walls
17. MECHANISMS IN THE BELL CELL
    damage: cracks in the arches; rotations and sliding of the pillars
    vulnerability: 1. lack of tie rods or hooping ties
    2. pillars too slender and roof too heavy and/or thrusting

BELL GABLE, SPIRES AND PROJECTIONS

18. OVERTURNING OF STANDING OUT ELEMENTS
    damage: global permanent rotations or sliding; cracks at the base of the element
    vulnerability: 1. lack of an effective connection with the church
    2. element too slender

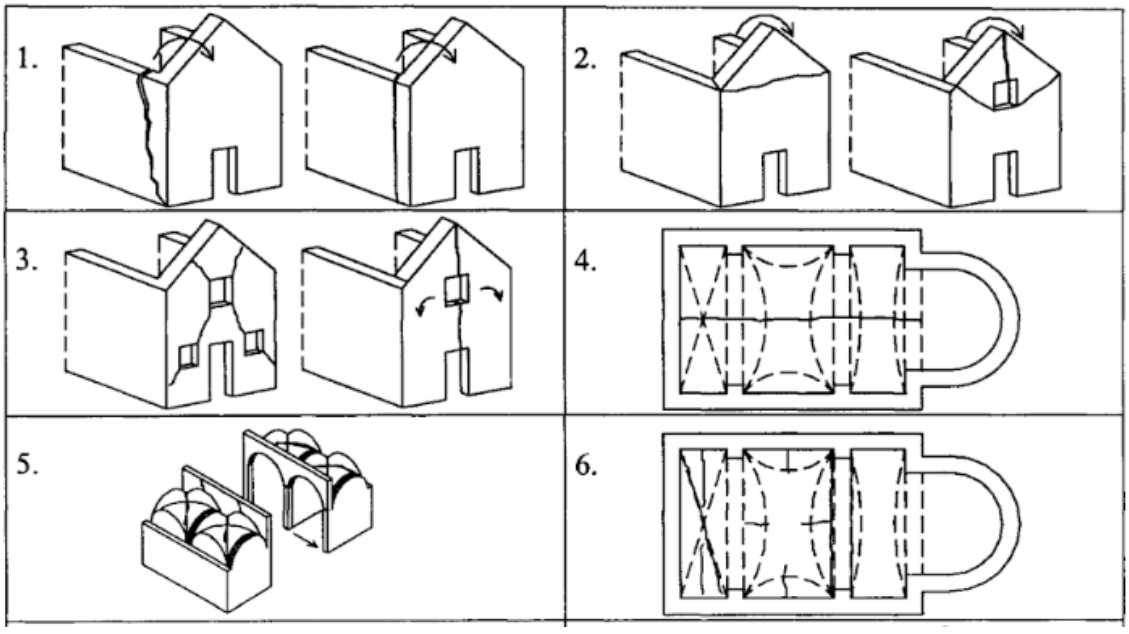

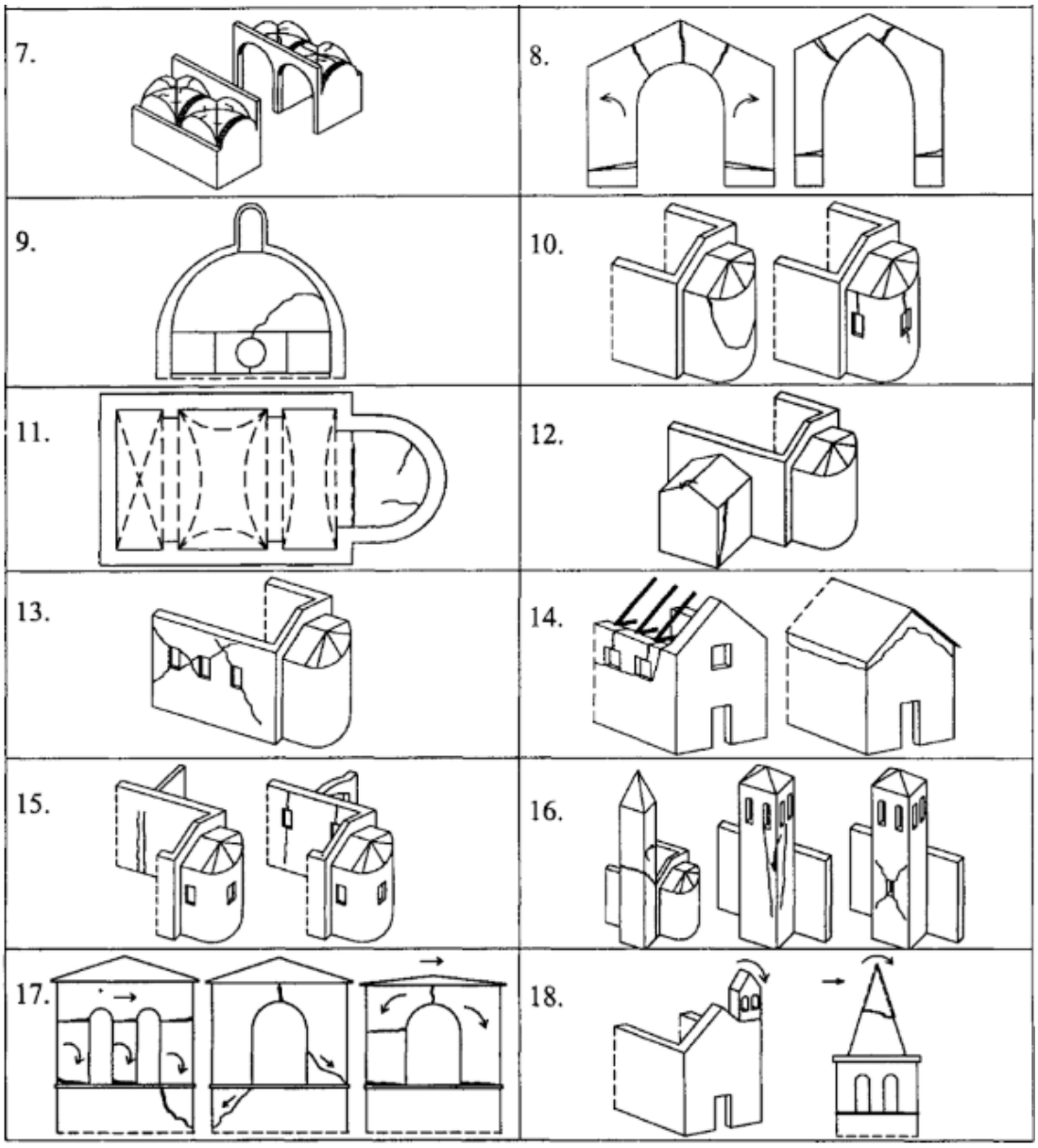
7.
8.
9.
10.
11.
12.
13.
14.
15.
16.
17.
18.

APPENDIX B: DESCRIPTION OF THE 28 MECHANISMS OF THE ITALIAN GUIDELINE

1 – Overturning of the façade	Detachment of the façade from the walls or evident out of plumb *Aseismic measures:* • Presence of longitudinal tie rods • Presence of element of contrast (buttress) • Good quality clamping *Vulnerability indicators:* • Presence of thrusting elements (roof, vault, arches) • Presence of large openings in side walls near corner	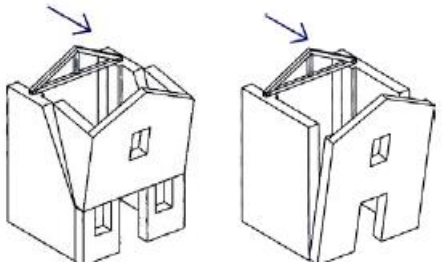
2 - Damage at the top of the façade	Overturning of the gable, with horizontal or V-shaped cracking. Disaggregation of masonry or shifting of tie beams. Rotation of the trusses *Aseismic measures:* • Presence of local connections to roof elements • Presence of roof braces • Presence of lightweight tie-beams *Vulnerability indicators:* • Presence of large openings (rose window) • Presence of large and heavy towering gable • Rigid tie-beams in R-C, heavy roof covering in R-C	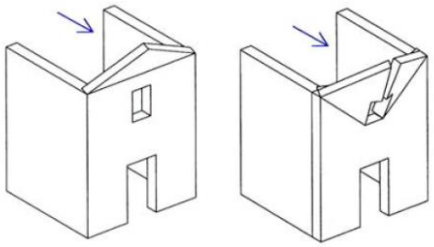
3 – Shear mechanism in the façade	Diagonal cracking (shear). Vertical or arched cracking (rotation). Other cracking or bulging *Aseismic measures:* • Presence of tie rods at the rear of the façade • Lateral contrast supplied by leaning building *Vulnerability indicators:* • Presence of large or numerous openings • Thin vertical elements	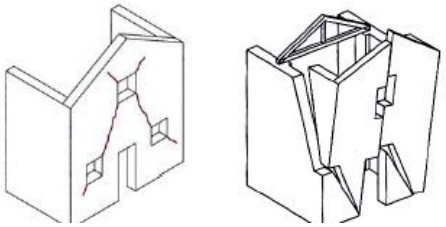
4 - Nartex	Cracking in the arches or in the trabeation due to column rotation. Detachment of the façade. Pounding *Aseismic measures:* • Presence of tie rods • Presence of adequately sized columns/pillars *Vulnerability indicators:* Presence of thrusting elements (roof, vault, arches)	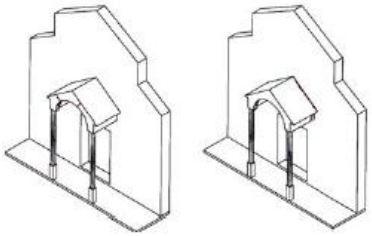

5 - Transversal vibration of the nave	Cracking in transversal arches (that might extend in the vaults). Rotation in side walls. Shear cracking in the vaults. Out of plumb and crushing of columns *Aseismic measures:* • Presence of pilasters or external buttresses • Presence of adjacent leaning building • Presence of transverse tie rods *Vulnerability indicators:* • Presence of very thin walls • Presence of vaults and arches	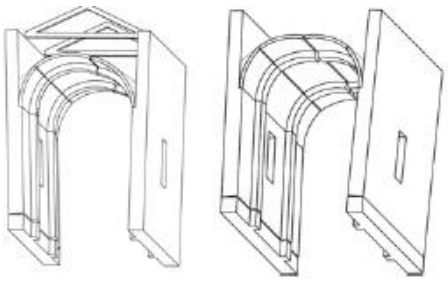
6 – Shear mechanism in the side walls	Diagonal cracking (single or crossed). Cracking next to wall discontinuity. *Aseismic measures:* • Good quality masonry (without different construction phase) • Presence of good architraves over the openings • Presence of lightweight tie-beams *Vulnerability indicators:* • Presence of large openings or wide zone with limited masonry thickness • Very rigid tie-beam, heavy roof covering	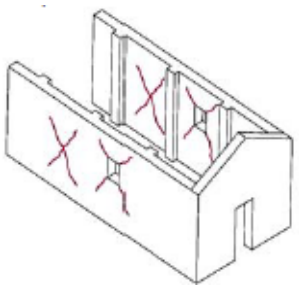
7 – Longitudinal response of the colonnade	Cracking in the arches or in longitudinal architraves. Crushing and/or cracking at the base of the pillars. Shear cracking in vaults or lateral naves. *Aseismic measures:* • Presence of longitudinal tie rods • Presence of buttress in the façade *Vulnerability indicators:* • Presence of large openings or wide zone with limited masonry thickness • Very rigid tie-beam, heavy roof covering	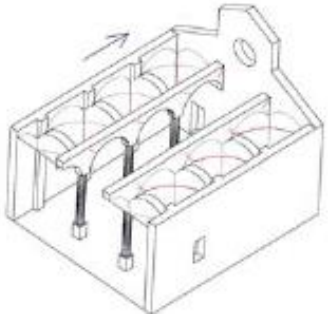
8 – Vault of the nave	Cracking in the vault or the central nave. Detachment of the vaults from the arches *Aseismic measures:* • Presence of effectively placed tie-rods • Presence of external or internal buttresses *Vulnerability indicators:* • Presence of concentrated loads from the roof • Thin vaults, especially if on a wide span • Presence of lunettes or interruption and irregularities	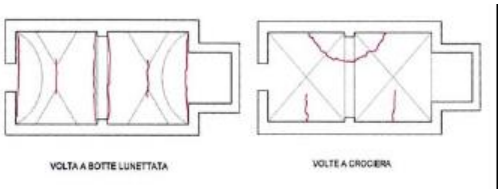

9 – Vault of the aisles	Cracking in the vaults or detachment from the arches or the side walls *Aseismic measures:* • Presence of effectively placed tie-rods • Presence of external or internal buttresses *Vulnerability indicators:* • Presence of concentrated loads from the roof • Thin vaults, especially if on a wide span • Presence of lunettes or interruption and irregularities	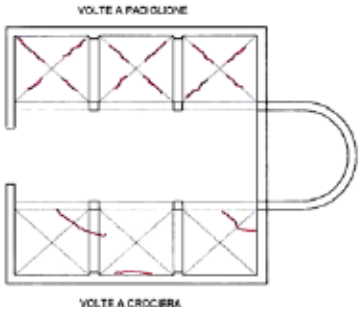
10 – Overturning of the transept façade	Detachment of the end wall from the side walls. Overturning or displacement of the gable *Aseismic measures:* • Presence of tie-rods • Presence of effective propping elements (buttresses, leaning building) • Good connection with roof covering • Good quality side wall to façade clamping • Presence of light weight tie-beams *Vulnerability indicators:* • Presence of rigid tie-beams, heavy roof • Presence of large openings in the façade • Presence of large and heavy towering gable	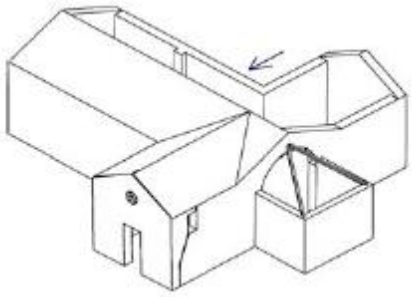
11 – Shear mechanism in the transept walls	Diagonal cracking (single or crossed). Cracking next to wall discontinuities *Aseismic measures:* • Good quality masonry (without different construction phase) • Presence of good architraves over the openings • Presence of lightweight tie-beams *Vulnerability indicators:* • Presence of large openings or wide zone with limited masonry thickness • Presence of stiff tie-beam, heavy roof covering	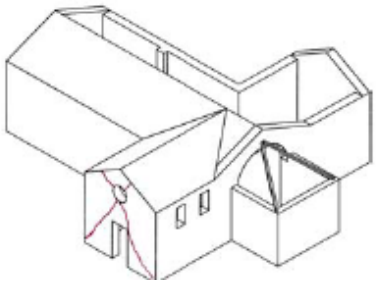
12 – Vault of the transept	Cracking in the vaultsor detachment from the arches and/or the side walls *Aseismic measures:* • Presence of effectively placed tie-rods • Presence of external or internal buttresses *Vulnerability indicators:* • Presence of concentrated loads from the roof • Thin vaults, especially if on a wide span • Presence of lunettes or interruption and irregularities	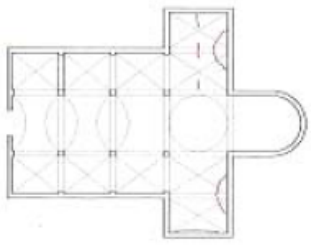

13 – Triumphal arches	Cracking in the arch. Sliding or the ashlars. Crushing or horizontal cracking at the base of piers *Aseismic measures:* • Presence of effectively placed tie-rods • Stiff lateral walls *Vulnerability indicators:* • Presence of heavy roof covering • Presence of dome, drum or tiburio	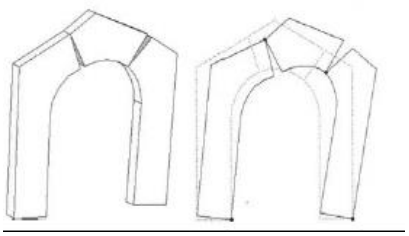
14 – Dome, drum and tiburio	Cracking in the dome (curved) with eventual continuation to the drum *Aseismic measures:* • Presence of external rings, at different height • Presence of external buttresses or pilasters in the drum • Dome placed directly on triumphal arches *Vulnerability indicators:* • Presence of large openings in the drum • Presence of concentrated loads from the roof covering	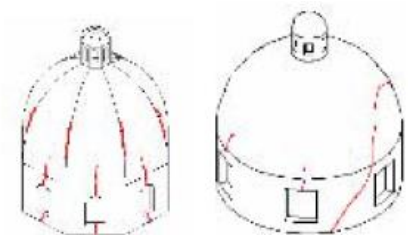
15 -Lantern	Cracking to the smaller dome in the lantern. Rotation or displacement of the piers *Aseismic measures:* • Presence of tie-rods or external reinforcement rings • Presence of buttresses or pilasters • Small size compared to the dome *Vulnerability indicators:* • Very thin lanterns, with large openings and slender pillars	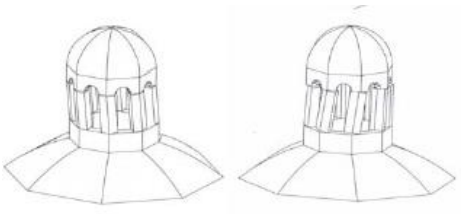
16 – Overturning of the apse	Vertical or curved cracking in the walls of the apse. Vertical cracking in polygonal apses. U-shaped cracking in semi-circular apses *Aseismic measures:* • Presence of reinforcement ring • Presence of effective propping elements (buttresses) • Presence of non-thrusting, braced-roof *Vulnerability indicators:* • Presence of weakness due to openings • Presence of thrusting vaults • Stiff tie-beams, heavy roof covering	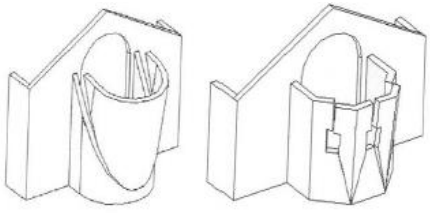

17 – Shear mechanism in the presbytery and the apse	Diagonal cracking (single or crossed). Cracking next to masonry discontinuity *Aseismic measures:* • Good quality masonry (without different construction phase) • Presence of good architraves over the openings • Presence of lightweight tie-beams *Vulnerability indicators:* • Presence of large openings or wide zone with limited masonry thickness • Presence of stiff tie-beam, heavy roof covering	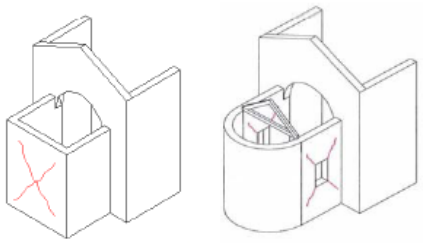
18 – Vault in the presbytery and the apse	Cracking in vaults or detachment from arches or side walls *Aseismic measures:* • Presence of effectively placed tie-rods • Presence of external or internal buttresses *Vulnerability indicators:* • Presence of concentrated loads from the roof • Thin vaults, especially if on a wide span • Presence of lunettes or interruption and irregularities	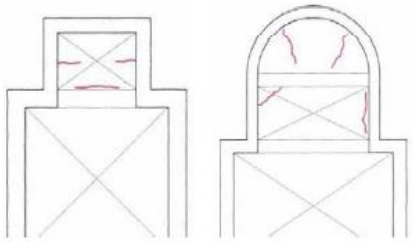
19 – Roof mechanism: side walls of nave and aisles	Cracking near the head of wooden beams, sliding of the beams. Detachment between tie-beams and masonry. Significant displacement of the covering carpet *Aseismic measures:* • Presence of light weight tie-beams • Presence of good wall to beam connections • Presence of roof braces • Presence of good connections between roof elements *Vulnerability indicators:* • Presence of static thrusts in the roof • Presence of rigid tie-beam, heavy roof	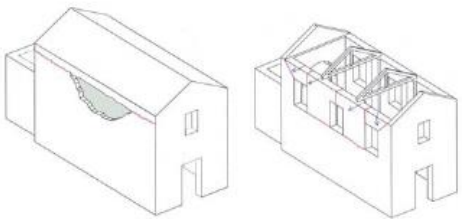
20 – Roof mechanism: transept	Cracking near the head of wooden beams, sliding of the beams. Detachment between tie-beams and masonry. Significant displacement of the covering carpet *Aseismic measures:* • Presence of light weight tie-beams • Presence of good wall to beam connections • Presence of roof braces • Presence of good connections between roof elements *Vulnerability indicators:* • Presence of static thrusts in the roof • Presence of rigid tie-beam, heavy roof	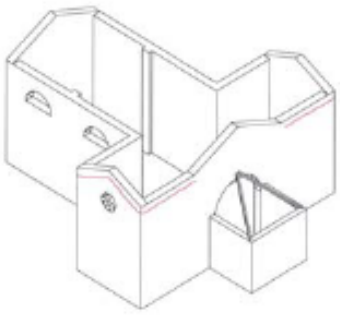

21 – Roof mechanism: apse and presbytery	Cracking near the head of wooden beams, sliding of the beams. Detachment between tie-beams and masonry. Significant displacement of the covering carpet *Aseismic measures:* • Presence of light weight tie-beams • Presence of good wall to beam connections • Presence of roof braces • Presence of good connections between roof elements *Vulnerability indicators:* • Presence of static thrusts in the roof • Presence of rigid tie-beam, heavy roof	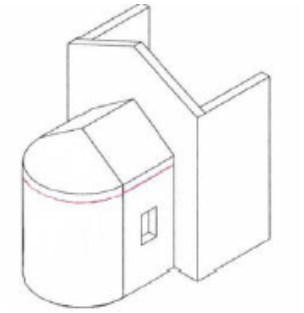
22 – Overturning of the chapels	Detachment of the end walls from the side walls *Aseismic measures:* • Presence of reinforcement ring or tie-rods • Presence of effective propping elements (buttresses) • Presence of non-thrusting, braced-roof • Good quality end wall to side wall clamping *Vulnerability indicators:* • Presence of great weakness due to walls openings	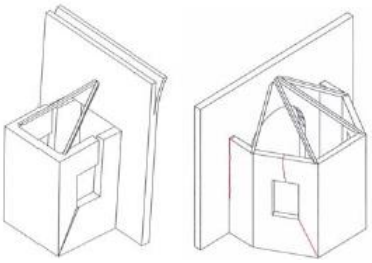
23 – Shear mechanism in the chapel walls	Diagonal cracking (single or crossed). Cracking next to masonry discontinuity *Aseismic measures:* • Good quality masonry (without different construction phase) • Presence of good architraves over the openings • Presence of lightweight tie-beams *Vulnerability indicators:* • Presence of large openings or wide zone with limited masonry thickness • Presence of stiff tie-beam, heavy roof covering	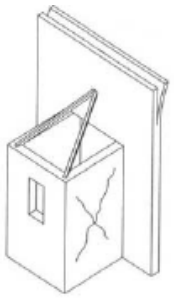
24 - Vaults of chapels	Cracking in the vaults or detachment from the walls *Aseismic measures:* • Presence of effectively placed tie-rods • Presence of external or internal buttresses *Vulnerability indicators:* • Presence of concentrated loads from the roof • Thin vaults, especially if on a wide span • Presence of lunettes or interruption and irregularities	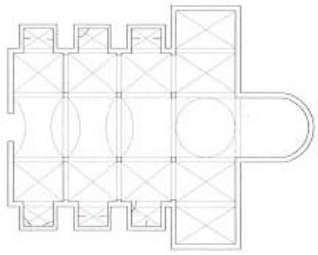

25 – Interactions with adjacent buildings	Displacement in correspondence with constructive discontinuity. Cracking in masonry due to pounding *Aseismic measures:* • Presence of adequate connections between the different phases of masonry construction • Presence of connecting tie-rods *Vulnerability indicators:* • Presence of a great difference in stiffness between the two buildings • Possibility of concentration of seismic actions in connecting elements	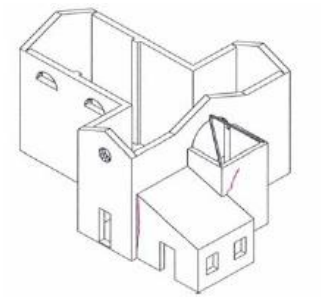
26 – Projections (gable belfry, spires, pinnacles, statues)	Permanent rotation or displacement. Cracking *Aseismic measures:* • Presence of connecting pins between the projection and the wall • Elements of small dimensions • Monolithic masonry *Vulnerability indicators:* • Very thin elements • Overhang support of the element on the underlying wall • Asymmetrical position of the element respect to the underlying structure	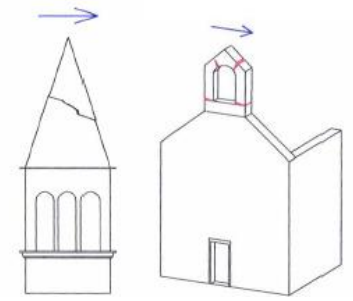
27 – Bell tower	Cracking next to the connection between the bell tower and the church. Shear cracking or sliding. Vertical or curved cracking (bulging of one or more corner) *Aseismic measures:* • Good quality uniform masonry • Presence of tie-rods at different height • Presence of an adequate joint between the church walls • Presence of good wall to wall connections in the church *Vulnerability indicators:* • Presence of large openings at different heights • Asymmetrical support on the church walls at its base • Irregular support elements at ground level of towers	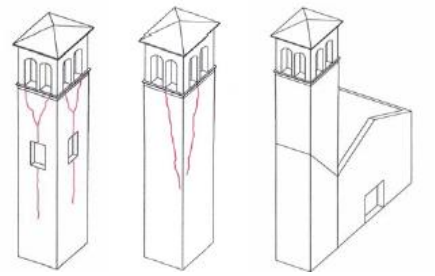
28 - Belfry	Cracking in arches. Rotation and sliding of piers *Aseismic measures:* • Presence of squat piers and/or arches with small openings • Presence of tie-rods or reinforcement rings *Vulnerability indicators:* • Presence of heavy covering or other significant weight • Presence of thrust from the roof covering	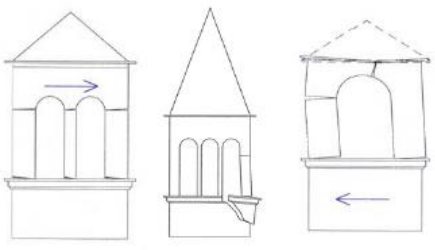

APPENDIX C: ILLUSTRATIONS OF THE GEOMETRY OF LA SEU D'URGELL

External views

External view of the apse

External view of the transept

Gable on the top of the dome

External view from the cloister

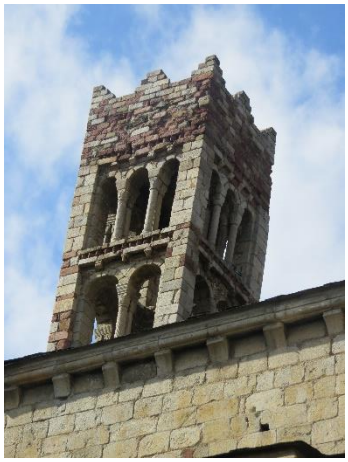

Bell tower on the top of the main façade

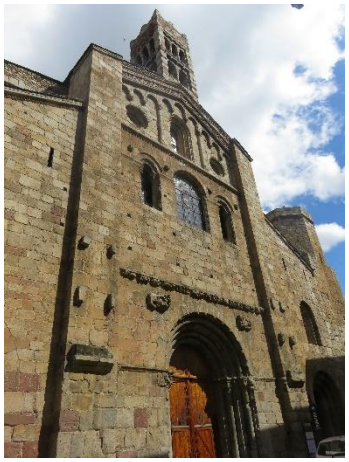

Main façade

Internal views

Vault of the central nave

Vault of the aisle

Apse

Dome

APPENDIX D: ILLUSTRATIONS OF THE DAMAGES OF LA SEU D'URGELL

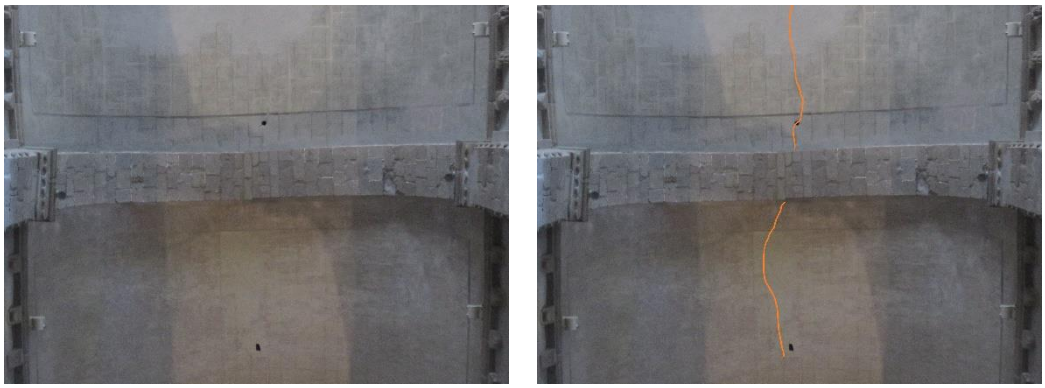

Crack and deformation of the central nave

Cracks in the side walls

Cracks in the transept

APPENDIX E: ILLUSTRATIONS OF THE GEOMETRY OF VILABERTRAN

External views

Main façade

External view of the apse

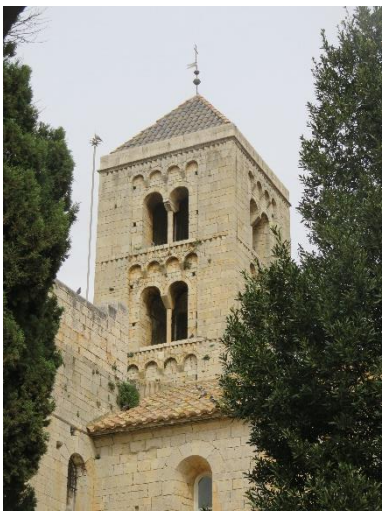

Bell tower from the cloister

Internal views

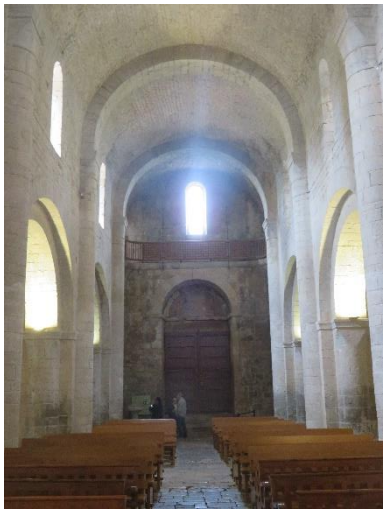

General view of the inside

Apse

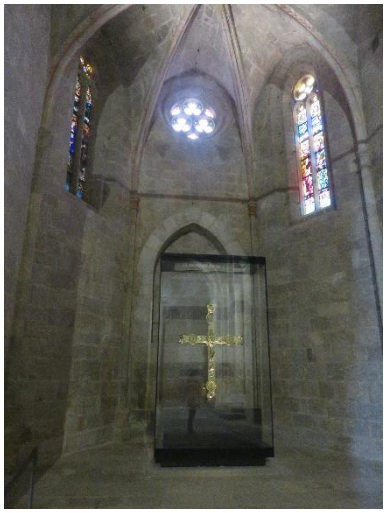

Transept

Chapel

APPENDIX F: ILLUSTRATIONS OF THE DAMAGES OF VILABERTRAN

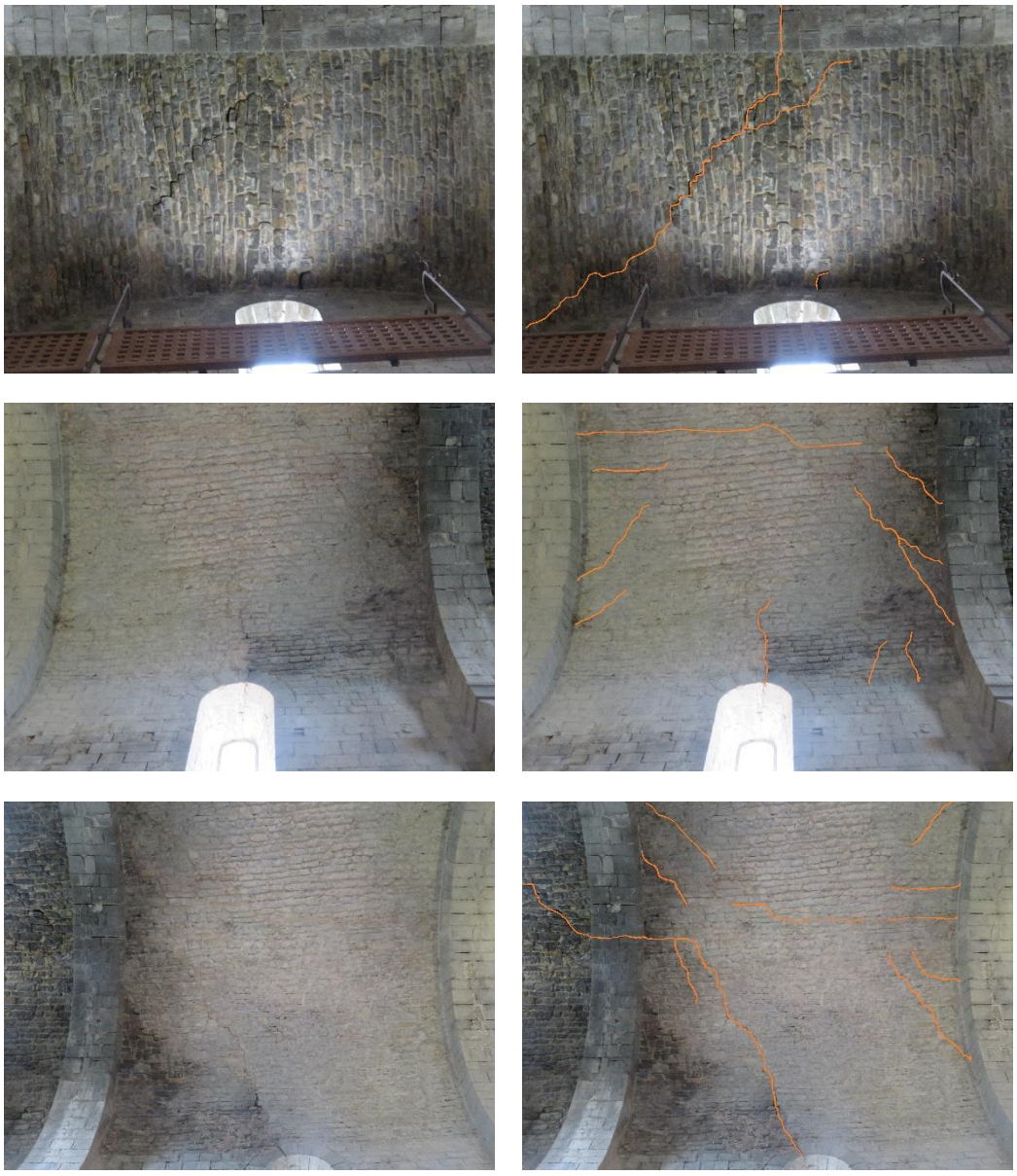

Cracks in the vaults


Cracks in the side wall

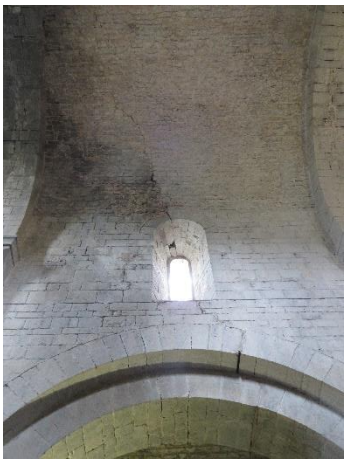
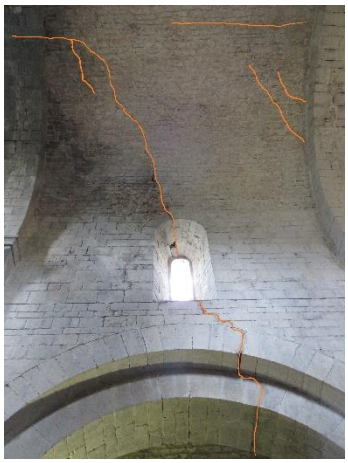

Cracks in thevault and the side wall


Cracks in the apse